Modifications of the tau protein and their varied effects on aggregation and function

By

Benjamin Neal Combs

Submitted to the graduate degree program in Molecular Biosciences and the Graduate Faculty of the University of Kansas in partial fulfillment of the requirements for the degree of Doctor of Philosophy.

_____

Chairperson Dr. Truman Christopher Gamblin

_____

Dr. Kristi Neufeld

_____

Dr. Berl Oakley

_____

Dr. James Orr

_____

Dr. Nancy Muma

Date Defended: April 11, 2013

The Dissertation Committee for Benjamin Neal Combs

certifies that this is the approved version of the following dissertation:

Modifications of tau protein and the varied effects on aggregation and function

_____

Chairperson Dr. Truman Christopher Gamblin

Date approved: 4/19/13

Abstract

Tau is a microtubule-associated protein that is typically found in the axons of neurons. Six isoforms of the protein can be generated through alternative mRNA splicing and all are found in the adult brain. The protein is closely associated with a group of neurodegenerative diseases, including Alzheimer's disease, collectively known as tauopathies. In these diseases tau dissociates from microtubules and begins to polymerize into aggregates that are typically fibrillary in nature. The deposition of these aggregates is closely linked to the death and dysfunction of neurons and eventually leads to atrophy of specific regions of the brain. Tauopathies display a wide variety of pathologies that distinguish them from each other, including aggregate morphology and isoform inclusion. Differential conformational changes in pathological forms of the protein may affect its propensity for aggregation and function. Hyperphosphorylation of tau or inherited mutations, known as FTDP-17 mutations, may induce these conformational changes and alter aggregation and function. The studies described here used in vitro assays to determine how hyperphosphorylation affects each of the tau isoforms and how various FTDP-17 mutations can alter aggregation and function. This information helps to describe how intrinsic differences due to modifications of tau can manifest themselves in the varying pathologies of tauopathies. This can be applied to *C. elegans* models of tauopathies to determine the effects in living neurons. The results demonstrate that similar phosphorylation patterns in tau can result in very different effects on the protein's aggregation and ability to stabilize microtubule polymerization depending on the isoform background. This suggests that phosphorylation pattern is sufficient to induce differential aggregation and may affect the morphology and isoform contents of aggregates. Similarly, FTDP-17 mutations also induced very different effects on tau aggregation and function. This indicates that these mutations may

be affecting disease pathologies in very different manners. Differences between tau isoforms and FTDP-17 mutations are likely affecting the phenotypes seen in animal models of disease and should not be ignored. This is being tested by developing several unique *C. elegans* models of tauopathies.

Acknowledgements

I would like to offer my biggest thank you to my graduate mentor, Dr. Chris Gamblin. It's impossible to imagine reaching this point without his knowledge, advice, and encouragement. I always felt that providing an environment where his students could be successful was among his top priorities and I'm grateful to have had the opportunity.

I'm also grateful to the past and present members of the Gamblin lab for their training, assistance, and friendship. Dr. Kellen Voss, Dr. Qian Sun, and Dr. Carolyn Rankin were always willing to point me in the right direction or explain a technique when I was still trying to find my footing in the lab. In the later years I've discovered that one of the best ways to learn something is to teach it to someone else so I thank Smita Paranjape and Yamini Mutreja for providing that experience and bringing new perspectives to the lab. Several undergraduate students have assisted my research in various ways and I would particularly like to acknowledge the hard work and dedication of Akosua Kernizan, James Odum, and Dakota Bunch.

Several members of the Molecular Biosciences department have played especially important roles in my development. Dr. Brian Ackley and the members of his lab, in particular Dr. Elvis Huarcaya Najarro and Mike Branden, taught me about *C. elegans* and allowed me to raid their supplies on a regular basis. Dr. David Davido took a chance on hiring a naïve post-undergraduate student who had some vague ideas about changing career paths and gave me my first real experience in a lab. Each of my committee members, Dr. Kristi Neufeld, Dr. Berl Oakley, Dr. Jim Orr, and Dr. Nancy Muma, have helped me in individual ways and I thank them for that.

Finally, I would like to thank my family for their unending support in every way imaginable, Candace Bailey for her ceaseless encouragement and acceptance of the long hours spent in the lab, as well everyone else that has helped me along the winding path it took to arrive at this point.

Table of Contents

Chapter I

Introduction

Chapter I Introduction

1.1 Tau Introduction

The tau protein was initially discovered in 1975 and noted for its ability to stabilize the assembly of tubulin into microtubules (*1*). Researchers continued to study the biochemical and functional properties of the protein over the next several years with most of the effort focusing on its relationships with microtubules (*2*). However, tau took on added importance in the mid-1980's when it was found to be the major component of intracellular neurofibrillary tangles, inclusions associated with Alzheimer's disease (AD) and first described in 1907 by Alois Alzheimer (*3-5*). Fibrillary inclusions primarily made up of aggregated tau were also found to be present in many other neurodegenerative disorders, collectively known as tauopathies (*6, 7*). The abnormal aggregation of the tau protein is found in all tauopathies and is also closely associated with neurodegeneration of certain regions of the brain (reviewed in (*8*)). In the nearly three decades since the protein was first linked with neurodegenerative disorders, scientists have learned more about the functions of tau and how its aggregation may be toxic to neurons. Despite this progress there are still significant gaps in our understanding of why tau begins to aggregate, how this aggregation may be exerting toxic effects, and how these aspects can be targeted by effective treatments.

The human tau gene is primarily expressed in the neurons of the central nervous system and the protein itself typically localizes to the axons of the neurons but can be found in the somatodendritic compartment as well (*9-11*). The gene is located on chromosome 17 and made up of 16 exons (*12, 13*). Alternative mRNA splicing is used to generate the six isoforms of tau that are found in the human brain (Figure 1.1) (*14*). These isoforms utilize 11 of the exons

Figure 1.1

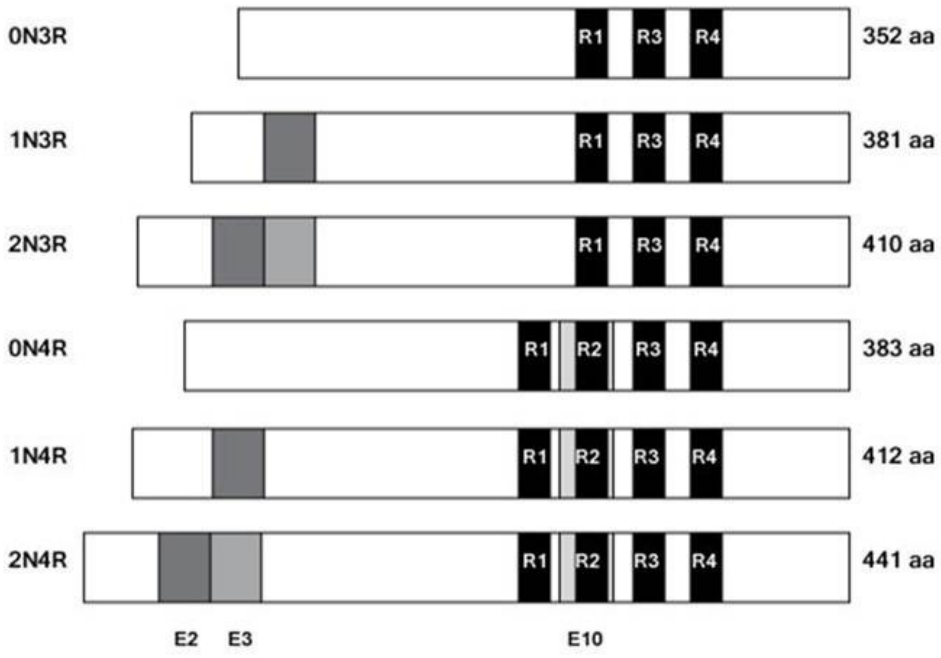

Figure 1.1 Tau isoforms with microtubule-binding repeats. In the human brain six tau isoforms are generated through alternative mRNA splicing of exons 2, 3, and 10 and range from 352 to 441 amino acids in length. Exon 10 contains the 2nd of four microtubule-binding repeat regions (MTBR). The nomenclature refers to the number of N-terminal exons (0N, 1N, or 2N) and the number of MTBR (3R or 4R) present in the isoform.

present in the tau gene and differ based on their inclusion of the 2nd, 3rd, and 10th exons. The nomenclature used to define these isoforms describes the presence or absence of exons 2 and 3, the N-terminal exons, as 0N, 1N, or 2N. The splicing of exon 3 depends on the presence of exon 2 and it is never included without the 2nd exon (*15*). The absence or presence of exon 10 is noted as 3R or 4R respectively due to that exon containing one of the four potential microtubule-binding repeat domains (MTBR). While the developing fetal brain only contains 0N3R tau, the adult brain expresses all six isoforms (*16*). The 3R to 4R ratio is approximately 1:1 while the breakdown of N-terminal exon inclusion is approximately 9% 2N, 54% 1N, and 37% 0N (*17, 18*).

Differences between the tau isoforms likely affect some of the protein's major functions of stabilizing and promoting the assembly of microtubules (*1, 19*). As mentioned above, the isoform nomenclature includes 3R or 4R depending on the number of MTBR present in the protein. These regions measure 31-32 amino acids in length and contain an 18-residue imperfect repeat followed by a 13 or 14 residue inter-repeat region (Figure 1.2) (*20*). The repeat and the inter-repeat regions are both involved in binding to microtubules but other sequences around the MTBR affect the interactions as well (*21, 22*). Each MTBR contains a conserved PGGG sequence that may form part of a β-turn motif that forms a loop upon binding to microtubules (*23*). Individually, each MTBR is able to bind microtubules relatively weakly, but, there appears to be a cooperative binding effect among the MTBR and the adjoining regions (*24, 25*). Due to the presence of MTBR2, the 4R isoforms bind more tightly than 3R isoforms and promote the assembly of microtubules more efficiently (*18, 26*). Upon binding, the N-terminal portion of the

Figure 1.2

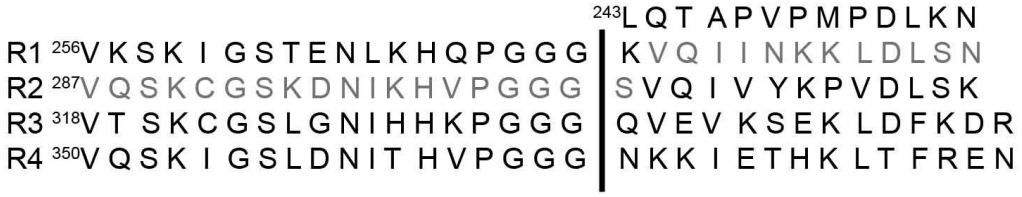

Figure 1.2 Sequence of Tau Microtubule-Binding Repeat Region. The amino acid sequence of the region including and surrounding the microtubule-binding repeat region (MTBR) of tau is displayed here. The amino acids left of the vertical line represent the repeat regions while those to the right of the line include the inter-repeat regions between the repeats as well as amino acids before and after the MTBR. The amino acids in gray represent those included in exon 10, subject to alternative mRNA splicing. They are included in the 4R isoforms and excluded in 3R isoforms.

protein remains unbound and is referred to as the "projection domain" (*27*). In vitro binding is saturated at a 2:1 tubulin to tau ratio, but, in neurons, tubulin is found at 20-40 μM concentrations while tau is typically found at ~1 μM (*19, 24, 28, 29*). Tau has demonstrated the ability to bind to the inside as well as the outside of microtubules (*23, 30*).

1.2 Tau function

The primary functions of tau seem to involve these direct interactions with microtubules. Tau has the ability to promote microtubule nucleation as well as their stabilization by inhibiting the dynamic instability (*1, 31-33*). Given the importance of microtubules in maintaining the shapes of projections it is not surprising that removal of tau prevents neurite growth (*34*). In addition to stabilization, tau also affects microtubule bundling and spacing, a process that is affected by the sizes of the tau isoform (*35-37*). The bundling may be important for maintaining axonal structure as well the transport of cellular cargo throughout the axon.

The transport of proteins and other cargo is particularly important for neurons due to the distances between the cell body and the tip of the axon and is carried out through the use of kinesin and dynein, motor proteins that pull the cargo along microtubules. Overexpression of tau inhibits the transport of cargo along microtubules, a process that occurs in an MTBR-dependent manner (*38, 39*). Tau may be inhibiting axonal transport by competitively binding to microtubules in place of motor proteins but this behavior has not been replicated in actual axons and at physiological conditions (*40, 41*).

In addition to the direct binding of microtubules, tau interacts with several other cellular components that may be related to other important tau functions. The protein's "projection domain" interacts with the plasma membrane and may be involved in anchoring the protein (*42*). Tau appears to be involved in remodeling of the actin cytoskeleton and may assist in mediating microtubule-actin interactions (*43-45*). Interactions between tau and other proteins may affect the functions of tau and the other protein itself. Included in these interacting partners are several kinases, phosphatases, and chaperone proteins. Tau can bind to several members of the src family, fyn being among the most characterized, and affect the localization of those kinases as well (*46, 47*). Tau also interacts with phosphatases, such as PP2A (*48*). Approximately 1 in 5 amino acids in tau is a potential phosphorylation site and the level and pattern of phosphorylation may have a large impact on its function. Phosphorylation and tau will be discussed in more detail below. Finally, the binding of certain chaperone proteins may affect the functions of tau and reduce its pathological aggregation (*49*).

1.3 Tau structure and domains

The fairly large number of binding partners for tau is partially due to some unique characteristics of the protein. Tau has been described as a "natively unfolded" protein due to its highly flexible nature and the lack of identifiable secondary and tertiary structures (*50, 51*). The protein is extremely hydrophilic and, in a normal state, will remain soluble at relatively high concentrations. The hydrophilic nature of the protein is due to the high number of polar amino acids, like serine and threonine, as well as the number of charged amino acids. Despite a net charge of only +2, the full-length tau isoform is made up of more than 25% charged amino acids. The highly flexible structure of tau allows it to promiscuously bind to other proteins and even

harsh treatments with heat and other denaturing agents do not have major effects on the ability of the protein to perform its normal functions (*52*). Despite this flexibility, there is some detectable secondary structure that is of particular importance for tau. Through nuclear magnetic resonance and other techniques, some of this secondary structure has been determined (Figure 1.3) (*51*). Of particular importance are β-strands that are found within the MTBR and which may be more prevalent when the protein is bound to microtubules (*53*). In addition to the secondary structures evidence suggests that higher order structure exists as well. The protein exists in what has been described as a "paperclip" or "global hairpin" conformation where the N- and C-terminal ends of the protein fold over to interact with each other and the interior domains of the protein (*54, 55*).

Included in these interior domains are the three or four MTBR, discussed earlier, and two proline-rich domains just upstream of them. The proline-rich region is contained between amino acids 150-240. Many of the prolines in this region are next to serines or threonines making them targets of proline-directed kinases. Additionally, other prolines are found in PXXP motifs that can bind to the SH3 domains of src-family kinases and other proteins (*46*). The proline-rich region is considered separate from the MTBR even though microtubule-binding interactions can be detected from amino acids 200 through 400 (*53, 56*). The "projection domain" refers to the N-terminal region of the protein because it projects from the microtubules when tau is bound to them (*27, 57*). This domain contains a higher proportion of acidic amino acids while the MTBR is more basic in nature, which likely assists in the binding to the acidic C-terminal ends of tubulin subunits (*58*).

Figure 1.3

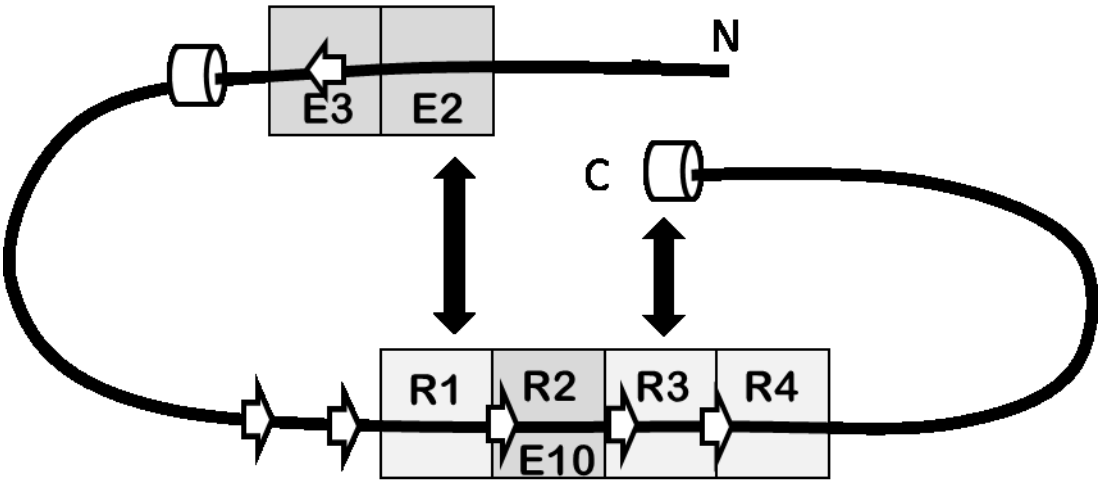

Figure 1.3 Global hairpin conformation of tau and its known secondary structure. The N- and C-terminal ends of tau interact with each other as well as the interior of the protein in a conformation that has been described as the "global hairpin." The tau protein is highly flexible and largely unstructured but NMR studies have determined that regions of transient secondary structure do exist. The β-strands are represented by arrows and α-helices are represented by cylinders.

While the evidence suggests several different functions for tau, mice lacking the tau gene initially seemed to suffer few observable defects outside of minor alterations in microtubule patterning (*59*). However, more recent studies have indicated some behavioral changes and brain atrophy occur in aged tau-knockout mice (*60, 61*). Despite the seeming lack of evidence for essential functions of the protein, tau has retained the focus of investigators for many years due to its obvious dysfunction in tauopathies.

1.4 Tauopathies

Tauopathies are a group of disorders characterized by an abnormal intracellular aggregation of the tau protein that is closely associated temporally and spatially with the degeneration and death of neurons in the brain. While tau aggregation and neuronal dysfunction generally characterize tauopathies, their specific pathologies can vary widely from each other. These differences manifest themselves in the morphologies of aggregates associated with the diseases, the locations and cell-types displaying the pathologies, and the related symptoms which correlate to the functions associated with the particular affected brain regions. Brief overviews of some of the major tauopathies and their pathologies will be discussed below.

1.4.1 Alzheimer's disease

The most common and widely-studied tauopathy is Alzheimer's disease. The two major characteristics of the disease are found in the brain and are intracellular neurofibrillary tangles, made up of the tau protein, and extracellular plaques, made up primarily of the β-amyloid (Aβ) peptide (*62*). The tau tangles can be found before plaques and mirror the loss of neuronal axons

and, as the disease progresses, the neurons themselves (*63*). The neurofibrillary tangles primarily contain hyperphosphorylated tau that has polymerized into paired helical filaments (PHF). The PHF are the predominant structure found in NFT but straight filaments (SF) are found as well and the two types of filaments combine to form a pyramidal shaped inclusion (*64*). PHFs appear as two filaments wrapped around each other and display a periodicity of around 80 nm and variable width (*65*). SFs lack periodicity and can also vary in their width (*66*). Aggregates in AD are made up of all 6 tau isoforms in roughly the same percentages as are found in a normal brain (*67, 68*). The disease is much more common in the elderly and the progression of the disease can require decades to reach the final stages (*69*). This progression can be described in stages based on the location and severity of the protein aggregation pathologies, which may be present before external symptoms appear (*62*). The initial tau pathology, found in projection neurons of the locus coeruleus, is known as the "pretangle phase" because hyperphosphorylated and aggregated tau can be detected through immunostaining but has not yet progressed to the level of full tangles (reviewed in (*70*)). Tangle pathology first develops on the entorhinal cortex and spreads to the amygdala and hippocampus before finally forming in all of cerebral cortex and parts of the midbrain and thalamus (*70*). The outward signs of the disease are usually not apparent until the later stages of the progression of tau pathology but are typified by dementia, including loss of memory and changes in emotional behavior.

Around 5% of AD cases are associated with a particular genetic polymorphism and typically present much earlier than the sporadic cases that have no apparent genetic mutations. These mutations occur in the amyloid precursor protein (APP) gene or 1 of the 2 presenilin genes (*71-73*). APP is the protein product that is cleaved to generate Aβ and presenilins are part of the

protease complex that cleaves APP indicating that Aβ pathology may be an initiating factor in the disease. A particular allele of the ApoE gene, associated with lipid metabolism, is also an associated risk factor for AD and may play a role in immune function or processing of Aβ.

While tau aggregation and neurodegeneration are closely correlated, the role of the protein's aggregation in the initiation of AD has been a divisive issue in the field. As mentioned above, AD displays aggregation of the tau protein but is also known for the extracellular accumulation Aβ (reviewed in (*74*)). Crosses of transgenic mice expressing mutant APP gene and a mutated tau gene enhanced tau pathology but not Aβ pathology compared to the initial transgenic line (*75*). This indicated that the presence of Aβ pathology led to tau pathology but not the reverse. The mutations in the APP gene can lead to early-onset forms of the disease but there is no mutation in tau associated with AD. These pieces of evidence led many AD researchers to focus primarily on Aβ for its roles in disease progression and potential therapeutic intervention but evidence supporting a greater role for tau in AD and other neurodegenerative diseases continues to mount.

While Aβ pathology may be upstream of tau, the locations of NFT more closely correlates with regions of neurodegeneration and the amount of tangles correlates with the levels of dementia (*76-79*). The discovery of several unique mutations in the tau gene that directly led to early-onset tauopathies provided evidence that alterations in the gene itself could result in tau aggregation and neurodegeneration (*80-82*). In addition, Aβ requires the presence of tau in order to exert toxic effects and reduction of tau levels decreases the effects on memory in mice (*83, 84*). Meanwhile, tau itself is able to exert toxicity as the overexpression of wild-type tau or

aggregate-prone tau constructs can cause toxicity in cultured cells or in various in vivo models (*85-87*). Finally, many other sporadic tauopathies described below display tau pathology and the related neuronal degeneration without any Aβ pathology (*8*). For these reasons many believe the tau protein to be the key mediator of toxicity in AD.

1.4.2 Pick's Disease

Pick's disease (PiD) is one such disorder that is characterized by aggregation of the tau protein but lacks Aβ pathology. However, instead of NFT, PiD is associated with Pick bodies, spherical inclusions primarily made up of tau filaments that are wider than those found in AD but also in straight and paired helical forms (*88-90*). The aggregates are made up almost exclusively of 3R tau isoforms, those lacking exon 10, and tau protein that has not been phosphorylated at S262 (*91, 92*). Different subsets of neurons are vulnerable to tau aggregation in PiD than in AD. In PiD, the frontotemporal lobar and limbic system are greatly affected as well as parts of the neocortex and dentate granular cells of the hippocampus (*90, 92*). Differences in tau aggregation relative to AD may be reflective of alternate initiating factors or symptomatic of the type of neurons that are affected. For example, the dentate granular cells primarily express 3R isoforms and may be disproportionately targeted if those isoforms are more likely to aggregate under certain conditions (*93*).

1.4.3 Progressive Supranuclear Palsy

Progressive supranuclear palsy (PSP) differs from many other tauopathies in that its symptoms are primarily characterized by movement defects (*94*). In addition to a loss of balance, eye

movement, and ability to swallow, the disease is associated with personality changes. The neuropathology displays the loss of neurons in the basal ganglia, subthalamus, and brainstem regions but not in the frontal cortex as in AD (*95*). This neuronal loss is associated with NFTs that are more globular in nature than those associated with AD and primarily formed from straight filaments that are narrower than PHFs (*7, 96, 97*). The tau found in the filaments is hyperphosphorylated and primarily 4R isoforms (*98, 99*). Increases in the levels of 4R tau mRNA in the brainstem of PSP-affected brains could help explain the preferential aggregation of that isoform (*100*).

1.4.4 Corticobasal Degeneration

Corticobasal degeneration (CBD) is a disease that is similar to PSP in many respects. The tau aggregates isolated from CBD brains are primarily made up of 4R isoforms that include 1 or both of the N-terminal exons that can be present (*99, 101*). However, CBD pathology is found in the cerebral cortex, cerebellum, and substantia nigra (*102*). The aggregates are similar to PHFs and SFs and combine to form fibrillary inclusions as well as neuropil threads, tau immunoreactive groups of fibrils associated with neurite projections (*6, 101*).

1.4.5 Chronic Traumatic Encephalopathy

Chronic traumatic encephalopathy (CTE) has recently entered the public consciousness due to revelations about its prevalence in military veterans and athletes who have been subjected to repeated brain traumas (*103*). The disease is characterized by severe atrophy of the frontal and temporal cortices, medial temporal lobe, and hippocampus, among other regions (*103, 104*).

Symptoms can include dementia, personality changes, and motor defects resembling Parkinson's disease (*105*). The tau pathology organized into variably shaped NFTs and neuritic threads while amyloid plaques were rare but occasionally present (*106*).

1.4.6 Frontotemporal Dementia with Parkinsonism Linked to Chromosome 17

The Frontotemporal Dementia with Parkinsonism Linked to Chromosome 17 (FTDP-17) disorders are actually a collection of tauopathies with overlapping phenotypes and a root cause tied to autosomal dominant mutations. This group of diseases has been subject to a complex and occasionally confusing nomenclature but, here, the FTDP-17 term will refer only to diseases associated with mutations in the tau gene itself. The discovery of several of these mutations in the late 1990's provided much support to the hypothesis that tau aggregation could itself be toxic to neurons (*80, 107, 108*). To date there are 31 known missense mutations and 10 silent mutations in the tau gene that are associated with early-onset tauopathies (Table 1.1). The aggregation of tau is prevalent in the brains of those affected by these diseases but the pathology can be highly variable between mutations and even, in some cases, among individuals with the same mutation. The tau pathology can be found in differing neuronal types as well as glial cells, can vary morphologically, and can display altered tau isoform expression and aggregation (reviewed in (*109*)). Due to the varied pathologies, the mutants are often described by their similarities to the symptoms and pathologies of AD, PiD, PSP, or CBD.

1.5 Tau aggregation

The presence of tau aggregation in all of these diseases strongly suggests that it may be having a toxic effect on neurons but very little is known about the mechanisms of this toxicity or why the aggregate morphologies can vary so widely. One aspect of the debate surrounding tau aggregation focuses on the type of tau aggregate that is toxic. Because the larger NFTs were easily identifiable and so closely associated with degeneration of neurons and the onset of dementia it was assumed that they must be toxic. More recent evidence suggests that the smaller aggregates, described as oligomers, are more toxic.

In order to understand tau toxicity it is useful to understand what is known about the aggregation of the protein. Tau monomers interact with each other through 2 hexapeptide motifs that take the form of β-strands that can polymerize through the formation of cross-β structure (*110-112*). The first sequence, ^{275}VQIINK, is located in the 2nd MTBR which is only found in 4R isoforms while the second sequence, ^{305}VQIVYK is in the 3rd MTBR. The sequences form intermolecular cross-β structure that make up the core of the tau fibril but detailed information about this structure remains elusive due to the flexible nature of the rest of the protein. Initially, monomers join together in this manner to form oligomers that are still soluble and more prevalent than previously thought (*113*). This step can be described as a nucleation event while the growth of oligomers is an elongation phase. The oligomers grow into larger, fibrous aggregates by joining together or through the addition of more monomeric tau. Often these aggregates take the form of PHF and display a periodicity of around 80 nm in AD (*64, 114, 115*). Less common are the SF, also found in AD and PiD, that contain some similarities to PHF but lack periodicity (*66, 116*). Both types of filaments have a core, made up of the regions of the protein around the

hexapeptide sequences described above, as well as a "fuzzy coat", made up of the N- and C-terminal regions of the protein (*65, 117*). The fuzzy coat is described as such because its flexibility makes it appear fuzzy next to the highly ordered core region (*118*). As the fibrils accumulate they form larger inclusions bodies that can be observed through direct visualization. The inclusions are typically NFT in AD but can vary morphologically in other diseases such as Pick bodies in PiD and globose tangles in PSP, (*119, 120*).

While tau aggregation seems to follow the path of nucleation, elongation, and finally formation of large inclusion bodies, information about why the highly soluble protein begins to aggregate in the first place is still lacking. Most of the early research focused on identifying how soluble tau differs from insoluble tau. In this way several key factors were identified and will be introduced here.

1.6 Tau phosphorylation

One difference that may have attracted the most attention is the phosphorylation of tau. Tau is normally phosphorylated at 2 to 3 sites in the normal brain but can have around 5-9 moles of phosphate per mole of tau in protein purified from AD brains (*121*). This phosphorylation may affect the function of the protein (*2, 122*). The tau found in PHF and other aggregates associated with tauopathies is often found to be hyperphosphorylated (*123-126*). Nearly 20% of the residues in full-length tau are potential phosphorylation sites and the protein can be phosphorylated by a wide range of kinases. These include proline-directed kinases such as GSK-3β and cyclin-dependent kinase 5 (cdk5) (*127-129*). Both kinases are highly expressed in the brain and have been found in conjunction with NFT and affected neurons in AD (*130-132*).

GSK-3β, in particular, phosphorylates tau at a higher level when it is overexpressed in cells and mice (*133, 134*). Prior phosphorylation by cdk5 increases the amount of tau phosphorylation by GSK-3β (*128*). Relevant to AD, the presence of Aβ has been demonstrated to promote the hyperphosphorylation of tau, possibly through localization or activation of kinases (*135, 136*).

Much effort has been expended in an attempt to determine how hyperphosphorylation of tau is affecting the protein and which sites are of particular importance. Phosphorylation by GSK-3β may lead to increased aggregation of the protein, as demonstrated with in vitro experiments and with *Drosophilia* models (*137, 138*). Several of the tau sites phosphorylated by GSK-3β are known to be phosphorylated when the protein is found in an aggregated form (*128, 139*). All of this indicates that phosphorylation by GSK-3β and other kinases may promote the polymerization of tau into fibrils. It is possible that the decreased microtubule-binding ability of hyperphosphorylated tau may be increasing the amount of unbound tau until it reaches a critical concentration, or the concentration of tau at which aggregation could begin. Additionally, hyperphosphorylation may be affecting the conformation of the protein such that the protein now exists in a pro-aggregant state. These theories are not mutually exclusive.

Phosphorylation of tau at certain sites, such as T231 or S262, inhibits its ability to carry out normal microtubule-related functions compared to other forms of the protein and can cause nearly all of the phosphorylated protein to dissociate from the microtubules (*140-142*). Many other sites are phosphorylated early in the course of the disease and lead to dissociation of tau from microtubules, including S199, S202, T205, S396, and S404, among others (*142-145*). The effect seems to be site-specific as phosphorylation at several other GSK-3β-phosphorylated sites

seemed to have very little effect on the function of the protein (*142*). Tau's reduced binding affinity for microtubules could lead to an increase in the amount of soluble protein inside of the neuron. Unbound and hyperphosphorylated tau may be more likely to aggregate in that state or could be further phosphorylated at other sites in order to induce conformational changes that lead to tau aggregation.

Studying phosphorylation of a protein, and particularly one with as many potential phosphorylation sites as tau, can present certain difficulties. For example, protein isolated from the brain is a heterogeneous mix of phosphorylation levels and phosphorylated sites making it difficult to determine which specific factors are of particular importance. It can also be difficult to mimic physiological conditions and control the overall level and specificity of phosphorylation during in vitro reactions. Pseudophosphorylation can be utilized in order to address some of these problems. This technique uses site-directed mutagenesis to alter serine and threonine residues, which are both potential phosphorylation sites, into aspartates or glutamates. The bulky and negatively-charged side groups of aspartates and glutamates are meant to mimic the effects of phosphorylation at that site. This technique has been used to confirm previous phosphorylation experiments and determine other site-specific effects (*146-148*).

Some of these site-specific effects of phosphorylation included decreased microtubule interactions as well as an increased propensity for aggregation at certain sites, including at the S202, T205, S396, and S404 sites (*149-152*). In the brain, these sites were often phosphorylated prior to aggregation while other sites, like S422, were phosphorylated later (*153*). Interestingly,

expression of pseduophosphorylated tau can also be toxic to cultured cells in the absence of tau aggregation, indicating that hyperphosphorylated tau may have toxic properties beyond increased tau polymerization (*154*). Any enhancement or inhibition of tau aggregation due to hyperphosphorylation is likely due to conformational changes induced by the post-translational modification. Hyperphosphorylated tau displays an SDS-resistant electrophoretic shift that results from an altered conformation and not the incorporation of phosphates (*155*). Pseudophosphorylation of tau, at individual or combinations of several key sites, altered the local and long-range intramolecular interactions that make up the global hairpin conformation (*156, 157*). Changing the conformation of tau could make some regions accessible to other tau molecules or stabilize secondary structures like the β-strands that are involved in tau-tau binding.

While hyperphosphorylation of tau may be changing the conformation of the protein, it does not necessarily mean that it is the causative agent of tau aggregation. However, tau hyperphosphorylation is known to occur prior to aggregation at many key sites and all tauopathies are associated with aggregated tau in a hyperphosphorylated state (*8, 158*). Some phosphorylation patterns seem to enhance tau polymerization in vitro while others may inhibit NFT formation and thereby trap tau aggregates in a more toxic oligomeric form (*149, 159*). Previous work in Chris Gamblin's lab attempted to answer some of the questions about the importance of several potential phosphorylation sites by using site-directed mutagenesis to create pseudophosphorylation mutants in several different combinations (*160*). A combination of 7 pseudophosphorylation mutations at sites known to be phosphorylated by GSK-3β induced the electrophoretic shift associated with pathological tau, decreased interactions with microtubules, and, when compared to normal tau in an in vitro polymerization assay, increased filament length

but decreased nucleation (*160*). Despite a wealth of evidence linking hyperphosphorylation to tau aggregation, its exact role remains complex.

1.7 Other tau post-translational modifications

Tau hyperphosphorylation is the most widely studied of the post-translational modifications and seems to have the most robust links to tau dysfunction but the protein also undergoes several other alterations that may be affecting its function and aggregation. These modifications can include truncation, ubiquitination, acetylation, glycoslylation, and oxidation. The effects of many of these modifications are still not well-characterized and may have a causative role in tau aggregation or merely a byproduct of other factors. Many of them affect or reflect an inability of neurons to properly degrade tau which may lead to increased concentrations of normal or modified tau. One example of this is the several species of truncated tau that can be found in NFTs (*161*). Some of these truncated forms of tau, such as those with the 20 C-terminal amino acid residues removed, can promote aggregation in an in vitro reaction (*162, 163*). The presence of ubiquitinated tau in NFT could indicate that the protein has been marked for degradation but the cell was unable to complete the task due to the protease- and proteasome-resistance of tau found in PHFs (*164-167*). Another modification of tau that may inhibit its degradation and promote aggregation is acetylation, particularly at the K280 residue (*168, 169*). Certain patterns of glycosylation have also been identified with aggregated tau and may be associated with hyperphosphorylation (*170*). Finally, oxidation of tau at its two cysteine residues may be leading to the formation of inter- or intra-molecular disulfide bonds that could affect the conformation and aggregation of the protein (*171*).

1.8 Nucleation of tau aggregation

Many of these post-translational modifications are associated with aggregated tau in disease-afflicted brains and affect the in vitro aggregation but cannot be definitively linked to a causal role in polymerization. In vitro aggregation of tau is very difficult to induce without the addition of a cofactor and it is possible that one is required in vivo as well. Typically the cofactors used for in vitro experiments are polyanions, free fatty acids, or planar aromatic dyes and include heparin (*172*), arachidonic acid (*173*), nucleic acids (*174*), and Congo Red (*85*). It is not known which cofactors, if any, are important for in vivo tau aggregation but it is possible that tau could be interacting with hydrophobic interfaces at the plasma membrane or coming into contact with nucleic acids at the ribosome. Due to its close association with microtubules it may be possible that nucleation of tau aggregation is occurring there as well, something that was recently demonstrated with taxol-stabilized microtubules (*175*). One of the most important recent developments in the tau field has been the demonstration that tau aggregates themselves can seed the formation of new in vitro and in vivo tau aggregates and the pathology can propagate through other synaptically-connected regions of the brain in a self-directed assembly mechanism similar to that of the prion protein (*176-180*).

Due to the difficulties of inducing in vivo and in vitro tau aggregation, FTDP-17 mutations have been used in order to enhance this activity. These variants of tau are associated with early-onset dementias and may have intrinsic factors that enhance their polymerization. Despite the unstructured nature of tau, changes to the limited local and global structures of the protein that do exist are probable and are likely to affect the aggregation of the protein in direct and indirect ways. Mutations that affect the structure and conformation of tau may enhance phosphorylation,

stabilize β-strands important for amyloid formation, expose regions of the protein that may be hydrophobic, or inhibit interactions with microtubules.

Most missense mutations are located in one of the four potential MTBR but can also be found at the N- or C-termini (Table 1.1, adapted from (*181*)). The potential for increased aggregation of FTDP-17 mutant forms of tau could be due to an enhanced level of phosphorylation. However, reports on the mutation-specific effects on phosphorylation have been mixed with some indications for more or less phosphorylation, even among the same mutations (*182, 183*). Despite the seemingly contradictory results, alterations in phosphorylation patterns far away from mutation sites indicate that the mutations are significantly changing the conformation of large segments of the protein.

Some FTDP-17 mutations affect the splicing of mRNA, particularly the silent mutations (reviewed in (*181*)). This imbalance in isoform ratio seems to be sufficient to induce aggregation of normal tau. Some missense mutations also affect splicing ratios while others have no apparent effect on mRNA splicing but the aggregated tau can still display altered isoform ratios similar to some of the sporadic tauopathies (*184, 185*). This indicates there may be mutation-specific effects that lead to differential aggregation propensities for individual tau isoforms.

1.9 Animal Models of Tauopathies

FTDP-17 mutations have frequently been used as enhancers of aggregation in transgenic animal models and, through the use of these models, there has been much progress made in understanding the role of tau aggregation in the progression of tauopathies. However, some of

these models have, at times, provided contradictory results. The mechanisms surrounding tauopathies appear to be quite complex and seemingly minor variations could result in drastically different phenotypes that cloud interpretation of the data. Many transgenic animal models of tauopathies utilize FTDP-17 mutated tau or hyperphosphorylation of tau to induce the protein's aggregation. Variations in the types of tau expressed could alter morphology within the same animal system. Some of the animal models that have been generated and their morphologies will be outlined here.

1.9.1 Mouse models

Mouse models of tauopathies have the benefits of taking place inside of a complex, mammalian brain. The mouse brain contains endogenous tau that is exclusively made up of 4R isoforms and can be left in or knocked out of the transgenic animals. It is possible for human wild-type tau to form aggregates in mice but it requires heavy overexpression and other attempts to generate wild-type tau models have not been successful (*186*). The addition of a dominant negative form of the PP2A phosphatase can also lead to hyperphosphorylation of tau and aggregation (*187*). Because of the difficulties inducing aggregation of endogenous or human wild-type tau, modified tau is often used in animal models. The most common modification is to use an FTDP-17 mutation. Transgenic models expressing FTDP-17 versions of tau will typically display NFTs that resemble those associated with AD and other tauopathies at lower concentrations that wild-type. The list of FTDP-17 mutations used to induce tau aggregation in mice includes G272V, P301L, P301S, V337M, K369I, and R406W (*188-192*). Based upon the differences associated with human forms of FTDP-17, it is not surprising that the pathologies among these mouse models varied as well, with differences arising in the location of tau aggregation and the

morphology of aggregates. Interestingly, these differences may correlate closely with human forms of the diseases. For example, the mice expressing K369I tau replicated several features of the PiD-like pathology associated with humans expressing the K369I tau variant as well as sporadic human PiD (*189*). Models of AD are particularly complicated due to the presence of Aβ plaques. The development of the "triple transgenic" mouse model has recapitulated most aspects of the disease by incorporating transgenes that contain mutated versions of presenilin 1, APP, and tau (*193*).

1.9.2 Invertebrate models

The use of invertebrate models allows the researcher to use a wide variety of genetic tools that allow faster and cheaper generation of transgenic models, compared to mice, while still being able to model the tauopathies in actual neurons. The most common invertebrate tauopathy model system to date has been in the *Drosophila* organism. One of the first *Drosophila* models utilized pan-neuronal expression of the wild-type 0N4R isoform, a model that displayed neuronal death with no detectable large aggregates (*87*). This lends support to the hypothesis that tau toxicity stems from a soluble form of the protein that may be in either a monomeric or oligomeric state. Later studies demonstrated that the tau isoforms had differential effects on neurons in the fly brains and that phosphorylation state was also important for toxicity in specific subsets of neurons (*194, 195*). Most *Drosophila* models lack fibrillar tau unless it is expressed in glial cells indicating that the cellular environment may affect when and how tau aggregates (*196*). As expected from other models, the addition of FTDP-17 mutations such as R406W enhanced toxicity while V337M had minor effects and seemed to ameliorate toxicity (*87, 194*). The totality of work in Drosophila suggests that mutations, phosphorylation patterns, and type of

FTDP-17 mutation can induce entirely different effects in the cell types affected and types of aggregation.

Somewhat more recently, nematodes have also been used to model tauopathies. Transgenic *Caenorhabditis elegans* expressed wild-type, P301L, or V337M tau in the 1N4R background (*197*). Expression of these constructs resulted in isolation of insoluble tau aggregates from the worms with more insoluble tau associated with the worms expressing FTDP-17 tau. In addition the worms displayed motor defects, indicative of neuronal dysfunction. Other models expressed 0N3R or 0N4R wild-type isoforms or 0N4R-R406W tau in the mechanosensory neurons (*198*). The worms expressing the mutant tau displayed greater dysfunction surrounding the morphologies and sensitiveness of those neurons, an effect which was exacerbated upon activation of GSK-3β in an isoform-specific manner. Aggregates were more prevalent in FTDP-17 transgenic worms but the aggregates were not filamentous. Additionally, neurodegeneration occurred in the presence and the absence of aggregates and with wild-type and mutant tau. Another model utilized the ΔK280 FTDP-17 mutation as a pro-aggregant form of tau and compared to a mutated form of tau that is unable to polymerize (*199*). The ΔK280 worms displayed much more aggregated tau as well as neuronal dysfunction when compared to the anti-aggregant tau, demonstrating the importance of aggregation to toxicity. This provides an example of utilizing multiple forms of tau in a model organism to answer a specific question about the toxicity of the protein and its aggregation.

1.9.3 Potential issues with model organisms

As demonstrated by the previous sections, there are many ways to generate animal models of tauopathies. These models can differ based on the presence of wild-type or mutant tau, the FTDP-17 mutation, which isoform is expressed, and what types of cells are expressing the tau gene. Evidence suggests that each of these factors may affect how, when, and where tau aggregates and what type of effect that aggregation will have on a particular cell or organism. Despite the possibility that these variables may be altering phenotypes in a manner that is not comparable to others, the models are often used interchangeably. This can complicate interpretation of results from different studies and can cloud some of the questions surrounding tauopathies. For example, the presence of NFTs was thought to be toxic to cells for many years until the creation of models that displayed toxicity without the large inclusion bodies cast doubt on this assumption. The answer to which species of tau is most toxic to neurons remains unresolved. The use of an FTDP-17 form of tau that forms one type of aggregate may not have the same effect as the use of another mutant that forms of a different type of aggregate. These differences between the two types of tau may affect the toxicity associated with a particular model and make answering these questions more difficult without knowing more about model-specific effects.

The choice of the isoform background is another aspect of generating models of tauopathies that may play a key role in the pathology associated with that particular model. Many studies have demonstrated that the tau isoforms have individual differences. For example, the 4R tau isoforms are more efficient at binding microtubules and aggregate more quickly than the 3R isoforms according to in vitro assays (*200, 201*). Similarly, the isoforms also interact differently

when together. Cross-seeding between 3R and 4R isoforms may not occur as efficiently as aggregation among like-types of tau (*202*), endogenous mouse tau can be incorporated into aggregates found in transgenic mice expressing one of the 4R human tau isoforms (*179*), and the presence of silent FTDP-17 tau mutations indicates that alteration of isoform expression levels is sufficient to induce tau aggregation in humans.

1.10 Thesis overview

Tauopathies are complex diseases and it is still not well known what initiates tau aggregation, why pathologies within this group of disorders are so varied, or what is the mechanism linking tau aggregation to its toxicity. Some of the difficulties involved in generating in vivo models of tauopathies have hampered efforts to find conclusive answers to these questions. First, it can be difficult to induce aggregation of the protein. This problem is typically solved by overexpressing modified versions of tau that can include FTDP-17 mutants or truncations. However, the mechanisms behind why these modified versions display increased aggregation are not well understood and it is possible that they do not correlate well to the behavior of wild-type tau in sporadic tauopathies. Second, it can be difficult to recapitulate certain aspects of human disease such as NFT or neuronal death. The pathologies of the various tauopathies are highly variable in humans and the current animal models can vary widely as well. The variability may arise in part from intrinsic differences within the types of tau used in the models. Elucidating differences between how the aggregation and function of tau are affected by these modifications can help explain the mechanisms of aggregation and its resulting toxicity. This information is relevant to understanding differences that exist in animal models of the disease as well as the progression of tauopathies in humans.

The studies described here were designed to characterize how the aggregation and functions of the tau protein are affected by isoform type or FTDP-17 mutation. They are part of a larger effort to use this information to examine how differences between these tau variants may be affecting pathology phenotypes and our interpretation of results from animal models of tauopathies. In addition, characterizing these differences will assist in elucidating the mechanisms of the initiation of tau aggregation as well as how it may be exerting its toxic effects. It is hoped that understanding these mechanisms will aid in the search for treatments of these diseases.

The study began with in vitro characterization of tau aggregation and function. One of the most obvious differences between normal tau and aggregated, disease-associated tau is the level of phosphorylation. Hyperphosphorylation of tau clearly affects its function and aggregation but that effect may not be the same for all six isoforms and could potentially affect the differential aggregation that is seen in some tauopathies. Seven pseudophosphorylation mutations were generated in each of the six isoforms. This combination of seven mutations was previously demonstrated to affect the conformation, aggregation, and function of tau in the 2N4R tau isoform. Through several assays designed to measure and characterize the aggregation of the protein, as well as its ability to stabilize microtubule polymerization, I determined differences in how the isoforms were affected.

Second, I examined how various FTDP-17 mutations affected tau. The in vitro polymerization of some mutated forms of tau had been characterized individually but a larger-scale direct

comparison had not been performed. A determination of mutation-specific effects could elucidate some of the initial causes of tau aggregation and demonstrate that changes to certain intrinsic properties of the protein can affect aggregate morphologies and potentially how the disease pathology progresses throughout the brain. These mutations are also often used interchangeably in animal models with little consideration about the potential intrinsic differences between the protein variants. These differences in how the mutations affect aggregation could explain the variable pathologies associated with FTDP-17 disorders and be applicable to sporadic tauopathies as well.

Finally, I began a project that expanded this work into a C. elegans system. Generating transgenic animals expressing various forms of tau is the first step in a larger project. The results from the in vitro biochemical assays will be used to determine how certain properties inherent in a particular variant of tau affect the disease pathology in an in vivo model. Differences in aggregate type or ability to interact with microtubules could be isolated and examined in similar organisms.

The main focus of research into tau-targeted therapeutics has focused on inhibitors of tau aggregation or phosphorylation under the assumption that large tau aggregates are toxic to the cells. However, some aggregation inhibitors may be preventing the formation of NFT by trapping the tau aggregates in a more toxic oligomeric state, potentially promoting disease progression rather than preventing it. Discovering the root causes of tau aggregation, how this aggregation is exerting its toxic effect, and what conditions lead to the differences in aggregate

morphology, isoform content, and location are some of the most pressing questions facing researchers today.

The use of in vitro techniques allows us to characterize the types of tau aggregates formed and what effects the modifications have on the function of the protein. The knowledge that is gained through these biochemical studies can then be applied to in vivo systems in order to examine the mechanisms of toxicity and explore potential differences between various animal models as a result of the type of tau expressed. Because we have an understanding of the types of aggregates that are formed by a particular FTDP-17 mutant and know how its interactions with microtubules are affected we can then design experiments to test how those aspects fit into toxicity of tau aggregation in an actual neuron. For example, one particular FTDP-17 mutation may induce smaller aggregates while another forms long fibers but both have no effect on microtubule interactions. Comparing these two tau variants in a similar animal background can provide evidence about the relative toxicities of the aggregates associated with each type of mutant and the driving forces behind this toxicity.

These studies demonstrate that similar pseudophosphorylation patterns do not induce the same effects on all isoforms and are sufficient to induce differential propensities for aggregation as well as morphological differences among the types of aggregates formed. FTDP-17 mutant versions of tau were very different from each other in the ways that they aggregated and stabilized polymerization of microtubules. The differences are likely to be an important factor in the progression of the familial frontotemporal dementias and may explain why the pathologies associated with the mutations are so widely varied. Finally, the type of tau expressed in

nematodes seems to alter the behavior, lifespan, and neuronal defects of the animals. This characterization of aggregation and function of various forms of tau is an important step toward elucidating the mechanisms of disease initiation and progression as well as how these differences may be affecting animal models of tauopathies.

Table 1.1 Known FTDP-17 Tau Missense Mutations

Missense Mutation	Location	Exon 10 Splicing Effect	Phenotype
R5H	Exon 1	No Change	FTDP-17
R5L	Exon 1	No Change	PSP-like
K257T	Exon 9, MTBR 1	No Change	PiD-like
I260V	Exon 9, MTBR 1	No Change	FTDP-17, 4R tau
L266V	Exon 9, MTBR 1	Decreased	PiD-like
G272V	Exon 9, MTBR 1	No Change	FTDP-17
G273R	Exon 9, MTBR 1	Unknown	No tau pathology?
N279K	Exon 10, IR 1-2	Increased	PSP-like
ΔK280	Exon 10, IR 1-2	Decreased	FTDP-17
N296H	Exon 10, IR 1-2	Increased	FTDP-17
ΔN296	Exon 10, MTBR 2	No Change	PSP-like
P301L	Exon 10, MTBR 2	No Change	FTDP-17
P301S	Exon 10, MTBR 2	No Change	CBD-like, FTDP-17
P301T	Exon 10, MTBR 2	Unknown	Unknown
G303V	Exon 10, MTBR 2	Increased	PSP-like
S305N	Exon 10, MTBR 2	Increased	CBD-like
L315R	Exon 11, IR 2-3	No Change	PiD-like
K317M	Exon 11, IR 2-3	No Change	PSP-like
S320F	Exon 11, IR 2-3	No Change	PiD-like
P332S	Exon 11, MTBR3	No Change	PiD-like/AD-like
G335V	Exon 11, MTBR3	Unknown	Unknown
G335S	Exon 11, MTBR3	No Change	FTDP-17?

Table 1.1 (Cont.)

Missense Mutation	Location	Exon 10 Splicing Effect	Phenotype
Q336R	Exon 12, MTBR3	No Change	PiD-like
V337M	Exon 12, MTBR3	No Change	FTDP-17
E342V	Exon 12, IR 3-4	Increased	PiD-like, FTDP-17
S352L	Exon 12, IR 3-4	No Change	Atypical
P364S	Exon 12, MTBR4	Unknown	Unknown
G366R	Exon 12, MTBR4	Unknown	Unknown
K369I	Exon 12	No Change	PiD-like
G389R	Exon 13	Increased/No N-terminal exons	PiD-like
R406W	Exon 13	No Change	PSP-like

Adapted from Alzforum.org and Cummings and Altman, 2005 (*181*).

Chapter II

Differential effects of pseudohyperphosphorylation on tau isoform aggregation and function

Chapter II Differential effects of pseudohyperphosphorylation on tau isoform aggregation and function

2.1 Abstract

The microtubule-associated protein tau exists as six isoforms created through the splicing of the second, third, and tenth exons. Hyperphosphorylated tau isoforms accumulate in insoluble aggregates in Alzheimer's disease and other tauopathies. These neurodegenerative diseases can be categorized based on the isoform content of the aggregates they contain. Hyperphosphorylated tau has the general characteristics of an upward electrophoretic shift, decreased microtubule binding, and an association with aggregation. Previously we have shown that a combination of seven pseudophosphorylation mutations at sites phosphorylated by GSK-3β, referred to as 7-Phos, induced several of these characteristics in full-length 2N4R tau and led to the formation of fewer but longer filaments. I sought to determine whether the same phosphorylation pattern could cause differential effects in the other tau isoforms, possibly through varied conformational effects. Using in vitro techniques, I examined the electrophoretic mobility, aggregation properties and microtubule stabilization of all isoforms and their pseudophosphorylated counterparts. I found that pseudophosphorylation affected each isoform but often inducing changes of varying magnitude or even completely opposite effects. Aggregation was inhibited for 3R isoforms but generally enhanced for 4R isoforms. Filament morphology was altered by generally increasing the length of the filaments that were formed in aggregation assays. Inclusion of N-terminal exons magnified inhibitory effects on the ability of tau to stabilize the assembly of microtubules. These results suggest that hyperphosphorylation pattern of tau could play a major role in determining the isoform composition of tau aggregates in disease and alter the downstream pathologies.

2.2 Introduction

The primary function of the tau protein is assisting in the assembly and stabilization of microtubules (*1*). The protein likely affects the spacing and localization of microtubules as well, a function that could be dependent on differences in length of the six isoforms. These isoforms are generated through alternative mRNA splicing of the second, third, and tenth exons (*203*). The second and third exons reside near the N-terminus of the protein and isoforms can be classified based on the presence or absence of these exons. If both exons are present the protein is referred to as 2N, if only the second exon is present it is known as 1N, and if neither is present it is classified as 0N. Exon 10 contains one of four microtubule-binding repeat regions (MTBR). If this exon is present in the isoform the protein is referred to as 4R and if it is absent the protein is classified as 3R (*204*).

In addition to affecting the spacing of microtubules, the various tau isoforms are involved in certain neurodegenerative diseases. In these disease states, tau dissociates from microtubules and aggregates inside of neurons, leading to neurodegeneration (*13, 205*). This group of disorders is collectively known as tauopathies. Tauopathies can be classified based on the isoform content and phosphorylation pattern found in tau aggregates (*205*). While aggregates from Class I tauopathies contain all six isoforms, Class II aggregates are characterized by a larger ratio of 4R to 3R tau, and Class III tauopathies are associated with aggregates containing mostly 3R isoforms. The Class III tauopathies are also characterized by a lack of phosphorylation at the 262 and 356 serine residues (*92, 206*). Aggregates from the fourth class of tauopathies typically contain only 0N isoforms (*205*). The various tauopathies can give rise to vastly different pathological effects and the changes in isoform content seen in the aggregates

could play a role in affecting these variations. While the root causes of differential isoform inclusion into pathological aggregates are unknown, it is possible that phosphorylation of the isoforms could differently alter their function and activity sufficiently to contribute to this phenomenon.

Several links between phosphorylation of tau and the pathology of Alzheimer's disease (AD) and other tauopathies have been described. A potential important factor is the increase in hyperphosphorylated tau found in AD-affected brains. Hyperphosphorylated tau can be identified by an upward electrophoretic mobility shift, even in the presence of SDS, and a decreased ability to stabilize microtubule assembly (*122, 207*). It is probable that several kinases and phosphatases are involved in generating hyperphosphorylated tau, but one kinase likely to be involved is glycogen synthase kinase 3β (GSK-3β) due to its association with the formation of neurofibrillary tangles and paired-helical filaments found in AD (*208-210*). In addition, several sites commonly found to be phosphorylated in pathogenic tau are known to be phosphorylated by GSK-3β (*128, 139*).

While the general effects of kinases are known, it can be difficult to study phosphorylation at specific sites in order to determine the effects they can have on the function and in vitro aggregation of the protein because it is nearly impossible to control the level and specific location of kinase activity on tau due to the large number of phosphorylation sites and the relative promiscuity of kinases toward tau (*127, 129, 211, 212*). This can complicate collection and interpretation of data. One method used to circumvent this issue is to utilize site-directed mutagenesis to create pseudophosphorylation mutants by changing a serine or threonine to an

aspartic acid or glutamic acid in order to mimic the size and the shape of a phosphate molecule (*146, 147*). Although the effects of pseudophosphorylation may not completely replicate the effects of actual phosphorylation events, the technique has previously been utilized effectively to examine conformational changes in the protein and behavioral effects that may arise from these changes (*54, 151, 156, 157, 160, 162, 213*).

A combination of pseudophosphorylation mutations, referred to as 7-Phos for the seven specific sites mutated, were previously created in 2N4R full-length tau (*160*). The 7-Phos mutation alters the following residues, numbered according to their position in 2N4R tau: S199E, S202E, T205E, T231E, S235D, S396E, and S404E. Five of these sites are phosphorylated by GSK-3β when the kinase is incubated in vitro with arachidonic acid-induced pre-polymerized tau and the S202 and S235 sites are often phosphorylated in conjunction with the S199 and T231 sites (*160, 208*). All of the selected sites are phosphorylated at elevated levels in AD and the combination of these mutations replicated several aspects of pathogenic tau (*212*). The 7-Phos mutations, in 2N4R tau, were shown to induce an electrophoretic mobility shift similar to that of the hyperphosphorylated protein seen in AD. Additionally, the 7-Phos mutation caused a decrease in the 2N4R tau isoform's affinity for microtubules and inducer-initiated nucleation of tau polymerization (*160*).

As described above, the pathology of tauopathies can vary based on the isoform content of their aggregates and tau phosphorylation patterns differ between the four classes of the diseases as well. The six isoforms have differences in their primary structures which could place the same phosphorylation sites in different structural contexts. Therefore, phosphorylation at the same

sites, but in different isoforms, could have widely varied effects on their conformation. These conformational changes could be sufficient to cause some isoforms to dissociate from microtubules and aggregate while others maintain their normal function, as seen in some tauopathy classes.

In this study I demonstrate that the 7-Phos mutation does affect the isoforms differently. The SDS-resistant upward shift in electrophoretic mobility was present in all isoforms but differed in magnitude. The mutation enhanced the polymerization of isoforms such as 0N4R while greatly inhibiting the aggregation of the 3R isoforms. The mutation also decreased the microtubule stabilization function of all isoforms but affected 0N4R less than the other five. These results suggest that phosphorylation patterns generated by the same set of kinases or phosphatases could be sufficient to increase the propensity of some isoforms to aggregate while reducing the aggregation of others, resulting in the differential isoform inclusion in pathological tau aggregates.

2.3 Experimental Procedures

2.3.1 Protein purification and site-directed mutagenesis. All wild-type and pseudophosphorylated mutant proteins were expressed and purified as described previously (*150*). The pT7C-tau plasmids were transformed into BL21 *E. coli* and grown in 1800 mL Luria Broth (LB) + ampicillin until an OD_{600} of 0.7-0.8 is reached. Protein translation is induced by adding IPTG to 1 mM. The cells are centrifuged and resuspended in buffer (500 nM NaCl, 10 mM Tris pH 8, 5 mM imidazole, and protease inhibitors) before being lysed with a French Press. Purification occurs by using an Acta fast protein liquid chromatography system. The protein is

tagged with a 6x-histidine tag that binds to nickel when passed through an affinity column before being released in Elution Buffer (500 mM NaCl, 10 mM Tris base pH 8, and 250 mM imidazole). The protein is then further purified by running it through a size-exclusion column in Sup200 Buffer (250 mM NaCl, 10 mM Hepes pH 7.64, and 0.1 mM EGTA, 0.1 mM DTT). The protein is aliquoted and frozen at -80°C before use. The mutations were made utilizing the Quikchange site-directed mutagenesis kit from Stratagene (La Jolla, CA). The following mutations were made in each of the 6 isoforms in order to create the "7-Phos" mutants: S199E, S202E, T205E, T231E, S235D, S396E, and S404E. Polymerization was induced using arachidonic acid (ARA) from Cayman Chemicals (Ann Arbor, MI).

2.3.2 SDS-PAGE. Each protein sample was incubated in buffer containing 2% SDS and 1% β-mercaptoethanol and then boiled for five minutes. One μg of each protein was loaded onto a 10% SDS-PAGE and resolved through electrophoresis. The urea-denatured protein samples were incubated in buffer containing 2% SDS, 1% β-mercaptoethanol, and 6 M urea (*160*). The protein samples were resolved on a 10% SDS-PAGE with 6 M urea and stained with Coomassie Brilliant Blue R-250.

2.3.3 ARA-induced Polymerization. Recombinant tau protein was incubated in polymerization buffer containing 10 mM HEPES (pH 7.64), 5 mM DTT, 100 mM NaCl, 0.1 mM EDTA, and 3.75% ethanol. Arachidonic acid was used as an inducer of tau polymerization. The effects of altering protein or ARA levels were found by varying final protein concentration from 0 to 4 μM with 75 μM ARA or varying the final ARA concentration from 0 to 150 μM with 2 μM protein (*209*). Based on these results a combination of 2 μM protein and 75 μM ARA were used in

subsequent experiments in order to approach maximum polymerization for each tau isoform and its corresponding 7-Phos mutant.

2.3.4 Thioflavin S fluorescence. Polymerization was measured by utilizing staining with thioflavin S (ThS) from Sigma-Aldrich (St. Louis, MO). Polymerization reactions were incubated for 18 hours at 25 °C. ThS was then added to the reactions in 96-well plates to a final concentration of 20 μM. The shift in fluorescence was measured with an excitation wavelength of 440 nm and an emission wavelength of 520 nm using a Cary Eclipse Fluorescence Spectrophotometer (Varian Analytical Instruments, Walnut Valley, CA). The PMT voltage was set to 650 V but the procedure was otherwise performed as described earlier (*150*).

2.3.5 Right-angle Laser Light Scattering. Polymerization reactions were transferred to 5 mm x 5 mm optical glass fluorometer cuvettes (Starna Cells, Atascadero, CA). The cuvettes were placed in the path of a 12 mW solid state laser at $\lambda = 532$ nm and operating at 7.6 mW (B&W Tek, Inc., Newark, DE). The level of polymerization was measured by capturing images of light scattered perpendicular to the beam using a SONY XC-ST270 digital camera. The images were captured at an aperture setting of f5.6-8. The intensities of the images were quantified using Adobe Photoshop CS5 version 12.0.1 (*214, 215*).

2.3.6 ARA-Induced Polymerization Kinetics. Polymerization reactions with 2 μM protein and 75 μM ARA, at the same reaction conditions described earlier, were mixed in 5 mm x 5 mm optical glass fluorometer cuvettes. Polymerization was measured at regular time intervals through right-angle laser light scattering (LLS) until an apparent steady-state was reached (*160*).

2.3.7 Transmission Electron Microscopy. The polymerization reaction samples were diluted 1:10 in polymerization buffer with glutaraldehyde added to a final concentration of 2%. After the five minute fixation with glutaraldehyde, 10 μL of each sample was added to a formvar carbon-coated grid for one minute. The grid was blotted on filter paper, washed with water, blotted, washed with 2% uranyl acetate, and blotted dry again. The grid was then stained with 2% uranyl acetate for one minute and blotted dry on the filter paper again. The grids were examined with a TECNAI G^2 20 electron microscope (FEI Co., Hillsboro, OR) and images were taken with the Gatan Digital Micrograph imaging system. The images were collected at a magnification of 3600X. The filament numbers and areas were quantified through the use of Image-Pro Plus 6.0 (*160*).

2.3.8 Tubulin Polymerization Assay. Polymerization of tubulin was measured by utilizing the Tubulin Polymerization Assay kit from Cytoskeleton, Inc. (Denver, CO). The reactions were measured in 96-well Costar black polystyrene flat-bottom plates (Corning, Inc., Corning, NY). Each well contained GTP at 1 mM and tubulin at 2 mg/mL in an 80 mM PIPES buffer (pH 6.9) with 2 mM $MgCl_2$ and 0.5 mM EGTA. Each of the wild-type or 7-Phos isoforms was added to a different well at a final concentration of 1 μM. Another well contained 1 μM paclitaxel in order to act as a positive control for polymerization and as a standard for normalizing the results for each of the other reactions. The two negative control reactions contained tubulin with no additional compound added. Upon addition of the protein or control reagent to the other wells, the plate was placed at 37 °C and shaken for 5 seconds in a FlexStation II Fluorometer (Molecular Devices Corporation, Sunnyvale, CA). The fluorescence was measured every minute

for one hour with a λ_{ex} of 355 nm and a λ_{em} of 455 nm. The resulting data were fit to the Gompertz equation

$y = ae^{-e^{-\frac{t-t_i}{b}}}$ as described in (*160*). The maximum amount of polymerization is found as *a*, the time from the initiation of the reaction to when polymerization is measured, or lag time, is calculated as $t_i - b$, and k_{app} is equal to *1/b* and proportional to the maximum rate of polymerization. These parameters were used to describe the characteristics of the polymerization curve.

2.4 Results

2.4.1 Generation of 7-Phos Mutants for All Tau Isoforms

Pseudophosphorylation mutants were generated in all six tau isoforms by making S199E, S202E, T205E, T231E, S235D, S396E, and S404E mutations (Figure 2.1A). The mutants were analyzed by SDS-PAGE and found to exhibit an upward mobility shift as had been previously described for the 2N4R isoform (*160*). All 7-Phos isoforms displayed a decrease in electrophoretic mobility when compared to their corresponding wild-type protein (Figure 2.1B). However, upon addition of 6 M urea, the upward mobility shift in the 7-Phos proteins was still present but largely decreased for all isoforms (Figure 2.1C). The electrophoretic shifts, in the absence of urea, were similar for all isoforms but slightly increased with the presence of additional N-terminal exons (Figure 2.1D). Because the wild-type and 7-Phos proteins have more similar migration distances in the presence of 6 M urea, but not in its absence, it is likely that the 7-Phos mutations are inducing an SDS-resistant conformational change in the proteins that can be interrupted with urea. This pseudophosphorylation-induced conformational change is the cause

Figure 2.1

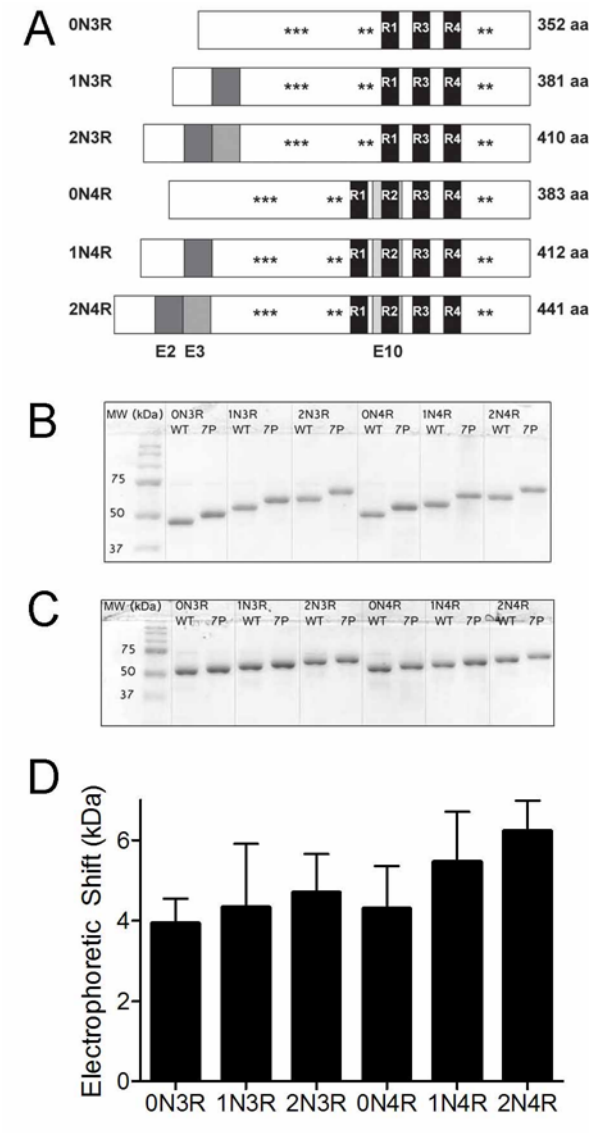

Figure 2.1. 7-Phos induces an SDS-resistant electrophoretic shift in all tau isoforms. (A) Six isoforms of tau are created through alternative mRNA splicing of the second, third and tenth exons. The latter contains the second of four microtubule-binding regions. Pseudophosphorylation mutations were made at seven sites commonly phosphorylated in Alzheimer's disease. This combination of mutations is referred to as 7-Phos. (B) 1 µg of the wild-type and 7-Phos variants for each of the six isoforms separated via 10% SDS-PAGE. MW refers to the molecular weight markers. The isoforms are labeled above the lanes with WT indicating wild-type protein and 7P indicating 7-Phos protein for each isoform. (C) The same amount of protein loaded onto a 10% SDS-PAGE with 6 M urea. (D) The mean values of the electrophoretic shifts (y-axis, in kDa) for each isoform (labeled below x-axis) separated via 10% SDS-PAGE. These values were calculated by subtracting the apparent molecular weight of wild-

type isoforms from the apparent molecular weight of the corresponding 7-Phos isoforms. Bars represent the mean shift from three gels with the standard deviation.

of the slowed electrophoretic migration and is similar to the retardation evident in hyperphosphorylated tau associated with disease.

2.4.2 Pseudohyperphosphorylation differentially affects ARA-induced polymerization of isoforms

In vitro experiments were performed to determine the effects of the 7-Phos mutation on the ARA-induced polymerization of the six isoforms. The concentration of the inducer was held constant and the protein concentration varied from 0-4 μM. The amount of polymerization generally increased with increases in protein concentration (Figures 2.2 and 2.3). The 7-Phos mutants containing only three MTBRs, or 3R isoforms, polymerized less than their corresponding wild-type 3R isoforms when measured by ThS staining (Figure 2.2A-C) and right-angle LLS (Figure 2.3A-C). In contrast, the 1N4R and 2N4R 7-Phos isoforms polymerized more similarly to their corresponding 1N4R and 2N4R wild-type proteins (Figures 2.2E-F and 2.3E-F) as compared to the 3R isoforms (compare Figures 2.2A-C, E-F and 2.3A-C, E-F). Unlike any of the other isoforms, the 0N4R 7-Phos protein polymerized more than its corresponding wild-type for most protein concentrations (Figures 2.2D and 2.3D).

To determine whether the 7-Phos modification altered the response to different concentrations of the inducer, the protein concentration was held constant and the concentration of inducer was varied from 0 μM to 150 μM. Data of this nature generally has a biphasic shape, with increasing polymerization up to a maximum level as the inducer concentration increases. After this maximum of polymerization is reached, any further addition of inducer decreases the amount of polymerization compared to the peak. The biphasic nature of inducer-mediated tau

Figure 2.2

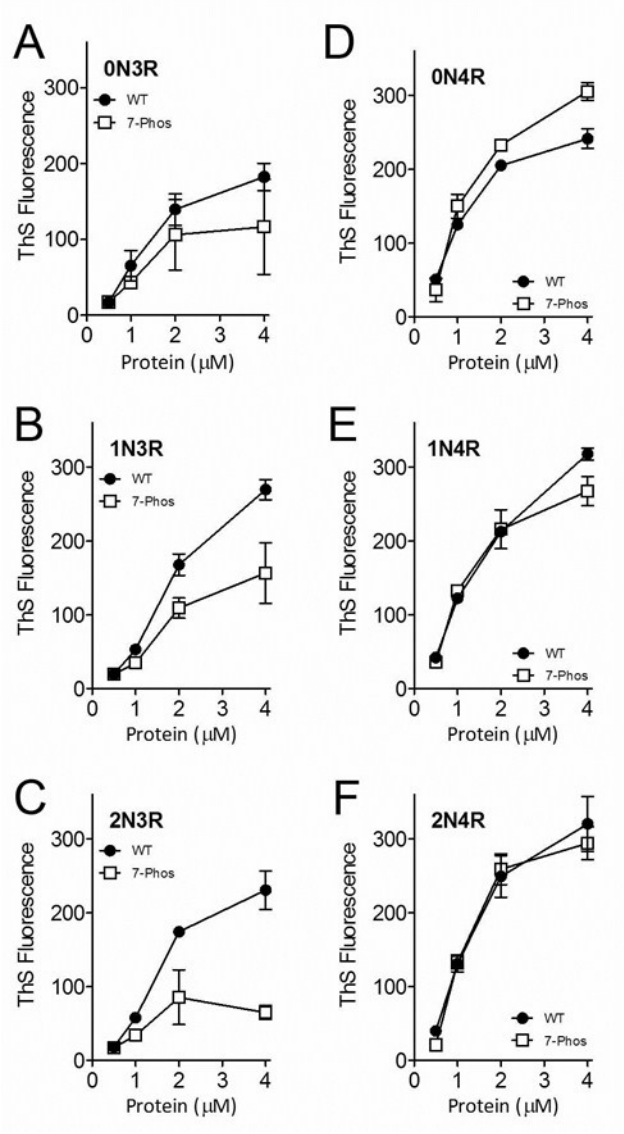

Figure 2.2. **Polymerization of varied tau concentrations measured by thioflavin S staining**. Wild-type (closed circles •) and 7-Phos tau isoforms (open squares □) polymerization reactions with 0 to 4 μM protein (x-axis) and 75 μM arachidonic acid were measured by thioflavin S fluorescence (y-axis) after 18 hours incubation at 25 °C. Individual graphs are shown for (A) 0N3R, (B) 1N3R, (C) 2N3R, (D) 0N4R, (E) 1N4R, and (F) 2N4R isoforms. Bars represent the mean from 3 experiments ± standard deviation.

Figure 2.3

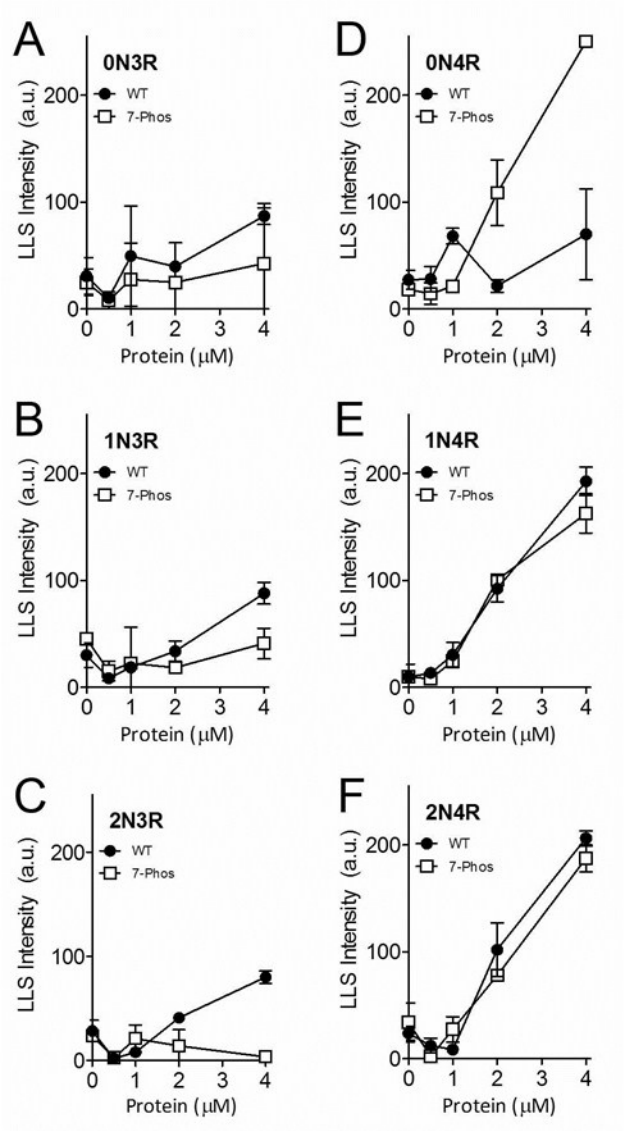

Figure 2.3. Polymerization of varied tau concentrations measured by right-angle laser light scattering. Wild-type (closed circles •) and 7-Phos tau isoform (open squares □) polymerization reactions with 0 to 4 μM protein (x-axis) and 75 μM arachidonic acid were measured by intensity of right-angle laser light scattering (y-axis) after 18 hours incubation at 25 °C. Individual graphs are shown for (A) 0N3R, (B) 1N3R, (C) 2N3R, (D) 0N4R, (E) 1N4R, and (F) 2N4R isoforms. Data are the mean from 3 experiments and bars represent ± s.d.

polymerization has been previously reported (*209, 216*). The polymerization for each of the 3R 7-Phos isoforms was lower than their corresponding non-modified 3R proteins, as measured by ThS staining (Figure 2.4A-C). Additionally, the 3R 7-Phos isoforms required a higher inducer concentration to reach maximum polymerization than the 3R wild-type isoforms. When the polymerization was measured by LLS, very little polymerization was detected for any of the 3R 7-Phos isoforms while the wild-type 3R isoforms also displayed the biphasic curve but with a sharp increase at the highest inducer concentrations (Figure 2.5A-C). Because these increases in light scattering, primarily seen at the 150 μM ARA concentration, are not replicated when measured by ThS staining (Figure 2.4A-F) or transmission electron microscopy (data not shown) they are likely due to formation of ARA micelles and not increased tau polymerization. Additionally, in Figures 2.4 and 2.5, the ARA to protein ratio has greatly been altered which has been shown to affect ThS and LLS readings differently (*209*).

The polymerization of 0N4R 7-Phos was greater than its corresponding wild-type at the higher inducer concentrations tested when measured by ThS fluorescence (Figure 2.4D). However, the LLS measurements indicated that polymerization of the 0N4R 7-Phos isoform was greater than that of the 0N4R wild-type isoform at 50 and 100 μM ARA but less than wild-type at the higher concentrations tested. The polymerization curves for 1N4R and 2N4R wild-type and 7-Phos variants were more similar to one another than what was observed for the other isoforms (Figure 2.4E-F and Figure 2.5E-F).

Any discrepancies between ThS staining and LLS readings could be due to subtle differences in how measurements from the two methods are affected by changes in length or other

Figure 2.4

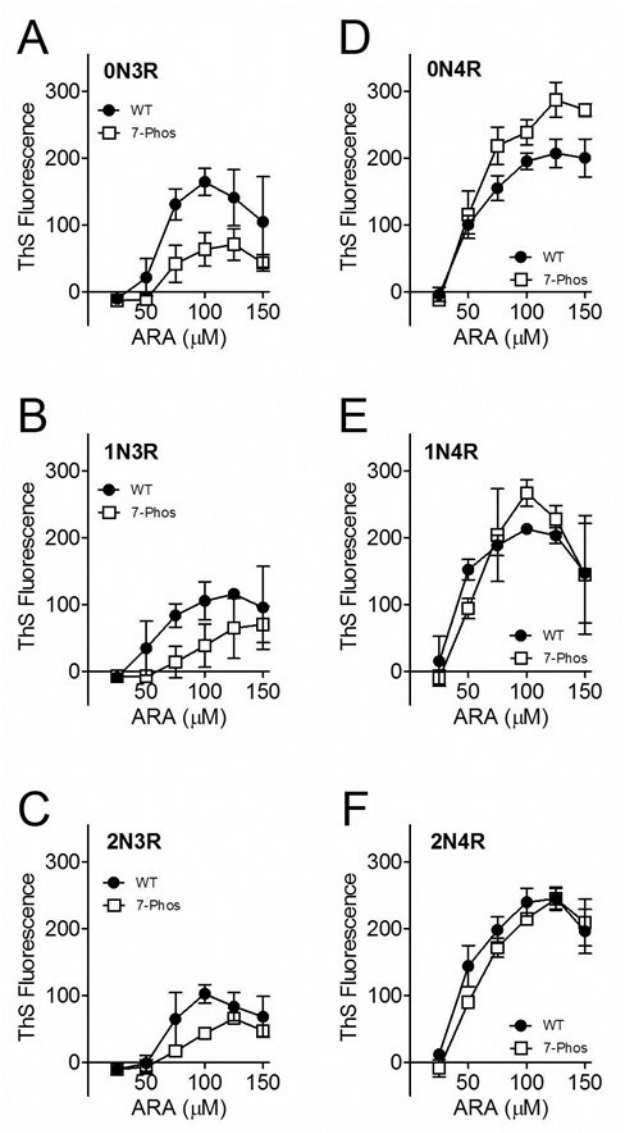

Figure 2.4. Polymerization of 2 μM tau with 0 to 150 μM ARA measured by thioflavin S fluorescence. Wild-type (closed circles •) and 7-Phos tau isoform (open squares □) polymerization reactions with 2 μM protein and 0 to 150 μM arachidonic acid (x-axis) were measured by thioflavin S fluorescence (y-axis) after 18 hours incubation at 25 ˚C. The fluorescence value of the 0 μM ARA reaction was subtracted from the other values. Individual graphs are shown for (A) 0N3R, (B) 1N3R, (C) 2N3R, (D) 0N4R, (E) 1N4R, and (F) 2N4R isoforms. Bars represent ± s.d. from 3 experiments.

Figure 2.5

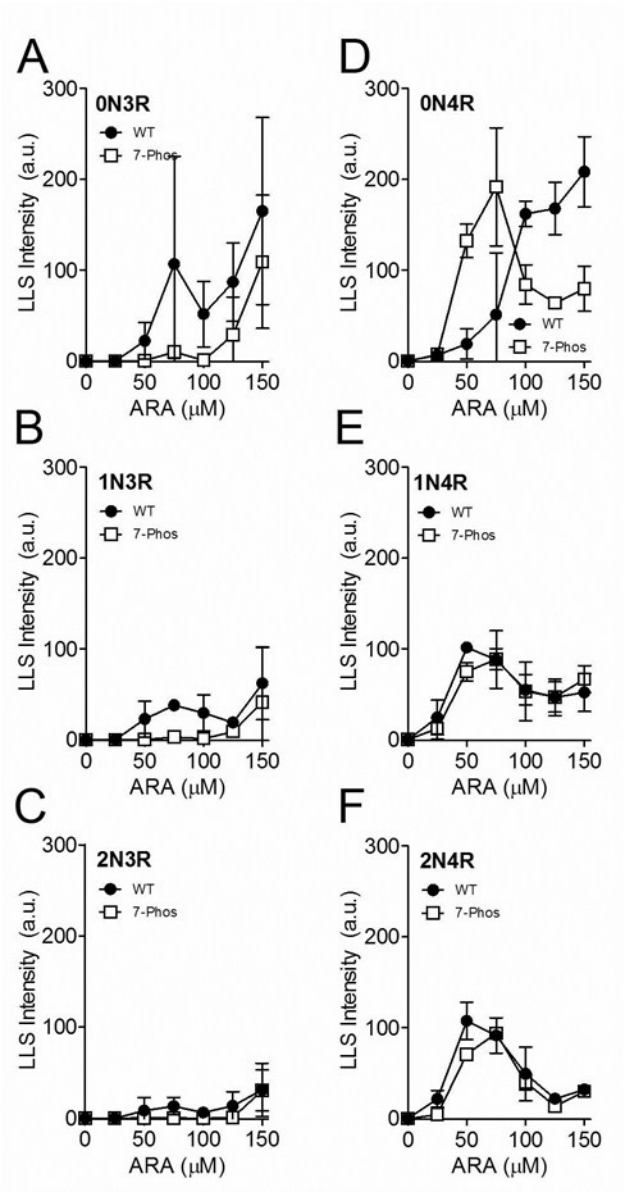

Figure 2.5. Polymerization of 2 μM tau induced with varied ARA concentration (0 μM to 150 μM) measured by right-angle laser light scattering. Wild-type (closed circles •) and 7-Phos tau isoform (open squares □) polymerization reactions with 2 μM protein (x-axis) and 0 to 75 μM arachidonic acid were measured by intensity of right-angle laser light scattering (y-axis) after 18 hours incubation at 25 ˚C. Individual graphs are shown for (A) 0N3R, (B) 1N3R, (C) 2N3R, (D) 0N4R, (E) 1N4R, and (F) 2N4R isoforms. Bars represent ± s.d. from 3 experiments.

morphological characteristics in the population of filaments (*209, 217-219*). Fewer, but longer, filaments may decrease the amount of light scattered but could have little change in ThS binding if the total amount of polymerization is similar. In addition, changes in morphology, such as a change in the β-sheet structure or the formation of straight filaments rather than paired helical filaments, could also affect the affinity of ThS binding. Factors other than morphology changes, such as the formation of ARA micelles, could also have an effect on LLS values. Because of these challenges I believe that utilizing both methods, as well as transmission electron microscopy, will give a clearer picture of alterations in the polymerization ability of these tau variants.

Visual inspection of the above curves revealed that most proteins at 2 μM concentration had a peak in polymerization either at or close to 75 μM ARA. As these polymerization conditions are routinely used for in vitro tau polymerization reactions, they were chosen for further analysis of the effects of the 7-Phos modification on the tau isoforms (*160, 173, 220*). The amounts of polymerization were determined after 18 hour incubation under these reaction conditions. The amounts of 7-Phos protein polymerization were normalized to their corresponding wild-type values to obtain a percent change from wild-type (Figure 2.6A and 2.6B). The 7-Phos pseudohyperphosphorylation mutation affected the 3R isoforms differently than it affected the 4R isoforms. The three 3R isoforms all showed a decrease in polymerization measured by ThS staining (Figure 2.6A) and a greater than 50% decrease in polymerization measured by LLS intensity (Figure 2.6B). In contrast, the 4R isoforms all had increased polymerization levels with the 7-Phos mutation according to ThS fluorescence (Figure 2.6A) and an increase or very little change in LLS values (Figure 2.6B).

Figure 2.6

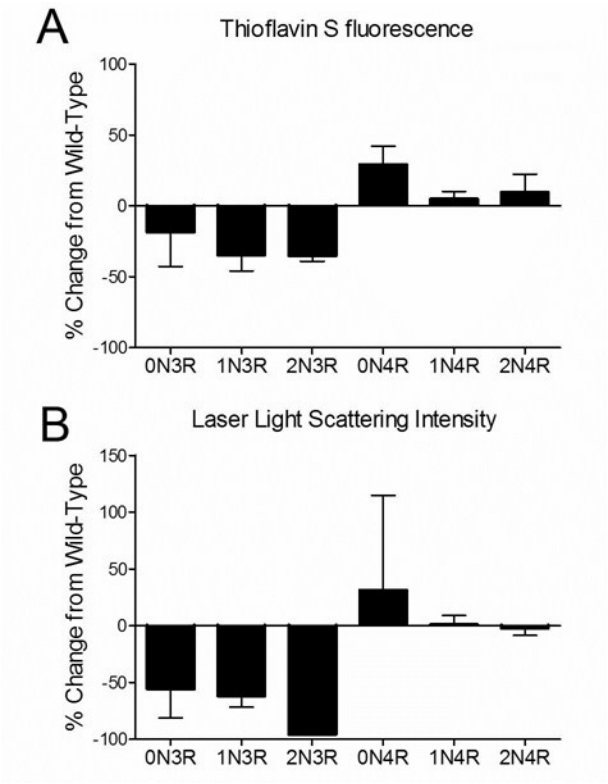

Figure 2.6. Percent change in polymerization of 2 µM 7-Phos protein and 75 µM ARA polymerization reactions as compared to wild-type protein. Polymerization reactions were prepared with 2 µM tau and 75 µM ARA and incubated for 18 hours at 25 °C. Polymerization was measured by (A) ThS fluorescence and (B) right-angle laser light scattering as described earlier. Results for each isoform are labeled on X-axis. Bars represent the average from 3 experiments ± s.d.

2.4.3 Pseudohyperphosphorylation affects the number and the morphology of tau filaments differently among the six isoforms

Samples of polymerization reactions under near optimal conditions (Figure 2.6) were examined by transmission electron microscopy to determine whether the 7-Phos mutation affected filament morphology (Figure 2.7). The mutation had varying effects on both the morphology and number of filaments present, although no changes were apparent in filament width or structure at higher magnification (data not shown). In general, filaments for the 7-Phos proteins were fewer in number, larger in size, and formed similar or less total mass of filaments (Figure 2.8). The exceptions were 0N4R 7-Phos (more filaments, more total mass) (Figure 2.8A and 2.8C), and 2N3R (shorter filaments) (Figure 2.8B). It should be mentioned that part of the effect seen on the number and morphology of 0N4R tau filaments is likely due to uneven distribution of wild type filaments, which is lessened by GSK-3β phosphorylation and is therefore likely to be decreased for 7-Phos 0N4R (*33*).

2.4.4 7-Phos affects the kinetics of polymerization

Polymerization reactions were monitored by LLS over time to measure the kinetics of polymerization. Wild-type 3R isoforms had very long lag times before polymerization was detected (Figure 2.9A-C), while the 4R isoforms had shorter lag times and reached maximum polymerization within approximately 80 minutes (Figure 2.9D-F).

The maximum amount of polymerization was greatly decreased for the 3R 7-Phos isoforms compared to their wild-type counterparts (Figure 2.9A-C). As expected, very little polymerization was detected for the 3R 7-Phos isoforms by LLS and the data could not be fit to a

Figure 2.7

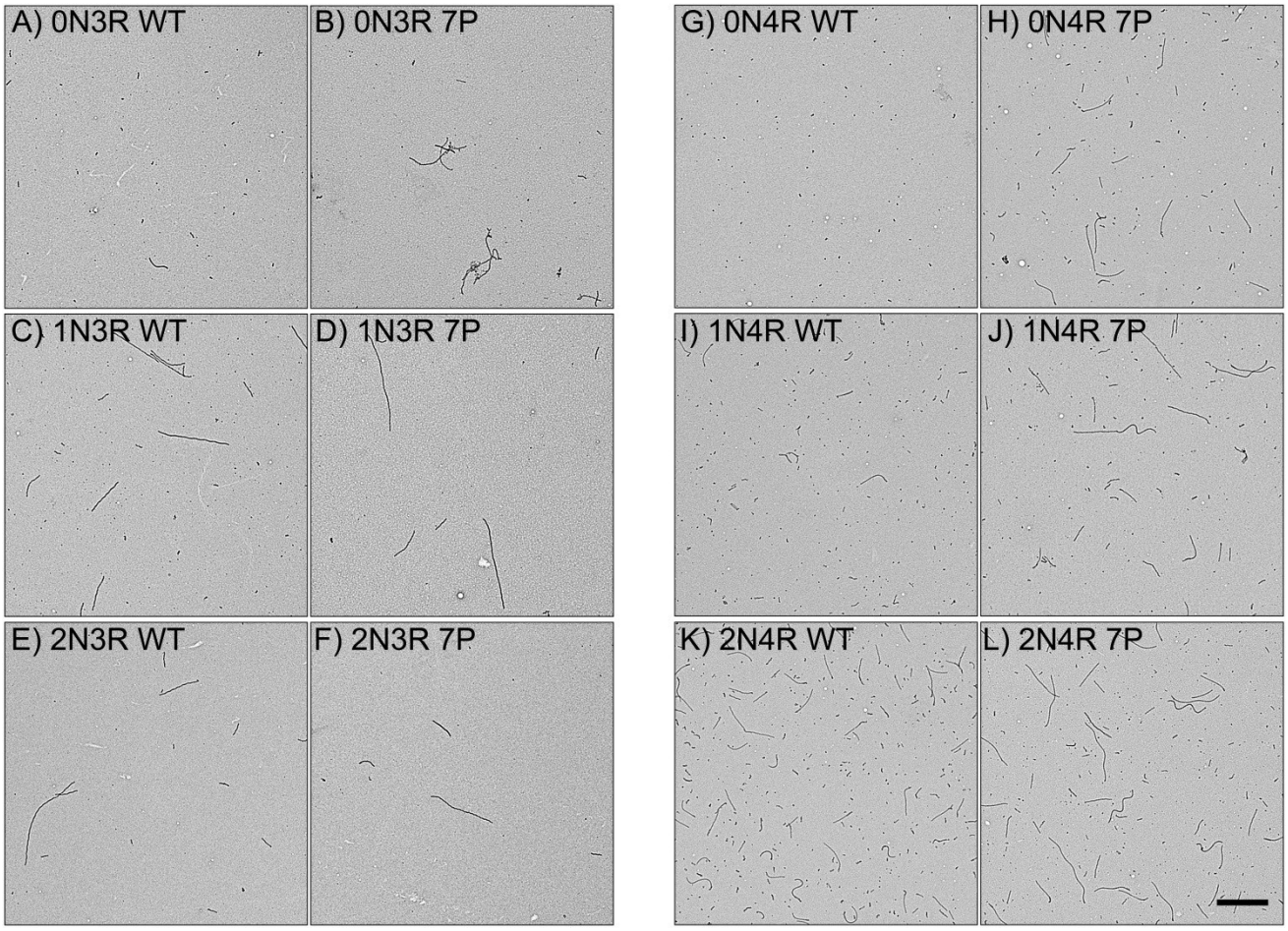

Figure 2.7. Electron Micrographs of 2 µM protein and 75 µM ARA polymerization reactions. Representative electron micrographs of polymerization reactions of wild-type isoforms (left): (A) 0N3R, (C) 1N3R, (E) 2N3R, (G) 0N4R, (I) 1N4R, and (K) 2N4R; and corresponding 7-Phos isoforms (right): (B) 0N3R, (D) 1N3R, (F) 2N3R, (H) 0N4R, (J) 1N4R, and (L) 2N4R. The images were taken at a magnification of 3600x and the scale bar in (L) represent 1 µm and applies to all images.

Figure 2.8

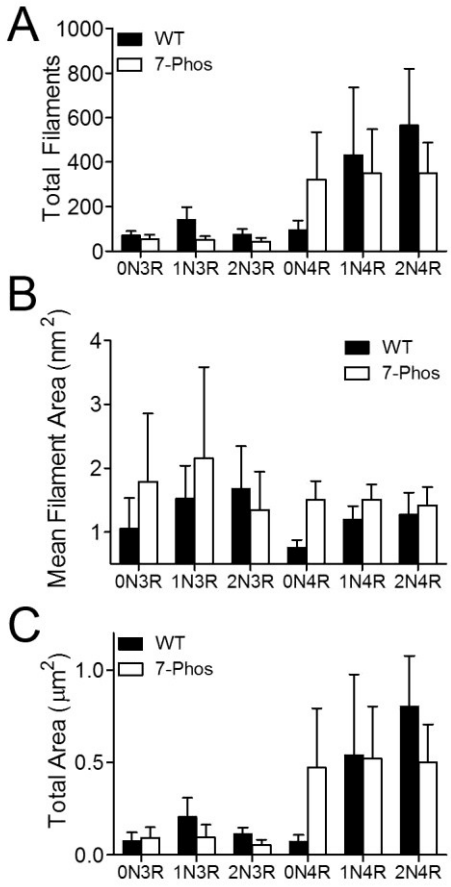

Figure 2.8. Quantitation of filaments from transmission electron micrographs. Quantitation of transmission electron micrographs from Figure 7 were performed as described in Materials and Methods. Values for (A) total number of filaments, (B) average filament length (μm), and (C) total length (number x average length) are shown for wild-type (black bars) and 7-Phos (white bars) for each isoform (labeled on x-axis). Data represent average values from 3 separate experiments ± s.d.

Figure 2.9

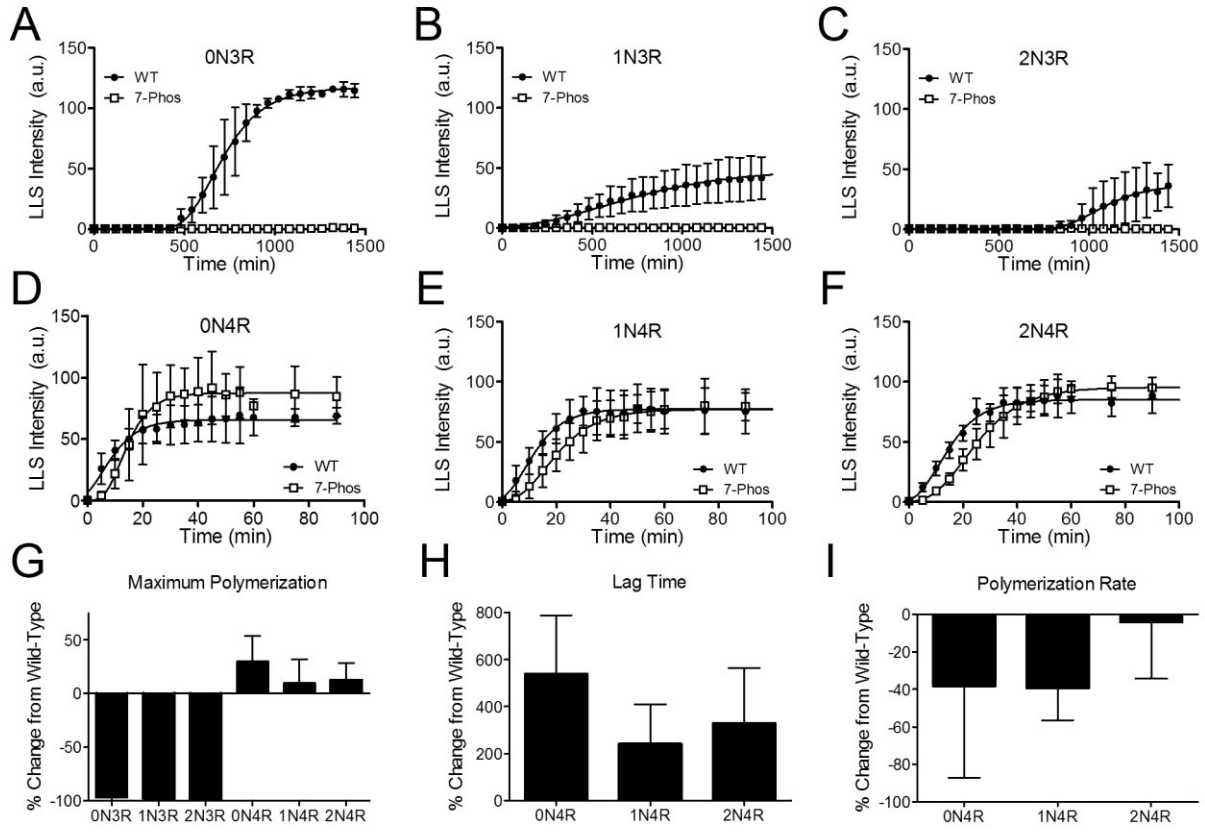

Figure 2.9. Kinetics of tau polymerization. Polymerization reactions were monitored by right-angle laser light scattering (arbitrary units, y-axis) at specific time points (minutes, x-axis) until the amount of polymerization approached an apparent steady-state. The experiment was repeated three times for the wild-type (closed circles •) and 7-Phos (open squares □) of (A) 0N3R, (B) 1N3R, (C) 2N3R, (D) 0N4R, (E) 1N4R, and (F) 2N4R. The equations were fit to the Gompertz equation and (G) the maximum amount of polymerization, (H) the lag time, and (I) the polymerization rate (k_{app}) for each was calculated. Isoforms are labeled on the x-axis. Data is shown as normalized values to the amount of wild-type polymerization (percent change from wild-type) for three separate trials. Error bars represent the s.d. from 3 experiments. Data is not included for the 3R isoforms in (H) and (I) because the data could not be satisfactorily fit to the kinetics equation.

kinetics equation (see Figure 2.5A-C). In contrast, the maximum amount of polymerization for the 4R 7-Phos isoforms were similar to or increased over their wild-type versions (Figure 2.9G) although their lag times before significant polymerization were longer (Figure 2.9H). The rate of polymerization was also slower (Figure 2.9I).

2.4.5 The ability of the protein to stabilize tubulin polymerization is affected by pseudohyperphosphorylation mutations

One of the normal functions of tau is the stabilization of microtubule assembly (*1, 31, 221, 222*). Phosphorylation of the protein can decrease its affinity for microtubules as well as its ability to induce the polymerization of tubulin dimers into microtubules (*142, 223-225*). An in vitro microtubule polymerization assay was used to measure the effect of the 7-Phos pseudohyperphosphorylation mutation on the ability of each isoform to stabilize tubulin polymerization (Figure 2.10A-F).

The 7-Phos mutation inhibited the ability of all six tau isoforms to stabilize the polymerization of tubulin. The rates of tubulin polymerization were decreased (Figure 2.10G), the lag times required to initiate microtubule polymerization were increased (Figure 2.10H), and the amounts of overall tubulin polymerization were reduced (Figure 2.10I). Of these, 7-Phos 0N4R seemed to be the least affected in all aspects.

Figure 2.10

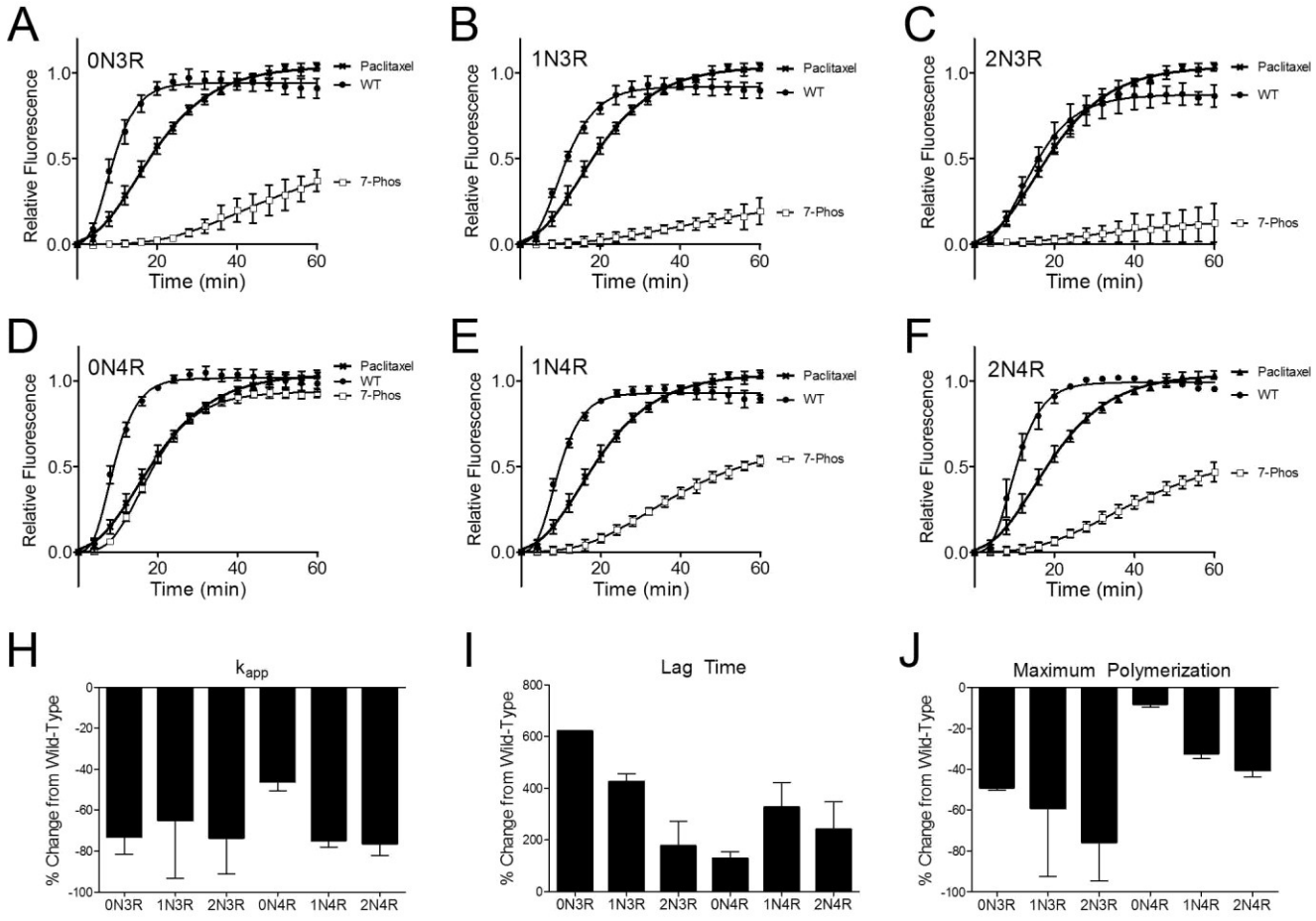

Figure 2.10. Tau isoform stabilization of microtubule polymerization. The ability of wild-type (•) and 7-Phos (□) tau isoforms to stabilize the polymerization of tubulin into microtubules was measured using a fluorescence assay. The relative fluorescence units (y-axis) are plotted against time (x-axis) for (A) 0N3R, (B) 1N3R, (C) 2N3R, (D) 0N4R, (E) 1N4R, and (F) 2N4R. Data points represent 3 separate trials ± s.d. The data was normalized to paclitaxel controls (crosshatches) that were performed in addition to tau reactions. Tau/tubulin reactions did not contain paclitaxel. Kinetics parameters were calculated from each of the three trials and the means of the percent change from wild-type with the addition of 7-Phos for (G) the k_{app}, or polymerization rate, (H) lag time, or the time from initiation of the reaction until polymerization is detected, and (I) the maximum polymerization after 60 minutes are shown ± s.d.

2.5 Discussion

The major common feature among neurodegenerative tauopathies is the polymerization of the tau protein into filamentous aggregates. While these aggregates are present in all tauopathies, the diseases can differ in the combination of tau isoforms included. The various combinations of isoforms present within the tangles can be used to classify the neurodegenerative tauopathies (*205*), indicating aggregation selectivity of certain isoforms in particular tauopathies. The causes of selective aggregation of tau isoforms are unknown but it is possible that phosphorylation plays an important role.

Phosphorylation of tau has long been associated with aggregation of tau in neurodegenerative tauopathies. The pathological tau found in neurofibrillary tangles is often hyperphosphorylated (*67, 123*). Kinases, such as GSK-3β, may display increased activity in Alzheimer's disease (*226*) and are associated with neurofibrillary tangles (*132*). In addition, the activities of phosphatases, such as PP2A, are decreased in many tauopathies (*227, 228*). The phosphorylation of tau can have profound effects on its conformation. Although tau typically exists as a natively unfolded protein, it has been shown to adopt a global hairpin conformation with the N- and C-termini folding over to interact with its MTBR (*54*). Pseudophosphorylation at certain sites can affect the compaction of the protein (*157, 229*). Because the isoforms of tau differ from each other by up to 89 amino acids (20-25%), it is reasonable that similar levels or similar patterns of phosphorylation could have significantly different effects on the isoform conformations and functions.

Pseudophosphorylation can provide a useful way to explore the effects of site-specific phosphorylation on the conformation and function of a protein. However, I also recognize that it may not exactly replicate an actual phosphorylation event and all of its effects. While limitations exist and caution should be used in interpreting implications of the results, pseudophosphorylation can be a valuable tool to explore site-specific effects of phosphorylation and, indeed, has been used in multiple in vitro and cell culture studies of tau (*147, 154, 229, 230*).

In one such study, it has previously been reported that pseudophosphorylation mutations at seven sites on full-length 2N4R tau replicated certain characteristics associated with hyperphosphorylated tau (*160*). One of these characteristics was an SDS-resistant electrophoretic mobility shift, likely due to a conformational change in the protein altering the accessibility of the protein backbone to SDS. The pseudophosphorylation mutations at the seven sites also negatively affected the normal interaction of the protein with microtubules compared to wild-type 2N4R tau (*160*). In addition, the 7-Phos mutation affected the in vitro polymerization of the isoform by inducing longer, but less frequent, filament formation (*160*). I therefore sought to determine whether the same level and pattern of pseudophosphorylation mutations would have different effects on the function of the other tau isoforms.

In this study I have shown that pseudophosphorylation at seven identical sites on the backbone of the six tau isoforms resulted in an SDS-resistant electrophoretic shift in each protein, indicating that the conformation of the proteins had been altered by the 7-Phos mutation. However, the magnitude of these changes was not equal. Previous studies have shown that

pseudophosphorylation of 2N4R tau at the S199, S202, S205, T212, S214, S396, and S404 sites induce conformational changes that increase the reaction of the protein with the conformational-dependent antibody MC1, an antibody that recognizes pathological tau associated with electrophoretic shifts (*229, 231*). However, there are conflicting results as to whether this pseudophosphorylation is causing a tightening or a loosening of the hairpin conformation (*157, 229*). Our results could coincide with either model but it seems likely that a global compaction of tau conformation would result in regions of tau becoming inaccessible, thereby reducing SDS binding and slowing electrophoretic migration. Our results would suggest that the level of compaction caused by pseudophosphorylation is not the same for the six isoforms, indicating that similar levels and sites of phosphorylation have different effects on the conformation of tau isoforms. These differential effects on conformation could lead to changes in the other properties of the protein.

In support of this, pseudohyperphosphorylation affected the ARA induction of tau polymerization differently among the isoforms. The 7-Phos 3R isoforms did not polymerize as well as their wild-type counterparts while 7-Phos 4R isoforms polymerized as well or better than wild-type 4R. This, combined with the differences in electrophoretic mobility, suggests the possibility that the MTBR of the 3R isoforms may be less accessible to ARA when they are in a conformation induced by the 7-Phos mutation. Previous results showing that the MTBR of tau isoforms differ from one another both structurally and mechanistically support this supposition (*232*). It is possible that different results could be obtained using different inducer molecules such as heparin, planar aromatic dyes, polyanionic microspheres, mRNA or alkyl sulfate detergents and these experiments should be performed in the future.

Because hyperphosphorylated tau is associated with aggregation in AD and other tauopathies one might expect that pseudophosphorylation would lead to increased polymerization in the in vitro reactions. However, for most of the isoforms, polymerization was similar or decreased compared to the corresponding wild-type isoforms. This could be due to the limitations of pseudophosphorylation as a model or the homogenous reactions give different results than a mixture of phosphorylated forms of tau. However, it is also possible that similar phosphorylation patterns could lead to different conformational effects on the isoforms. The varied conformational effects could then lead to increased aggregation for some isoforms while decreasing the likelihood of aggregation for others. Variable conformational changes could help explain why the isoform content of aggregates can vary by tauopathy.

Compaction of the carboxy-terminus toward the MTBR would be expected to inhibit tau aggregation (*152, 233*), while compaction of the amino-terminus toward the MTBR would be expected to enhance tau aggregation (*220, 229*). If this is the case, inhibition caused by compaction of the carboxy-terminus would likely be relatively similar among the isoforms since that region does not differ between them. However, the compaction of the amino terminus caused by phosphorylation would be expected to be different between the isoforms due to the presence or absence of exons 2 and 3, and one would therefore expect this compaction of the amino terminus to have more varied effects on polymerization of the isoforms. Indeed, polymerization of the 0N 7-Phos isoforms seems to be less inhibited compared to its wild-type counterparts than was observed for the 1N and 2N isoforms. In fact, polymerization of the 0N4R 7-Phos in enhanced compared to wild-type 0N4R tau under certain conditions. The absence of

exons 2 and 3 could lead to a tighter compaction of the amino-terminus when these sites in the proline-rich region are phosphorylated. This tighter compaction could then lead to increased tau aggregation.

In general, the four-repeat isoforms seem to be less affected by pseudo-phosphorylation and compaction than the three-repeat isoforms, presumably due to the additional MTBR. This additional repeat reduces the impact of conformational-dependent enhancement or inhibition of tau aggregation leading to similar aggregation for wild-type and 7-Phos of each isoforms. It is likely that the additional repeat either results in a structural conformation that protects the MTBR from the amino and carboxy terminals, or that the additional repeat provides a second site for inducer interactions, thereby overcoming inhibition or enhancement by mass action.

Other differences in the polymerization of 7-Phos isoforms existed at the optimal ratio of 2 μM protein and 75 μM ARA. All of the 7-Phos isoforms polymerized more slowly than wild-type and fewer, but longer, filaments were formed for many of the 7-Phos isoforms. This also suggests that compaction due to phosphorylation could negatively affect the ARA-induced nucleation of filaments but could also stabilize filament elongation. This compaction could be differentially affecting the accessibility of the MTBR as discussed above, resulting in less nucleation and slower growth, causing the differences in morphology observed between isoforms. The effect was greatest in 0N4R tau which displayed an increase in polymerization, number of filaments formed, and length of filaments with the 7-Phos pseudophosphorylation mutation. Part of this effect could be due to increased or improved filament distribution on the electron microscopy grids (*215*) but the agreement between the SDS-PAGE migration,

quantitative electron microscopy, LLS, and ThS fluorescence data suggest that the 0N4R 7-Phos has a more accessible MTBR.

Differences in accessibility of the MTBR would be expected to affect the ability of tau to stabilize microtubule polymerization as well. The 7-Phos mutation caused a reduction in the ability of all six isoforms to stabilize microtubules. The overall amount of tubulin polymerization was decreased, the lag times were increased, and the rate of polymerization was decreased. The degrees of changes were not equal among the isoforms. For example, 0N4R tau had much less severe defects in its ability to stabilize microtubules. Additionally, the 0N3R 7-Phos stabilized microtubule growth more readily than the other 3R 7-Phos isoforms did. This indicates that phosphorylation of 0N isoforms could cause the MTBR to be more accessible than in 1N or 2N isoforms. In general, pseudohyperphosphorylated 4R isoforms had more similar aggregation and microtubule stabilization characteristics as compared to their wild-type counterparts than the 3R isoforms. This indicates that compaction of tau due to phosphorylation may be obscuring the MTBRs more for 3R isoforms than 4R isoforms.

In summary, our results are consistent with similar levels and patterns of phosphorylation having substantially different effects on tau isoforms. This result is important considering efforts to target phosphorylation as a therapeutic intervention for tauopathies. Our results suggest that such therapies will have different effects on the six isoforms of tau which could lead to complications. They also suggest that animal models used to study the effects of phosphorylation on the toxicity of tau would be affected by the choice of isoforms. Future studies will be required to determine whether these results are specific to these sites and this

inducer or whether similar results will be obtained using alternative inducers or different sites to generate alternative pseudohyperphosphorylated versions of tau isoforms.

Chapter III

FTDP-17 Tau Mutations Induce Distinct Effects on Aggregation and Microtubule Interactions

Chapter III FTDP-17 Tau Mutations Induce Distinct Effects on Aggregation and Microtubule Interactions

3.1 Abstract

FTDP-17 mutations in the tau gene lead to early-onset frontotemporal dementias characterized by the pathological aggregation of the microtubule-associated protein tau. These mutations are primarily located in or near the microtubule-binding repeat regions of tau and can induce vastly different effects on the aggregation and function of the protein. The pathologies associated with FTDP-17 can vary widely as well. Despite this variety, several of the mutations are commonly used interchangeably as aggregation inducers for in vitro and in vivo models of tauopathies. The recombinant forms of 12 FTDP-17 mutations, chosen for their predicted effects on the charge, hydrophobicity, and secondary structure of the protein, were generated. I then examined the effects that the mutations induced on the properties of in vitro aggregation of the protein and its ability to stabilize microtubule assembly. The group of mutations induced very different effects on the total amount of aggregation, the kinetics of aggregation, and filament morphology. Total aggregation could be enhanced or inhibited by the mutations. Some mutants formed primarily oligomeric aggregates while others formed much longer filaments. Several of the mutations inhibited the microtubule-stabilizing ability of tau while others had very little effect compared to wild-type tau. These results indicate that the mechanisms of disease progression may differ among FTDP-17 mutations. Additionally, the effects of the varying mutations may not be equal in all model systems and the type of mutation and its effects should be considered when generating and comparing these in vivo models.

3.2 Introduction

The pathological aggregation of the microtubule-associated protein tau is characteristic of the group of neurodegenerative disorders known as tauopathies. Although tau can be found in a variety of tissues, it is predominantly found in neurons where its primary functions are to promote the assembly and stability of microtubules in addition to interacting with cellular membranes and playing a role in regulation of microtubule spacing as well as axonal transport (*1, 37, 42, 46, 234*). The tau gene contains sixteen exons that, in the central nervous system, give rise to six distinct isoforms that differ by their pattern of inclusion or exclusion of exons 2, 3 and 10. Exon 10 encodes one of four potential microtubule-binding repeat regions (MTBR) that are the primary source of tau interactions with microtubules. Each MTBR contains a highly-conserved 18 amino acid repeat and an inter-repeat regions of 13 or 14 amino acids, both of which make significant contributions microtubule binding (*21, 93, 204*).

Tau MTBR were found to comprise the core of pathologically aggregated tau filaments (*235*) and have been found to be necessary and sufficient for tau aggregation into straight and paired-helical filaments (*110, 236*). Within the MTBR, the sequences ^{275}VQIINK in exon 10 and ^{306}VQIVYK in exon 11 misfold into β-strands that subsequently interact with adjacent tau molecules to form characteristic amyloid structure (*110-112, 237, 238*). The nucleation step, formation of oligomers, is likely the first step in tau aggregation and can be followed by a slower elongation phase that leads to the formation of longer straight or paired helical filaments from these oligomers (*239, 240*). Aggregated tau then accumulates in pathological structures such as neurofibrillary tangles, neuropil threads, Pick bodies and others that correlate with the type and severity of clinical impairment in neurodegenerative tauopathies (reviewed in (*8, 205*)).

In AD and other related tauopathies, tau aggregation is oftentimes associated with other pathological structures such as beta-amyloid extracellular senile plaques. It was therefore unclear whether tau aggregation played a role as a causative agent in neuronal cell death or was simply a byproduct of other toxic mechanisms. The potential for a causative role was greatly strengthened with the identification of a group of mutations in the tau gene that led to early-onset frontotemporal dementias (*80, 82*). Many of the mutations cause increased propensities for aggregation and decreased microtubule interactions which could represent toxic gain and loss of functions respectively (*112, 182, 214, 241-248*), Several of the mutations have also been utilized in a diverse set of model organisms, including nematodes, flies, *Xenopus*, and mice ((*192, 197, 214, 249, 250*), reviewed in (*251*)). These naturally-occurring mutations have provided an invaluable tool to the study of tau aggregation, but their effects have not always been consistent across the spectrum of mutants or model organisms (*252*).

It is possible that some of the observed differences in the effects of tau aggregation in cellular and animal models are a direct result of the various FTDP-17 mutations employed to generate aggregated tau. Certain FTDP-17 mutations have been shown to increase the rate or total amount of tau aggregation both in vitro and in vivo which may be leading to early-onset tauopathies (*192, 220, 241, 244, 253*); some FTDP-17 mutants show decreased binding to microtubules and an impaired ability to stabilize polymerization of tubulin while others have little effect (*242, 254*). In addition, the progression and pathologies of FTDP-17 can vary greatly depending on the specific mutation, indicating that initial causes of the disease may vary as well (reviewed in (*255*)). I therefore sought to compare several FTDP-17 mutations under the

same conditions to determine how they affected aggregation and microtubule interaction, two factors that may have causative roles in the toxicity of these diseases, and whether differences in the intrinsic effects of FTDP-17 mutations could be correlated to these changes. From the 25 known FTDP-17 missense mutants of tau, we chose to model the 12 mutations predicted to have the most significant impact on tau charge, hydrophobicity (*256*) and structure (*257*). Our predictions were based on an analysis demonstrating that these parameters were the primary determinants of aggregation rates (*258*). These mutants were modeled in the background of full-length 2N4R tau in vitro to provide direct side-by-side comparisons to assess the impact of the structural modifications.

I found that the FTDP-17 mutants had very different effects on the aggregation and microtubule interactions of tau. These changes in aggregate amounts, rates and morphologies could help in our understanding of the varied pathologies and toxicities resulting from the mutations. While some of the mutations had similar effects on tau function and aggregation, I found that there was not a simple correlation between the effects on tau and the protein's charge, hydrophobicity or predicted structure. This indicates that predictive methods are insufficient for determining the impact of tau mutations on the severity of impairment.

3.3 Experimental Procedures

3.3.1 Selection of FTDP-17 mutations. Mutations were selected based on their predicted changes to average hydrophobicity, charge, α-helical structure, β-strand structure, and turns. These predictions were calculated across 7 amino acid-long sequences for the entire 2N4R tau isoform using Kyte-Doolitte values to estimate hydrophobicity (*256*) and Chou-Fassmann

parameters for effects on secondary structure (*257*). The effect of each mutant was ranked according to each of these factors and the total effect was estimated based on summation of rankings for each variant. The 11 mutants predicted to have the largest effects on the structure of the protein were chosen along with V337M, a mutant commonly used to generate tau aggregation in in vivo models.

3.3.2 Protein expression and purification. All wild-type (WT) and FTDP-17 mutant protein was expressed and purified as described previously (*150*). The FTDP-17 mutations were created using the Quikchange site-directed mutagenesis kit from Stratagene (La Jolla, CA). The following mutations were generated in a full-length 2N4R tau background contained in a pT7C vector: R5L, G272V, ΔN296, P301L, G303V, L315R, S320F, V337M, E342V, S352L, K369I, and G389R.

3.3.3 Arachidonic acid-induced polymerization. Recombinant WT and mutant tau protein, at a concentration of 2 μM, was incubated in buffer containing 0.1 mM EDTA, 5 mM dithiothreitol, 10 mM Hepes buffer (pH 7.64), 100 mM NaCl, and 3.75% ethanol in a 1.5 mL microcentrifuge tube. The polymerization inducer molecule was arachidonic acid (ARA) at a concentration of 75 μM. Reactions were allowed to proceed overnight at 25 °C.

3.3.4 Thioflavin S fluorescence. The total amount of aggregation was measured utilizing the binding of thioflavin S (ThS) from Sigma-Aldrich (St. Louis, MO). 150 μL of each reaction was added to separate wells in a 96-well, white, flat-bottom plate. ThS was diluted in water and added to the well to a final concentration of 20 μM. The fluorescence shift was measured by

using a Cary Eclipse Fluorescence Spectrophotometer (Varian Analytical Instruments, Walnut Valley, CA) with an excitation wavelength of 440 nm and an emission wavelength of 520 nm. PMT voltage was set to 650 V. Readings from a reaction with 2 μM protein and 0 μM ARA were used as a blank and subtracted from the reading for each reaction (*150*).

3.3.5 Right-angle laser light scattering. Aggregation of the protein was also read by adding 180 μL of the reaction to a 5 mm x 5 mm optical glass fluorometer cuvette (Starna Cells, Atascadero, CA). A 12 mW solid state laser, with a wavelength of λ=532 nm and operating at 7.6 mW, was aimed at the cuvette. The amount of light scattered by particles in the reaction was measured by capturing the amount of light perpendicular to the angle of the beam using a SONY XC-ST270 digital camera. The images were captured at varying aperture settings (from f4 to f11) and analyzed using the histogram function of Adobe Photoshop CS5 version 12.0.1. (*214*).

3.3.6 ARA-induced polymerization kinetics. ARA was added to our polymerization buffer (0.1 mM EDTA, 5mM dithiothreitol, 10 mM Hepes buffer (pH 7.64), 100 mM NaCl) to a final concentration of 75 μM and 3.75% ethanol in a 5 mm x 5 mm optical glass fluorometer cuvette. Tau polymerization was measured by collecting images of the right-angle scattered light at specific time points beginning from the initiation of the reaction upon addition of protein, at a final concentration of 2 μM, and the ending once the reaction had reached a steady-state. The data were fit to the Finke-Watzky 2-step mechanism, designed to describe the nucleation and elongation of protein aggregation (*259*). The mechanism assumes simplified nucleation $\left(A \overset{k_1}{\rightarrow} B\right)$ and elongation $\left(A + B \overset{k_2}{\rightarrow} 2B\right)$ steps to yield the following equation:

$$[B]_t = [A]_0 - \frac{\frac{k_1}{k_2}+[A]_0}{1+\frac{k_1}{k_2[A]_0}exp(k_1+k_2[A]_0)t}$$

The k_1 and k_2 rate constants are used to qualitatively compare the rates of nucleation and elongation, respectively, of our protein aggregation reactions.

3.3.7 Transmission electron microscopy. The ARA-induced polymerization reactions were diluted 1:10 in polymerization buffer and 2% glutaraldehyde. After a five minute incubation, a formvar-coated copper grid (Electron Microscopy Sciences, Hatfield, PA) was placed on top of a 10 μL drop of the diluted sample for 1 minute. The grid was then blotted on filter paper, placed on a drop of water, blotted with filter paper, placed on a drop of 2% uranyl acetate, and blotted dry. The grid was then placed on another drop of 2% uranyl acetate for 1 minute and blotted dry for a final time. For all tau variants a single grid was prepared and examined from each of three separate reactions. The grids were examined using a TECNAI G^2 20 electron microscope (FEI Co., Hillsboro, OR). Images were collected with the Gatan Digital Micrograph imaging system at a magnification of 3600X. Five images were collected from each grid and analyzed. The aggregated tau in each of the 15 images was quantified by using Image-Pro Plus 6.0. The macro was designed to recognize filaments with a total perimeter of greater than 30 nm. This captured what I felt were legitimate aggregates while eliminating background noise. The perimeter of each filament was measured and divided by two in order to estimate the filament's length. These values were totaled in order to estimate the total amount of aggregated material in each image. The total polymerization/image was calculated by taking the mean of all total polymerization values. The mean of all filament lengths was also determined by calculating the mean length of

all filaments in a given image and reported as a mean of those values with the error bars representing standard deviation.

3.3.8 Tubulin polymerization assay. The Tubulin Polymerization Assay kit from Cytoskeleton, Inc. (Denver, CO) was used to measure the polymerization of tubulin. The reaction conditions included WT tau or one of the tau variants at 1 μM, or a control compound, added along with 1 mM GTP, 2 mg/ml (~36 μM dimerized) tubulin, 2 mM $MgCl_2$, and 0.5 mM EGTA in 80 mM PIPES buffer at a pH of 6.9. The reaction proceeded in a black, flat-bottomed polystyrene 96-well plate. Paclitaxel was used at 3 μM in one reaction to serve as a positive control for tubulin polymerization, as well as a way to normalize separate reactions. One well contained no additional compound as a negative control. After addition of the compounds the plate was inserted into a FlexStation II Fluorometer (Molecular Devices Corporation, Sunnyvale, CA) set at a temperature of 37 °C and the reactions were mixed by shaking for 5 seconds. The fluorescence was measured with an excitation wavelength of 355 nm and an emission wavelength at 455 nm at 1 minute intervals for 1 hour. The data were fit to the Gompertz equation

$$y = ae^{-e^{-\frac{t-t_i}{b}}}$$

as described earlier (*160, 260*). The maximum amount of tubulin polymerization is described by *a*, the lag time from reaction initiation to the start of polymerization is $t_i - b$, and k_{app}, or *1/b*, is proportional to the rate of polymerization.

3.3.9 Statistical analysis. An unpaired two-tailed Student's t-test was used to compare means of WT values to mean values of each mutant for thioflavin S fluorescence, right-angle laser light

scattering, quantitative electron microscopy, and kinetics parameters. A paired two-tailed t-test was used to compare the values for the microtubule assembly assay. P-values less than or equal to 0.05 were indicated with one asterisk (*), less than or equal to 0.01 with two asterisks (**), and less than or equal to 0.001 with three asterisks (***). Because variation among the mutants is also important to consider, statistical variation in the entire groups was measured by using a one-way ANOVA analysis with a Tukey's Multiple Comparison test and compiled in tables. The p-values for this comparison were also indicated using the asterisk system described above.

3.4 Results

3.4.1 Selection of FTDP-17 mutations

A list of 25 known FTDP-17 mutations was generated and ranked based on the total predicted changes to the structure of the protein. The 11 mutations predicted to induce the largest structural changes were selected along with V337M which was selected because it has previously been used in several model organisms. The majority of the chosen FTDP-17 mutations can be found within, or very near to, one of the 4 MTBR while R5L and G389R are found in the N- and C-terminal regions respectively (Figure 3.1).

3.4.2 FTDP-17 mutations induce varying effects on total polymerization

In vitro experiments were used to examine the effects of the 12 mutations on the ARA-induced polymerization of tau at 2 μM protein and 75 μM ARA (*209*). After the reactions proceeded overnight, the total amount of aggregation was measured by ThS fluorescence and right-angle laser light scattering (LLS). Half of the mutant proteins displayed an increase in ThS

Figure 3.1

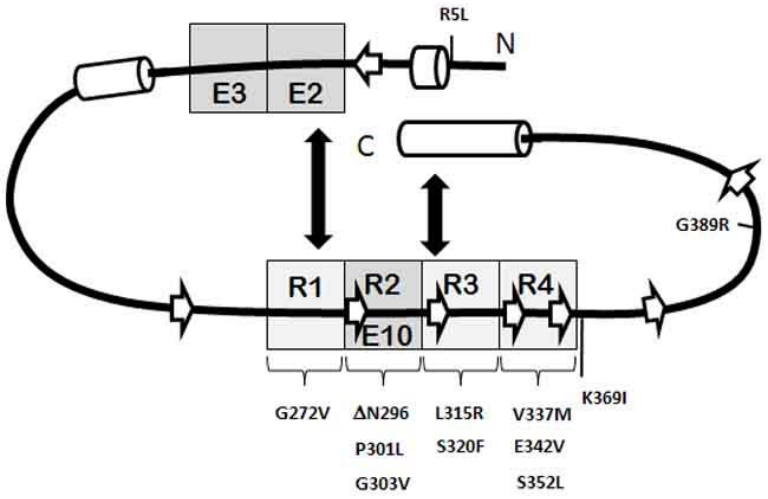

Figure 3.1. Schematic of FTDP-17 mutations in 2N4R tau. Each of the naturally-occurring FTDP-17 mutations indicated in the figure was created in a full-length 2N4R tau background. E2, E3, and E10 represent exons that can be excluded from other tau isoforms. Regions predicted to exhibit transient secondary structure are indicated by cylinders (α-helices) or arrows (β-strands). Boxes R1-R4 represent microtubule-binding repeat regions.

fluorescence compared to WT tau protein (G272V, P301L, G303V, S320F, S352L and G389R), indicating that more protein had polymerized in those reactions. Others had levels of polymerization that were similar to WT tau (R5L, ΔN296, V337M and E342V), while two of the mutants showed a clear decrease (L315R and K369I) (Figure 3.2A).

LLS can be used as another method to measure relative amounts of protein aggregation (*214*). However, in this case the results differed from those found in ThS fluorescence. Only three mutants showed a clear increase over WT (R5L, P301L and S352L), while five of the mutants showed a decrease in scattered light (G272V, G303V, L315R, S320F and K369I) and four mutants had levels similar to WT (ΔN296, V337M, E342V and G389R) (Figure 3.2B). Results from one-way ANOVA analyses with Tukey's multiple comparison tests can be found in Tables 3.1 and 3.2. This analysis demonstrates that not only are many of the mutants different from WT, but there is also a wide range in variation between mutants as well.

3.4.3 FTDP-17 mutations induce varying effects on aggregate morphology

Because LLS is known to be affected by the length distribution of the aggregates (*214*) and the structure of tau recognized by ThS is unknown (*216, 239*), the aggregates of tau were viewed directly by electron microscopy (Figure 3.3). Direct visualization of the aggregates can help in elucidating some causes of the apparent variation between the ThS and LLS results (Figure 3.2). WT tau displays a characteristic mixture of longer filaments and smaller aggregates less than 100 nm in length, hereafter described as oligomers (Figure 3.3A). Examination of the images made it abundantly clear that the mutations were inducing very different effects on the aggregation of the

protein. Some of the mutants, such as G303V and S320F are almost entirely made up of Figure 3.2

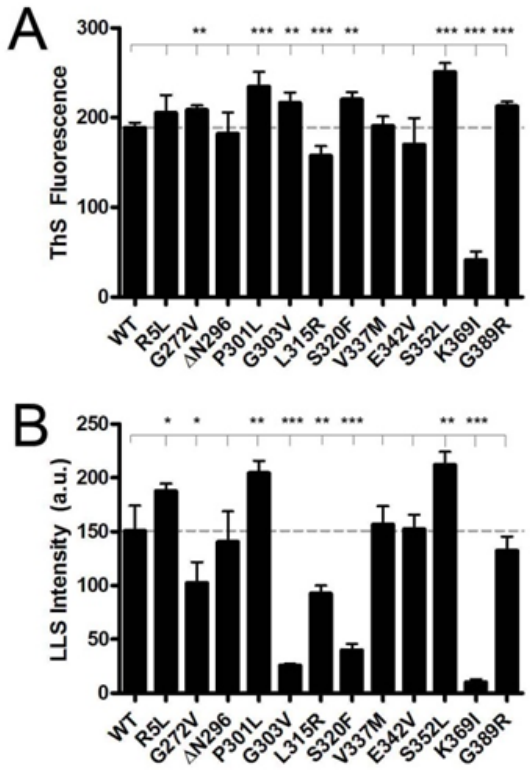

Figure 3.2. Polymerization of wild-type and FTDP-17 mutant tau measured by thioflavin S staining and right-angle laser light scattering. Polymerization reactions contained 2 μM of WT or one of 12 FTDP-17 mutant versions of tau and 75 μM ARA. Reactions were incubated overnight at 25° C. The final extent of polymerization was measured by (A) ThS fluorescence and (B) right-angle LLS as described in the Experimental Procedures. Data represent the mean from 3 experiments ±SD. Stars represent p-value results from Student's unpaired t tests comparing means from each mutant to WT. (*), $p < 0.05$; (**), $p < 0.01$; (***), $p < 0.001$. More extensive statistical analysis can be found in Tables 3.1 and 3.2.

Figure 3.3

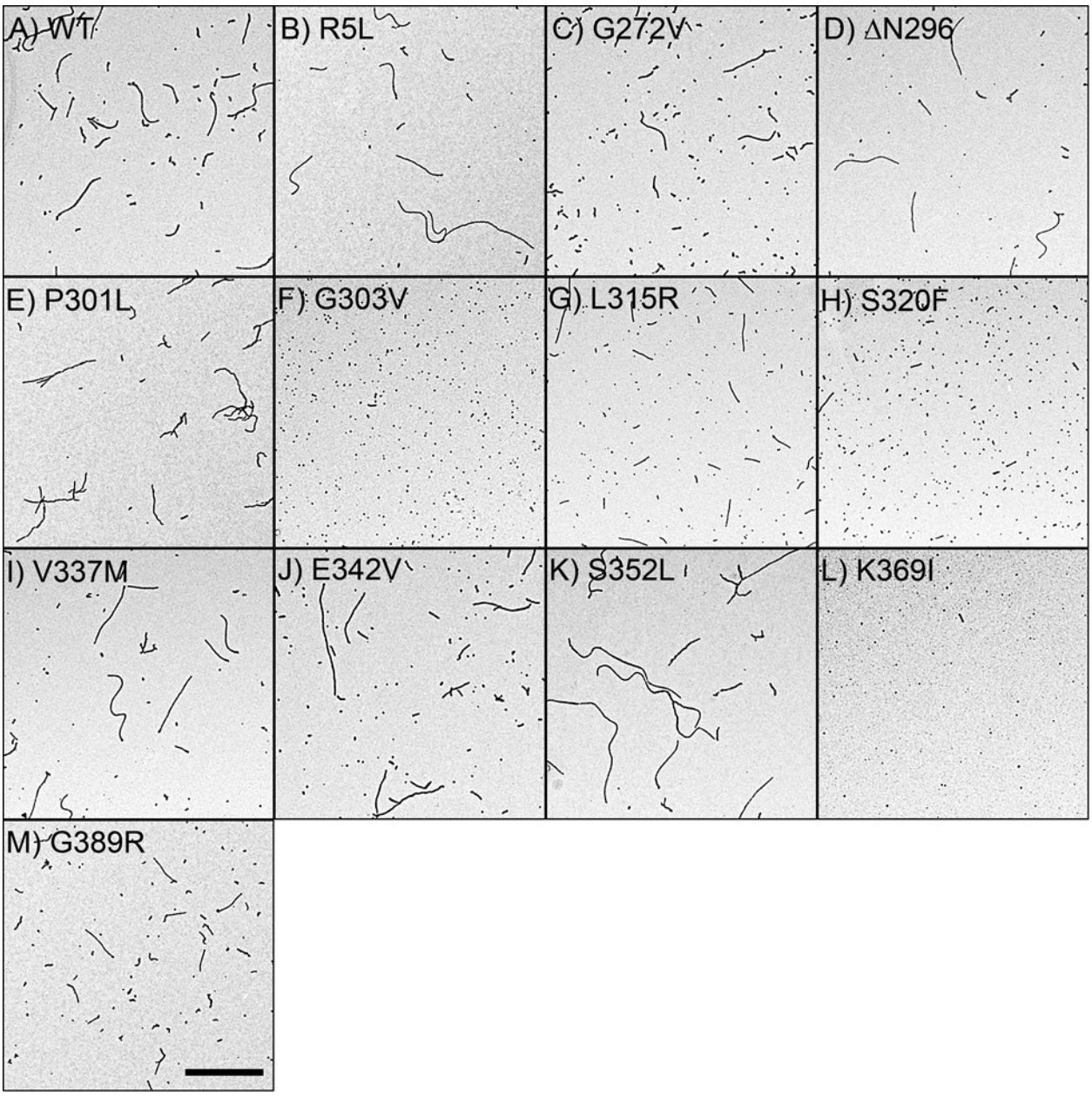

Figure 3.3. Electron micrographs of polymerization reactions containing 2 μM protein and 75 μM ARA. A representative electron micrograph for (A) WT tau, (B) R5L, (C) G272V, (D) ΔN296, (E) P301L, (F) G303V, (G) L315R, (H) S320F, (I) V337M, (J) E342V, (K) S352L, (L) K369I, and (M) G389R. The scale bar in (M) represents 1 μm and is applicable for all images.

oligomers (Figures 3.3F and H). Others, including R5L, S352L, and P301L seem to be lacking oligomers and display longer filaments than WT tau (Figures 3.3B, E, and K). Very few aggregates were associated with K369I which confirms earlier ThS and LLS results (Figures 3.2 and 3.3L). I next sought to determine if the apparent observed differences could be detected by quantitative methods and whether these differences were significant. To accomplish this I measured the number and length of filaments displayed in five representative images from each of three different reactions for each tau variant.

Quantitation of the total amount of aggregated material indicated that most of mutant forms of tau variants polymerized to a similar extent as WT tau but images from G303V, S320F, and E342V all contained more total polymerized tau than WT (Figure 3.4A). In contrast, K369I and G389R displayed less polymerization than WT in these images. K369I had considerably fewer aggregates than WT and these aggregates were very short in nature and in general did not stain as intensely as tau aggregates associated with WT and the other mutants, again indicating low levels of polymerization (Figures 3.3L and 3.4B).

The differences in aggregation, apparent in Figure 3.3, were confirmed by comparing the average lengths of all filaments for each tau variant. Several mutants (G272V, G303V, L315R, S320F, and G389R) displayed shorter average filament lengths while filaments from R5L, P301L, and S352L were much longer on average than WT (Figure 3.4B). Average filament lengths are not amenable to statistical analysis due to their exponential distribution. Therefore, the data from each of the 15 electron micrographs were plotted as average filament length versus the number of filaments formed to demonstrate the variation in the data (Figure 3.5). These plots also

Figure 3.4

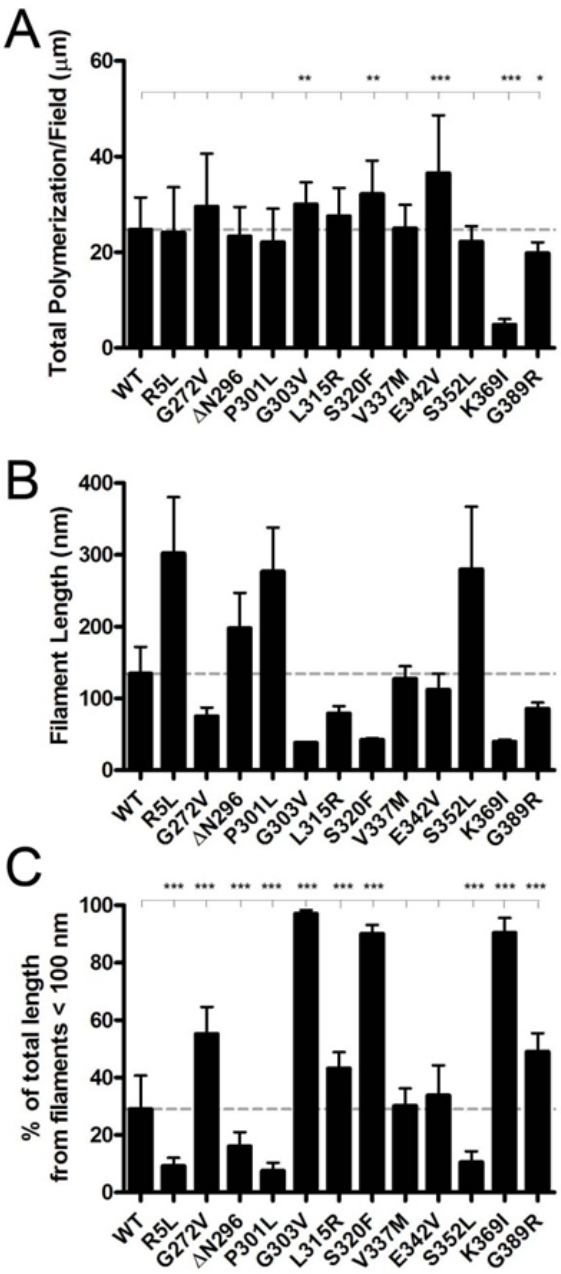

Figure 3.4. Quantitation of polymerized tau protein in electron micrographs. Images in the electron micrographs from Figure 3 were quantified using Image-Pro Plus 6.0 as described in the Experimental Procedures. The graphs display (A) the mean of the total length (μm) of polymerized tau filaments/image, (B) the mean length of filaments (nm), and (C) the percent of the total length coming from filaments less than 100 nm in length for each of the tau variants. Data in (A) represent the mean of 5 images from each of 3 separate reactions ±SD for a total of n=15. Data in (B) represent the means of the mean filament length for each of the 15 images ±SD. Data in (C) represent means of the sum of all filament lengths less than 100 nm as a percent of the total length for each image ±SD, n=15. Stars

represent p-value results from Student's unpaired t tests comparing means from each mutant to WT. (*), $p < 0.05$; (**), $p < 0.01$; (***), $p < 0.001$.

Figure 3.5

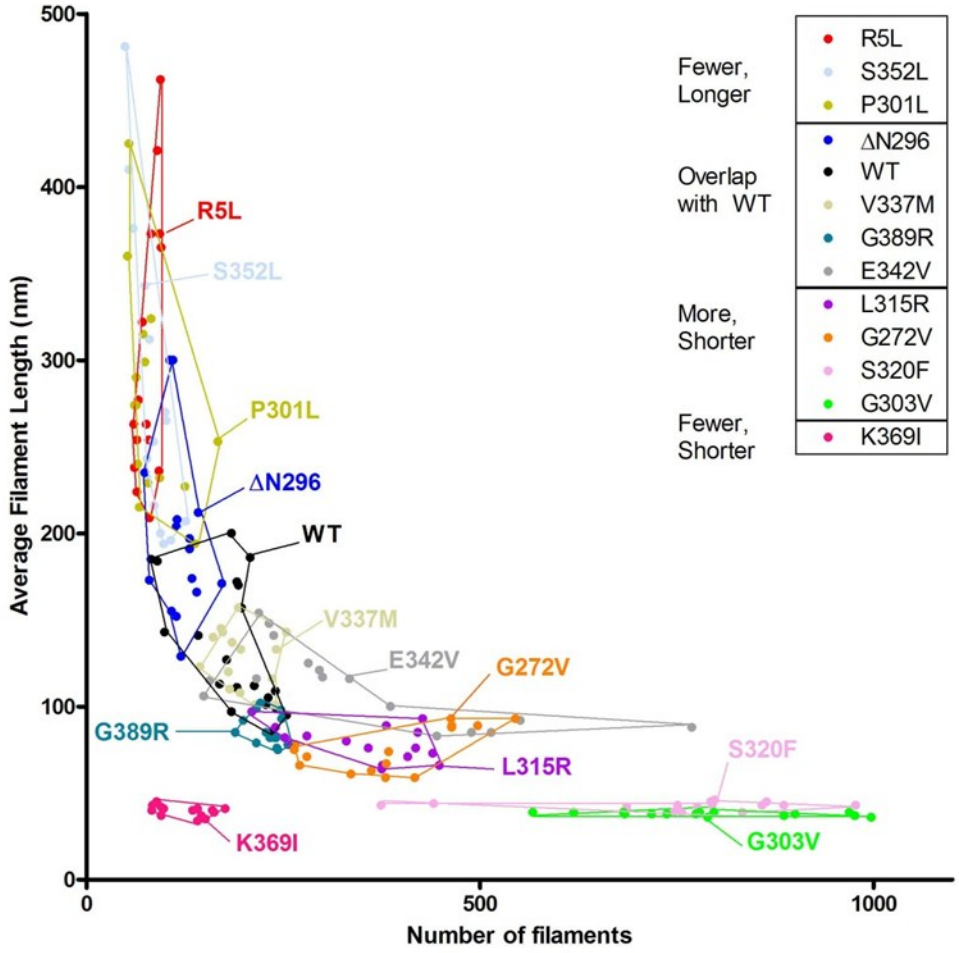

Figure 3.5. Average filament length vs filament number for all electron micrographs. The quantitated values for average filament length and number of filaments per image are displayed here. The values for each form of tau were grouped together to indicate differences and similarities among the aggregate morphologies in this assay. The figure legend ranks each tau variant in order of average filament length and groups them based on the general trends of the mutation-induced effects on filament number and average filament length and how much these traces overlap with WT tau.

supported the differences in filament morphology described above. Further variation can be observed by determining how much of the total polymerization is due to very short filaments. I calculated the percent of the total polymerized material that was made up of filaments shorter than 100 nm (Figure 3.4C). Around 30% of polymerized WT tau was contained in short filaments while oligomers made up greater than 90% of the total for G303V, S320F, and K369I. Others, such as R5L, ΔN296, P301L, and S352L, again induced a very different effect and contained much lower percentages, indicating that longer filament lengths and fewer oligomers were present (Figure 3.4C).

In light of the quantitative EM data, the discrepancy between ThS fluorescence and LLS measurements of tau mutant aggregation is likely due to the disparate morphologies of the resulting filaments. In fact, there is a direct correlation between filament length, as measured through electron microscopy (Figures 3.3 and 3.4B), and the ratio of ThS fluorescence to LLS values (Figure 3.6). Therefore, the amount of light scattering from two populations of filaments of very different length distributions may not be equally proportional to the mass of filaments.

3.4.4 Kinetics of polymerization varies by FTDP-17 mutant

Because the morphology of tau aggregates can be influenced by the rate of polymerization (*209*), I sought to determine whether the mutations were affecting the kinetics of polymerization. Polymerization reactions for each mutant were followed by LLS and were then fit to a two-step model of polymerization to determine nucleation and elongation rates (Figure 3.7). The K369I mutant had nearly undetectable levels of polymerization in this assay and could therefore not be fit to the model.

Figure 3.6

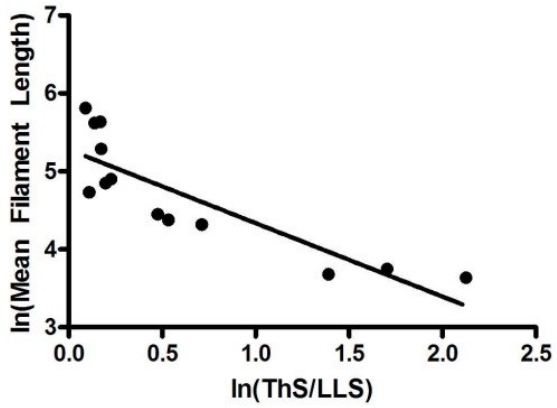

Figure 3.6. Correlation between natural log of mean filament length and natural log of ThS to LLS ratio. This plot displays correlation between the natural log of the mean filament length calculated from electron micrographs (Figure 3.4B) versus the natural log of the ratio of ThS values to LLS values (Figure 3.2). This indicates that larger differences between ThS and LLS values are due to decreases in filament size. The r^2 value is 0.7339.

Figure 3.7

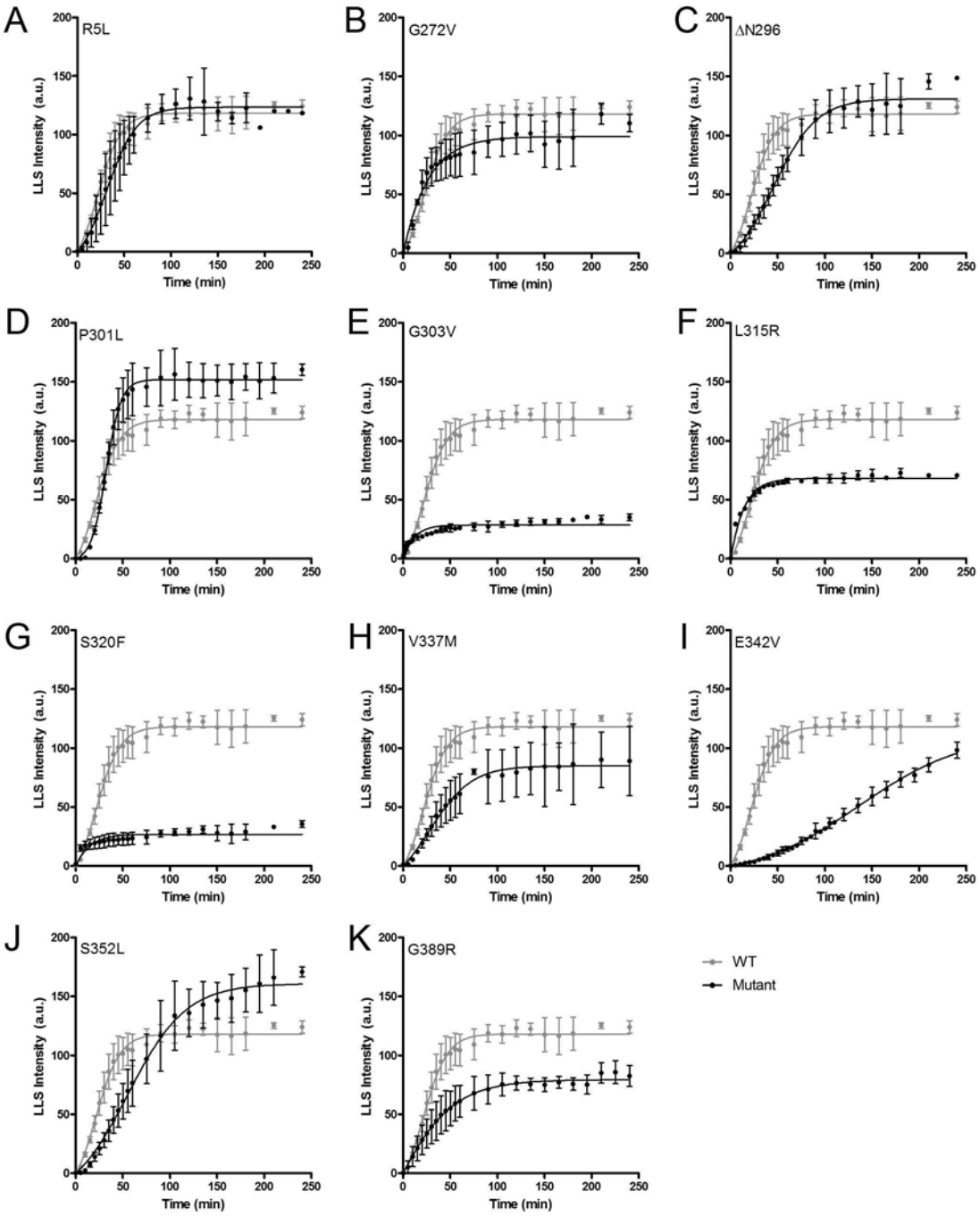

Figure 3.7. Kinetics of tau polymerization. Polymerization reactions containing 2 μM tau were initiated by the addition of 75 μM ARA. LLS readings were measured at specific time intervals until the reactions reached a steady-state. The traces here represent mean values ±SD from 3 reactions fit to the Finke-Watzky mechanism described in the Experimental Procedures and displayed over 250 minutes for WT tau protein (light gray) and various FTDP-17 mutant tau protein (black) including (A) R5L, (B) G272V, (C)

ΔN296, (D) P301L, (E) G303V, (F) L315R, (G) S320F, (H) V337M, (I) E342V, (J) S352L, and (K) G389R.

A visual inspection of the curves indicated a wide range of polymerization kinetics between mutants (Figure 3.7). A comparison of nucleation rates (k1, Figure 3.8A) indicated that G272V, G303V, L315R, and S320F had significantly increased nucleation rates as compared to WT while R5L, P301L, E342V, and S352L had significantly decreased nucleation rates (Figure 3.8A). G303V, L315R and S320F also had greatly reduced elongation rates as compared to WT (k2, Figure 3.8B), such that the elongation phase was essentially undetectable. E342V and S352L had elongation rates that were significantly reduced compared to WT but elongation was still detectable (Figure 3.8B). The only mutant with a faster elongation rate than WT was P301L (Figure 3.8B). In addition to these differences from WT protein, further analysis of the data using one-way ANOVA with Tukey's multiple comparison tests demonstrates that many of the mutants are significantly different from one another. For example, the kinetics of elongation (k2) of the P301L mutant is significantly different from G303V, L315R, S320F, V337M, S352L and G389R (Tables 3.3 and 3.4).

3.4.5 FTDP-17 mutations can inhibit ability of tau to stabilize microtubule assembly or have little effect

I then sought to determine whether the FTDP-17 mutations would have differential effects on one of tau's normal functions of stabilizing microtubules. Microtubule polymerization was monitored using a fluorescence based assay and the resulting curves (Figure 3.9) were fit to a Gompertz function in order to determine maximal extent of microtubule polymerization, the rate of elongation, and lag time in the presence of the FTDP-17 mutants (Figure 3.10). Most proteins stabilized microtubules to similar levels as WT tau, but G303V, L315R, and S352L did not (Figure 3.10A). P301L, G303V, S320F, and S352L induced microtubule elongation at a slower

Figure 3.8

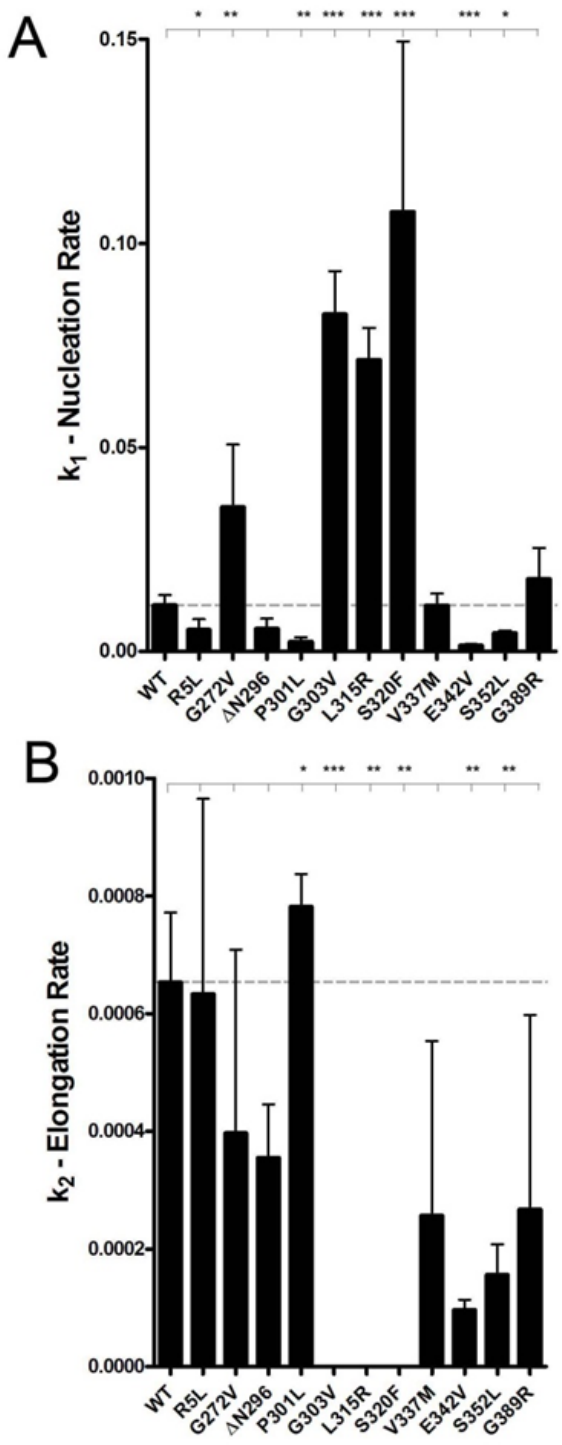

Figure 3.8. Comparison of tau polymerization kinetics. The parameters describing the tau polymerization kinetics curves fit to the Finke-Watzky mechanism are displayed. The first

parameter is (A) k_1, representing the rate of nucleation or formation of oligomers. The second parameter is (B) k_2, the rate of elongation or extension of the oligomeric tau aggregates into filaments. Data represent means of values for fits of at least 3 separate reactions ±SD. Stars represent p-value results from Student's unpaired t tests comparing means from each mutant to WT. (*), $p < 0.05$; (**), $p < 0.01$; (***), $p < 0.001$. More extensive statistical analysis can be found in Tables 3.3 and 3.4.

Figure 3.9

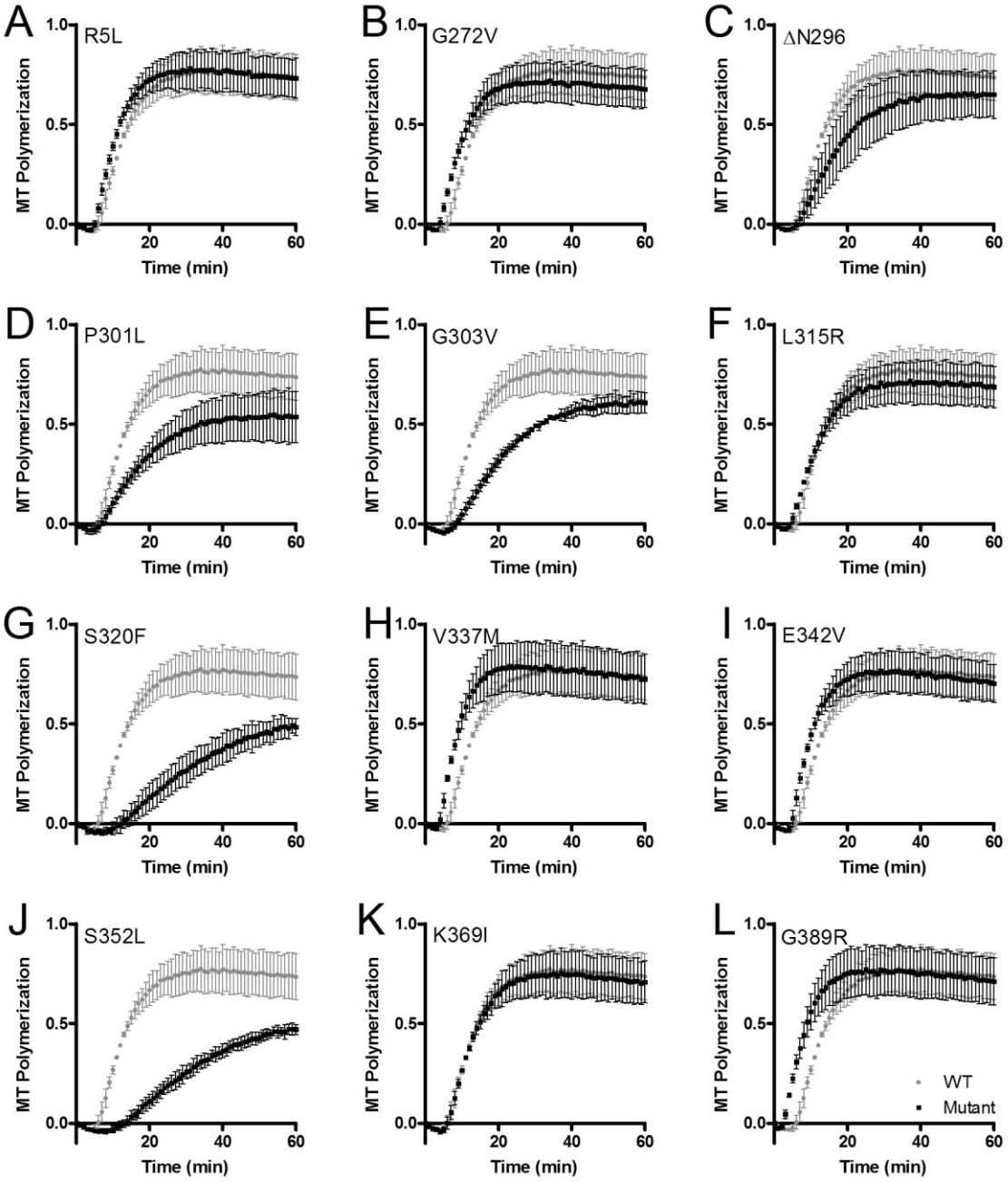

Figure 3.9. Microtubule assembly curves in the presence of tau. Each point represents a mean value of the amount of tubulin polymerized into microtubules in the presence of wild-type tau (light gray) or tau with mutations of (A) R5L, (B) G272V, (C) ΔN296, (D) P301L, (E) G303V, (F) L315R, (G) S320F, (H) V337M, (I) E342V, (J) S352L, (K) G389R (black). The values are fluorescence readings normalized to paclitaxel-stabilized polymerization of microtubules.

rate while V337M and E342V actually increased the rate of tubulin polymerization (Figure 3.10B). The lag time for tubulin polymerization was decreased in the presence of G272V, L315R, V337M, E342V, and G389R but increased in the presence of G303V and S352L (Figure 3.10C). In addition to these differences in FTDP-17 mutants as compared to WT, results from one-way ANOVA analyses with Tukey's multiple comparison tests demonstrate that there were many statistically significant differences between FTDP-17 mutants as well (Tables 3.5-3.7).

Figure 3.10

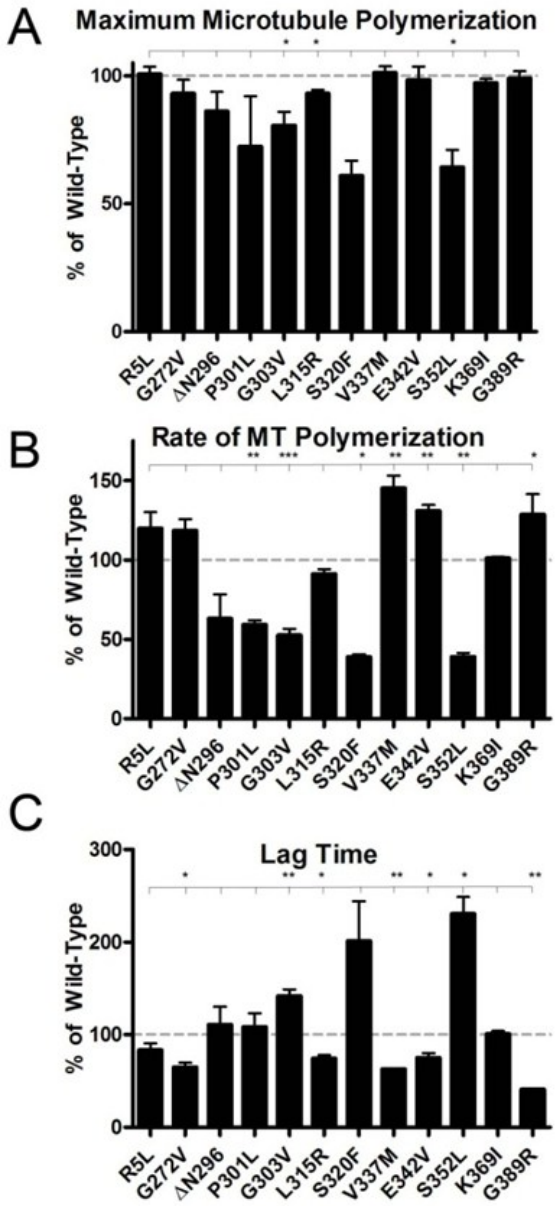

Figure 3.10. Stabilization of microtubule assembly by tau protein. The tau variants were incubated with tubulin and its polymerization was measured via a fluorescence assay. Numbers were normalized to values of polymerization in the presence of paclitaxel. The relative fluorescence units (*y*-axis) were plotted vs. time (*x*-axis) and fit to the Gompertz equation as described in the Experimental Procedures. From the parameters describing these curves, the percent of WT values for the (A) maximum amount of microtubule polymerization in presence of each protein, (B) k_{app} or rate of microtubule polymerization, and (C) lag time, the time before microtubule polymerization is detected. The values in (A-C) are mean values of the percent

changes from WT in three separate experiments ±SD. Stars represent p-value results from Student's paired t tests comparing means from each mutant to WT. (*), $p < 0.05$; (**), $p < 0.01$; (***), $p < 0.001$. More extensive statistical analysis can be found in the Tables 3.5-3.7.

3.5 Discussion

FTDP-17 mutations in tau are extremely rare but play a particularly important role in the study of tau aggregation associated with familial and sporadic tauopathies. Some of these mutations are commonly used in disease models in order to enhance protein aggregation. However, among the FTDP-17 mutants there exists significant variability in symptoms and pathology of diseases, indicating that there may be differing root causes of the disease. While most known mutations are found within one of the four MTBRs, the locations vary from the N- to the C-terminal regions. The amino acid substitutions or deletions result in increased or decreased hydrophobicity and charge, as well as induce a variety of potential changes in the transient secondary structure of the protein. In addition, other factors such as alterations in splicing or phosphorylation pattern could be playing a major role in the neurodegenerative process.

Because of the differences in pathology of aggregation and disease progression, it is important to determine how the mutations are changing the properties of the tau protein as well as how these changes could be affecting the associated neurodegeneration patterns. Previous work has shown that the rate of tau aggregation into amyloid could be predicted by calculating expected changes in hydrophobicity, charge, and secondary structure due to three known FTDP-17 mutations (*258*). In addition, other studies have examined the in vitro properties of small numbers of known mutants (*214, 241, 244*). I sought to directly compare aggregation and function of WT and a wider variety of FTDP-17 mutant forms of tau under similar conditions, using the same mechanisms for inducing aggregation, as well as to determine whether these predictive tools would apply to an expanded field of mutations.

After studying the effects of FTDP-17 mutations on the in vitro aggregation of tau and its microtubule-stabilization properties I determined that the mutants had very distinct profiles from WT tau as well as each other. I was able to group some of the mutants together based on their common properties and speculate on some of the causes for these general trends although I could not detect a clear pattern between the effects in these assays and the intrinsic changes predicted to occur due to mutations. Some of the mutations induced similar effects on filament morphology that may be tied to their aggregation kinetics, but the overall trends pointed to large differences in the behavior of the mutated versions of tau in our assays.

Several of the mutants displayed shorter average filament lengths than WT which seemed to be due to an increase in the number of oligomers and a decrease in the length and number of longer filaments. The increase in the number of oligomers from this group may be explained by the increased rate of nucleation that was also associated with these four mutations. Fast nucleation would take up large amounts of monomeric tau quickly and drop the protein level below the critical concentration of aggregation before elongation could begin. Interestingly, four of the mutations with decreased filament length occur directly before and after the ^{275}VQIINK and ^{306}VQIVYK sequences, important for aggregation of tau, and may be causing increased nucleation through enhancements of the β-strand character (*110, 261*). G272V, G303V, and S320F are predicted to enhance β-strand structure and extension of the β-strands in these regions has been shown to enhance polymerization in other mutants, although with slightly different effects (*262*). The fourth mutation, L315R, is not predicted to enhance β-strand character, but it would replace a hydrophobic amino acid with a positive charge on the polar/charged side of an amphipathic β-strand which may help promote the cross-β amyloid structure (*262*).

Strengthening the β-strand secondary structure in these key regions may increase nucleation; making it more likely that tau will begin to aggregate, leaving little tau left for the elongation phase of polymerization. Therefore the rate of nucleation is an important determinant of the ratio of oligomers to fibrils formed under these conditions.

Another group of mutations induced the opposite effects on the filament morphology phenotype. R5L, P301L, and S352L all induced fewer, but longer filaments, than WT or the other mutant versions of tau. These were slower to nucleate than WT tau which could be another indication of the importance of nucleation rate on filament morphology. Despite the similarities in the rates of nucleation, the elongation rates of these three tau mutants varied widely compared to WT; R5L was similar, P301L was faster, and S352L was slower. Even though each of these mutants aggregated into long filaments with few oligomers, the mechanisms of aggregation were quite dissimilar.

It may seem unusual that R5L, a mutation that is far away from the MTBR, would have such large effects on the aggregation of the protein but the N-terminal region has been shown to have an enhancing effect on aggregation which may be due to alterations in the global hairpin conformation (*54, 220, 229*). The P301L mutation is much closer to the ^{306}VQIVYK hexapeptide than R5L and the removal of a proline in the PGGG sequence preceding it could assist in the formation of a β-strand in such a way as to stabilize the formation of longer filaments with an altered morphology (*263*). S352L also enhances the β-strand character around the ^{350}VQLKI sequence which is very similar to the ^{275}VQIINK and ^{306}VQIVYK sequences that

form the amphipathic β-strands crucial for the formation of tau filaments. The addition of another amyloidogenic sequence could assist in stabilizing longer filaments.

While the mutants discussed above had obvious effects on the morphology of the aggregates, other mutants, such as ΔN296, V337M, and E342V, displayed aggregates that were much more similar to WT protein. These mutants aggregated into mixes of short and long filaments with roughly the same number of filaments as WT tau. These mutations are further from the ^{275}VQIINK and ^{306}VQIVYK sequences and may not have as strong of effects on those regions even if they are enhancing the β-strand character around them. These minor changes may indicate that the root causes of these tauopathies may lie somewhere other than direct increases in tau aggregation. For example, the N296 position is also associated with other FTDP-17 mutations that can lead to splicing defects and V337M can lead to increased phosphorylation ((*182*) and reviewed in (*264*)).

While general trends in the aggregation of mutated proteins could be identified, the interactions with microtubules followed an alternate pattern. Only mutations that occur within one of the 18 amino acid repeats in the MTBR displayed effects on the ability of the protein to stabilize assembly of microtubules, confirming previous results with other FTDP-17 mutations (*265*). Of the mutants that fell outside of the MTBR or in one of the interrepeats (R5L, L315R, V337M, E342V, K369I, and G389R) only L315R displayed any decrease from WT tau in the total amount of microtubule polymerization. This was a relatively minor change compared to the effects of the other mutants and was in agreement with previous results (*184*). All of the mutants located within one of the repeat regions were unable to stabilize the same maximum level of

microtubule polymerization, stabilized a slower rate of polymerization, or altered the lag time compared to WT tau. These results, combined with the large percentage of FTDP-17 mutations located in a MTBR, indicate that interactions with microtubules may play a key role in the progression of these tauopathies. Further research is needed to determine how altered microtubule interactions may be affecting tau aggregation as well as if affected microtubule dynamics may be playing a more direct role in toxicity.

Direct comparisons of our results to previous studies can be difficult due to differing experimental setup. The most common differences involve the type of tau aggregation inducer employed, the buffer conditions, and the tau isoform used in the assays. Our data confirm previous results indicating that P301L is a very fast aggregator compared to WT, several of these FTDP-17 mutants have decreased abilities to stabilize assembly of microtubules and increased aggregation, and K369I typically forms smaller aggregates (*214, 266-268*). Occasionally, differences were seen in the kinetics of aggregation that may be ascribed to how the data are measured and what type of curve they are fit to. The Finke-Watzky mechanism appears to be best able to describe the complex process of tau aggregation in a simplified manner and accurately represented differences in the mechanisms of aggregation for the studied mutations.

The fact that significant differences exist in how these mutants aggregate, the types of aggregates that are seen, as well as their ability to perform normal functions of tau in vitro should not be particularly surprising given the diversity in disease phenotype associated with FTDP-17 cases and tauopathies in general. Conformational differences among the mutations are likely to affect the protein's aggregation in complex ways which could then have a direct impact on disease

progression. These differences could manifest themselves in the initiation, morphology, or spread of aggregation. While the end result may always be aggregation of tau and degeneration of neurons, the mechanisms by which the various diseases reach that point may be drastically different and alternate therapeutic interventions may be required based on the initiating cause of the disorder. As it is likely that sporadic tauopathies also differ in their initiating factors, information about how certain FTDP-17 mutations affect tau may be applicable to the progression of those diseases as well.

In order to attempt to explain some of these initiating factors I attempted to find correlations between the intrinsic effects of our chosen mutations and their effects on tau in the various assays. However, I was unable to detect any correlations among these components. It is likely that these effects are complicated and dependent on the specific location of the mutation.

Given the importance of the MTBR in the function and dysfunction of tau, it is likely that location is a very important factor for how these mutations are affecting the aggregation of the protein. Mutations that increased the hydrophobicity and β-strand character, especially in the MTBR, seem to increase the rate of nucleation and decrease the average filament length but exceptions to this exist as well. The causes of familial tauopathies are likely quite complex. Mutation-induced effects on intrinsic properties of tau may alter its propensity for aggregation or the morphology of its aggregates and lead to early-onset tauopathies. However, changes in mRNA splicing, interactions with microtubules, or phosphorylation levels could also lead to aggregation of the protein or neuronal death. In addition, the mutations could also affect other

properties of the protein including interactions with protein degradation systems, kinases, or fast axonal transport among others.

Because of the variation in location and effects on intrinsic properties of tau, significant differences exist in how FTDP-17 mutations affect the protein. While these mutations can be quite useful for in vitro and in vivo models of tau aggregation and tauopathies, it may be important to consider the differential effects when comparing results from various model systems. Further work on characterizing these mutations and their effects on in vivo organisms may help explain how the various FTDP-17 mutations are leading to tauopathies and how these mechanisms are affecting our understanding of the progression of sporadic tauopathies.

Table 3.1. **One-way ANOVA analysis with Tukey's multiple comparison test for ThS results.**

One-way ANOVA with Tukey's multiple comparison post test

ThS

	WT	R5L	G272V	ΔN296	P301L	G303V	L315R	S320F	V337M	E342V	S352L	K369I	G389R
WT	x	ns	ns	ns	*	ns	ns	ns	ns	ns	***	***	ns
R5L	ns	x	ns	ns	ns	ns	ns	ns	ns	ns	ns	***	ns
G272V	ns	ns	x	ns	ns	ns	*	ns	ns	ns	ns	***	ns
ΔN296	ns	ns	ns	x	***	*	ns	**	ns	ns	***	***	*
P301L	*	ns	ns	***	x	ns	***	ns	ns	**	ns	***	ns
G303V	ns	ns	ns	*	ns	x	**	ns	ns	ns	ns	***	ns
L315R	ns	ns	*	ns	***	**	x	**	ns	ns	***	***	**
S320F	ns	ns	ns	**	ns	ns	**	x	ns	*	ns	***	ns
V337M	ns	ns	ns	ns	ns	ns	ns	ns	x	ns	**	***	ns
E342V	ns	ns	ns	ns	**	ns	ns	*	ns	x	***	***	ns
S352L	***	ns	ns	***	ns	ns	***	ns	**	***	x	***	ns
K369I	***	***	***	***	***	***	***	***	***	***	***	x	***
G389R	ns	ns	ns	*	ns	ns	**	ns	ns	ns	ns	***	x

ns – No statistically significant differences
* P < 0.05
** P < 0.01
*** P < 0.001

Table 3.2. **One-way ANOVA analysis with Tukey's multiple comparison test for LLS results.**

One-way ANOVA with Tukey's multiple comparison post test

LLS

	WT	R5L	G272V	ΔN296	P301L	G303V	L315R	S320F	V337M	E342V	S352L	K369I	G389R
WT	x	ns	**	ns	**	***	***	***	ns	ns	***	***	ns
R5L	ns	x	***	*	ns	***	***	***	ns	ns	ns	***	**
G272V	**	***	x	ns	***	***	ns	**	*	*	***	***	ns
ΔN296	ns	*	ns	x	**	***	*	***	ns	ns	***	***	ns
P301L	**	ns	***	**	x	***	***	***	ns	*	ns	***	***
G303V	***	***	***	***	***	x	**	ns	***	***	***	ns	***
L315R	***	***	ns	*	***	**	x	*	**	**	***	***	ns
S320F	***	***	**	***	***	ns	*	x	***	***	***	ns	***
V337M	ns	ns	*	ns	ns	***	**	***	x	ns	*	***	ns
E342V	ns	ns	*	ns	*	***	**	***	ns	x	**	***	ns
S352L	***	ns	***	***	ns	***	***	***	*	**	x	***	***
K369I	***	***	***	***	***	ns	***	ns	***	***	***	x	***
G389R	ns	**	ns	ns	***	***	ns	***	ns	ns	***	***	x

ns – No statistically significant differences
* P < 0.05
** P < 0.01
*** P < 0.001

Table 3.3. **One-way ANOVA analysis with Tukey's multiple comparison test for tau polymerization nucleation, k_1 rate constant, results.**

One-way ANOVA with Tukey's multiple comparison post test

Kinetics k1

	WT	R5L	G272V	ΔN296	P301L	G303V	L315R	S320F	V337M	E342V	S352L	G389R
WT	x	ns	**	ns	ns	***	***	***	ns	ns	ns	ns
R5L	ns	x	**	ns	ns	***	***	***	ns	ns	ns	ns
G272V	**	**	x	**	***	***	***	***	ns	***	**	ns
ΔN296	ns	ns	**	x	ns	***	***	***	ns	ns	ns	ns
P301L	ns	ns	***	ns	x	***	***	***	ns	ns	ns	ns
G303V	***	***	***	***	***	x	ns	***	***	***	***	***
L315R	***	***	***	***	***	ns	x	***	***	***	***	***
S320F	***	***	***	***	***	***	***	x	***	***	***	***
V337M	ns	ns	ns	ns	ns	***	***	***	x	ns	ns	ns
E342V	ns	ns	***	ns	ns	***	***	***	ns	x	ns	ns
S352L	ns	ns	**	ns	ns	***	***	***	ns	ns	x	ns
G389R	ns	ns	ns	ns	ns	***	***	***	ns	ns	ns	x

ns – No statistically significant differences
* $P < 0.05$
** $P < 0.01$
*** $P < 0.001$

Table 3.4. **One-way ANOVA analysis with Tukey's multiple comparison test for tau polymerization elongation, k_2 rate constant, results.**

One-way ANOVA with Tukey's multiple comparison post test

Kinetics k2

	WT	R5L	G272V	ΔN296	P301L	G303V	L315R	S320F	V337M	E342V	S352L	G389R
WT	x	ns	ns	ns	ns	**	*	*	ns	ns	ns	ns
R5L	ns	x	ns	ns	ns	***	**	**	ns	*	*	ns
G272V	ns	ns	x	ns	ns	ns	ns	ns	ns	ns	ns	ns
ΔN296	ns	ns	ns	x	ns	ns	ns	ns	ns	ns	ns	ns
P301L	ns	ns	ns	ns	x	***	***	***	*	***	**	*
G303V	**	***	ns	ns	***	x	ns	ns	ns	ns	ns	ns
L315R	*	**	ns	ns	***	ns	x	ns	ns	ns	ns	ns
S320F	*	**	ns	ns	***	ns	ns	x	ns	ns	ns	ns
V337M	ns	ns	ns	ns	*	ns	ns	ns	x	ns	ns	ns
E342V	ns	*	ns	ns	***	ns	ns	ns	ns	x	ns	ns
S352L	ns	*	ns	ns	**	ns	ns	ns	ns	ns	x	ns
G389R	ns	ns	ns	ns	*	ns	ns	ns	ns	ns	ns	x

ns – No statistically significant differences
* $P < 0.05$
** $P < 0.01$
*** $P < 0.001$

Table 3.5. **One-way ANOVA analysis with Tukey's multiple comparison test for results of total polymerization of microtubules.**

One-way ANOVA with Tukey's multiple comparison post test

MT Polymerization Total

	WT	R5L	G272V	ΔN296	P301L	G303V	L315R	S320F	V337M	E342V	S352L	K369I	G389R
WT	x	ns	ns	ns	ns	ns	ns	***	ns	ns	***	ns	*
R5L	ns	x	ns	ns	ns	*	ns	***	ns	ns	***	ns	ns
G272V	ns	ns	x	ns	ns	***	ns	***	ns	ns	***	ns	ns
ΔN296	ns	ns	ns	x	ns	ns	ns	***	ns	ns	***	ns	**
P301L	ns	ns	ns	ns	x	ns	ns	***	ns	ns	***	ns	**
G303V	ns	*	***	ns	ns	x	**	**	***	**	***	ns	***
L315R	ns	ns	ns	ns	ns	**	x	***	ns	ns	***	ns	ns
S320F	***	***	***	***	***	**	***	x	***	***	ns	***	***
V337M	ns	ns	ns	ns	ns	***	ns	***	x	ns	***	ns	ns
E342V	ns	ns	ns	ns	ns	**	ns	***	ns	x	***	ns	ns
S352L	***	***	***	***	***	***	***	ns	***	***	x	***	***
K369I	ns	ns	ns	ns	ns	ns	ns	***	ns	ns	***	x	*
G389R	*	ns	ns	**	**	***	ns	***	ns	ns	***	*	x

ns – No statistically significant differences
* $P < 0.05$
** $P < 0.01$
*** $P < 0.001$

Table 3.6. **One-way ANOVA analysis with Tukey's multiple comparison test for results of the rates of microtubule polymerization.**

One-way ANOVA with Tukey's multiple comparison post test

MT Polymerization Rate, kapp

	WT	R5L	G272V	ΔN296	P301L	G303V	L315R	S320F	V337M	E342V	S352L	K369I	G389R
WT	x	ns	ns	**	***	***	ns	***	***	*	***	ns	*
R5L	ns	x	ns	***	***	***	*	***	ns	ns	***	ns	ns
G272V	ns	ns	x	***	***	***	ns	***	ns	ns	***	ns	ns
ΔN296	**	***	***	x	ns	ns	*	ns	***	***	ns	**	***
P301L	***	***	***	ns	x	ns	*	ns	***	***	ns	***	***
G303V	***	***	***	ns	ns	x	**	ns	***	***	ns	***	***
L315R	ns	*	ns	*	*	**	x	***	***	**	***	ns	**
S320F	***	***	***	ns	ns	ns	***	x	***	***	ns	***	***
V337M	***	ns	ns	***	***	***	***	***	x	ns	***	***	ns
E342V	*	ns	ns	***	***	***	**	***	ns	x	***	*	ns
S352L	***	***	***	ns	ns	ns	***	ns	***	***	x	***	***
K369I	ns	ns	ns	**	***	***	ns	***	***	*	***	x	ns
G389R	*	ns	ns	***	***	***	**	***	ns	ns	***	ns	x

ns – No statistically significant differences
* P < 0.05
** P < 0.01
*** P < 0.001

Table 3.7. **One-way ANOVA analysis with Tukey's multiple comparison test for results of the lag times of microtubule polymerization.**

One-way ANOVA with Tukey's multiple comparison post test

MT Polymerization Lag Time

	WT	R5L	G272V	ΔN296	P301L	G303V	L315R	S320F	V337M	E342V	S352L	K369I	G389R
WT	x	ns	ns	ns	ns	ns	ns	***	ns	ns	***	ns	*
R5L	ns	x	ns	ns	ns	*	ns	***	ns	ns	***	ns	ns
G272V	ns	ns	x	ns	ns	***	ns	***	ns	ns	***	ns	ns
ΔN296	ns	ns	ns	x	ns	ns	ns	***	ns	ns	***	ns	**
P301L	ns	ns	ns	ns	x	ns	ns	***	ns	ns	***	ns	**
G303V	ns	*	***	ns	ns	x	**	**	***	**	***	ns	***
L315R	ns	ns	ns	ns	ns	**	x	***	ns	ns	***	ns	ns
S320F	***	***	***	***	***	**	***	x	***	***	ns	***	***
V337M	ns	ns	ns	ns	ns	***	ns	***	x	ns	***	ns	ns
E342V	ns	ns	ns	ns	ns	**	ns	***	ns	x	***	ns	ns
S352L	***	***	***	***	***	***	***	ns	***	***	x	***	***
K369I	ns	ns	ns	ns	ns	ns	ns	***	ns	ns	***	x	*
G389R	*	ns	ns	**	**	***	ns	***	ns	ns	***	*	x

ns – No statistically significant differences
* P < 0.05
** P < 0.01
*** P < 0.001

Chapter IV

Generating and characterizing novel tauopathy models in *C. elegans*

Chapter IV Generating and characterizing novel tauopathy models in *C. elegans*

4.1 Abstract

The mechanisms of aggregation and toxicity in tauopathies are not entirely understood but a variety of transgenic animal models have been developed to study these questions in an in vivo setting. Data from Chapters II and II indicate that the choice of isoform background or FTDP-17 mutation can directly and significantly impact the mechanisms of aggregation, aggregate morphology, and ability of the protein to perform its normal functions. I set out to develop and characterize novel in vivo models of tauopathies in order to determine how some of the factors described earlier affect these models and to use the models to address how these factors affect disease pathologies. *Caenorhabditis elegans* was selected as the model organism due to the ease of genetic manipulation and the relative simplicity of their nervous systems. To begin, I generated several *C. elegans* lines that express various types of tau. These included wild-type 2N4R tau, a P301L FTDP-17 mutant, a 7-Phos pseudophosphorylation mutant, and 3PO, a modified version of tau optimized for aggregation. Several of the resulting phenotypes were characterized for these lines in order to compare the effects of expressing various forms of tau. Worms expressing the types of tau associated with enhanced aggregation, P301L and 3PO, displayed decreased head-thrashing compared to worms expressing only GFP or wild-type tau. The lifespans of these worms appeared to be slightly decreased compared to worms expressing wild-type tau but not to a statistically significant degree. These worms also displayed axonal defects that may be leading to neuronal dysfunction. This demonstrates that *C. elegans* can be a useful system to analyze the differential effects of tau variants.

4.2 Introduction

Biochemical techniques and assays can be very useful in determining how modifications of tau, such as phosphorylation or inherited mutations, affect the aggregation of the protein or how it interacts with microtubules. While this can be very important, these techniques are unable to describe how those changes in aggregation and function affect neuronal dysfunction and death in a living organism. However, this limitation can be overcome by applying results obtained from biochemical assays to make rational decisions when designing an animal model. These could include using properties such as aggregate morphology or an altered ability to interact with microtubules to answer specific questions about how these properties affect toxicity. For example, the results from Chapter III indicate that some FTDP-17 mutations induce the formation of very long filaments while others induce aggregates that remain in a primarily oligomeric state. A transgenic worm line could be generated that expresses a form of tau associated with long filaments and another could be generated that expresses a form of tau associated with oligomeric aggregation. A variety of physiological and morphological characteristics could then be used to compare the effects of expressing each type of tau. Differences in these phenotypes would likely be due to the differential effects induced by each specific aggregate-type. In this manner, rational decision-making can be used to generate transgenic models that will allow us to isolate and compare the effects of specific traits associated with certain tau variants.

Tauopathies have been modeled in many different organisms including mice, flies, nematodes, and fish (*87, 197, 269, 270*). The model organism *C. elegans* was chosen for this study because it is relatively simple and inexpensive to generate multiple lines of transgenic animals making it

suitable for comparing the effects of various strains. Previous versions of *C. elegans* tauopathy models have typically used one of the FTDP-17 mutations in order to enhance tau aggregation and exacerbate its negative effects. One of the earliest models used V337M and P301L in the 1N4R isoform (*197*). The pan-neuronal expression of these tau variants induced a locomotion defect, known as "unc" for uncoordinated, that demonstrates neuronal defects within the worms. Degenerating neurons were confirmed by transmission electron microscopy. Insoluble tau was associated with these neurons and could be isolated from worms expressing FTDP-17 tau (*197*). Another model used P301L or R406W expressed in the mechanosensory neurons (*198*). Again, the transgenic worms expressing mutant tau forms displayed more functional and morphological defects in their neurons than those expressing wild-type forms of tau (*198*).

A more recent study utilized a truncated background, known as F3 and containing primarily MTBR regions, with a ΔK280 mutation as a pro-aggregant form. An anti-aggregant form was generated by adding the I277/308P mutations (*199*). The proline for isoleucine substitutions at those locations interrupts the β-strand character in the hexapeptide motifs that are so important for aggregation (*271*). The nucleation rates of the tau fragments were slow until a full-length version of tau with the V337M mutation was added. The combination of the F3ΔK280 fragment along with full-length V337M resulted in the formation of tau aggregates that were largely absent with the F3ΔK280-PP anti-aggregant form. The ability to aggregate was closely associated with morphological defects in the neurons that occurred in the form of axonal gaps, pre-synaptic defects, and mislocalized mitochondria (*199*). Interestingly, the addition of a known aggregation inhibitor reduced levels of insoluble tau and induced small reductions in the numbers of axonal gaps (*199*).

These models demonstrate that expression of tau in worms can result in protein aggregation and neuronal defects, two key aspects of tauopathies. With this in mind I set out to examine how expression of some of the various forms of tau described in Chapters II and III affected worms and their neurons. Some of the initial characterization and preliminary results from this study are presented here. This is an entirely new undertaking for my group and was carried out with the assistance and guidance of Dr. Brian Ackley and his group. The project is ongoing and will continue to expand but the first steps were designed to demonstrate that the models could be generated and that differential phenotypes could be detected that were simple to read and demonstrative of relative toxicity.

Initially, transgenic models expressing one of four different forms of tau were generated at varying expression levels. This study included wild-type 2N4R tau, P301L tau, and 7-Phos tau along with an extremely pro-aggregant form of the protein known as 3PO tau. This was treated as a positive control for aggregation and was originally optimized for that purpose by removing pattern breaking sequences in the first three potential MTBR with a purpose of enhancing β-strand character and propensity for aggregation (*272*). Based on previously published results 3PO tau was supposed to aggregate very quickly and induce the most severe phenotypes.

4.3 Experimental Procedures

4.3.1 Generation of transgenic worms. The *C. elegans* N2 strain was used for the microinjection and maintained at 20-22.5°C as described earlier (*273*). All tau used was in the 2N4R isoform background. Wild-type tau (*Prgef-1::tau::gfp*), P301L tau (*Prgef-*

1::tau(P301L)::gfp), pro-aggregant tau (*Prgef-1::tau(3PO)::gfp*), and pseudohyperphosphorylated tau (*Prgef-1::tau(7-Phos)::gfp*) were injected into the animals at varying concentrations including 0.5, 5, and 50 ng μl^{-1}. The Pstr-1 co-injection marker was injected at a concentration of around 5 ng μl^{-1}.

4.3.2 Motility assays. The motility of the worms was measured through a thrashing assay. A single adult worm was placed in M9 buffer and the number of head thrashes/minute was counted. A head thrash was defined as a full movement from one side of the worm to the opposite side.

4.3.3 Lifespan assays. 20 worms at the L4 stage were placed onto a plate. They were counted after 24 hours, which was the "Day 0" time point. The worms were counted every 24 or 48 hours after that point until at least half of the worms had died.

4.3.4 Imaging of neurons. Z-stacks of the neurons were collected using an Olympus FV1000 confocal microscope with multi-tracking parameters and a 60x Plan-apochromat objective.

4.4 Results

4.4.1 Motility defects associated with transgenic tau expression

The transgenic expression of tau induced an assortment of behavioral defects in the worms. One predominant example is the Unc, or uncoordinated, phenotype. This is characterized by an abnormal and inhibited locomotion and coiling when stationary. The severity of the phenotype was quantified by counting the head thrashes of worms suspended in M9 buffer. Transgenic

worms expressing only GFP were used as a tau-negative control. All of the worm lines expressing tau at injection concentrations of 5 ng/μL displayed impaired head thrashing ability compared to the GFP-control (Figure 4.1A). The mean number of head thrashes per minute decreased by around 18 for worm lines expressing wild-type tau at an injection concentration of 0.5 ng/μL when compared to GFP-only worms and around 12 for the worms expressing 7-Phos tau at the same concentration but these values were not considered significant according to an unpaired t-test (Figure 4.1B). However, the motility of lines expressing P301L and 3PO tau variants were significantly inhibited (Figure 4.1B).

4.4.2 Shorter lifespans for P301L and 3PO worms

The lifespans of transgenic *C. elegans* expressing wild-type, P301L, and 3PO tau at 5 ng/μL were measured and were affected by the tau variant expressed. The lifespans of P301L and 3PO worms were, on average, shorter than the wild-type tau worms (Figure 4.2). As the P301L and 3PO animals aged they became progressively less mobile, an event that appeared earlier than in the wild-type animals. These worms began dying earlier than wild-type tau worms. An average of 10% of these worms had died within 11 days of reaching adulthood while no wild-type tau worms died by that same time point. The means of the median survival time for each trial were 16.5 days for the wild-type tau worms, 15.25 days for the P301L worms, and 14.63 days for the 3PO worms.

Figure 4.1

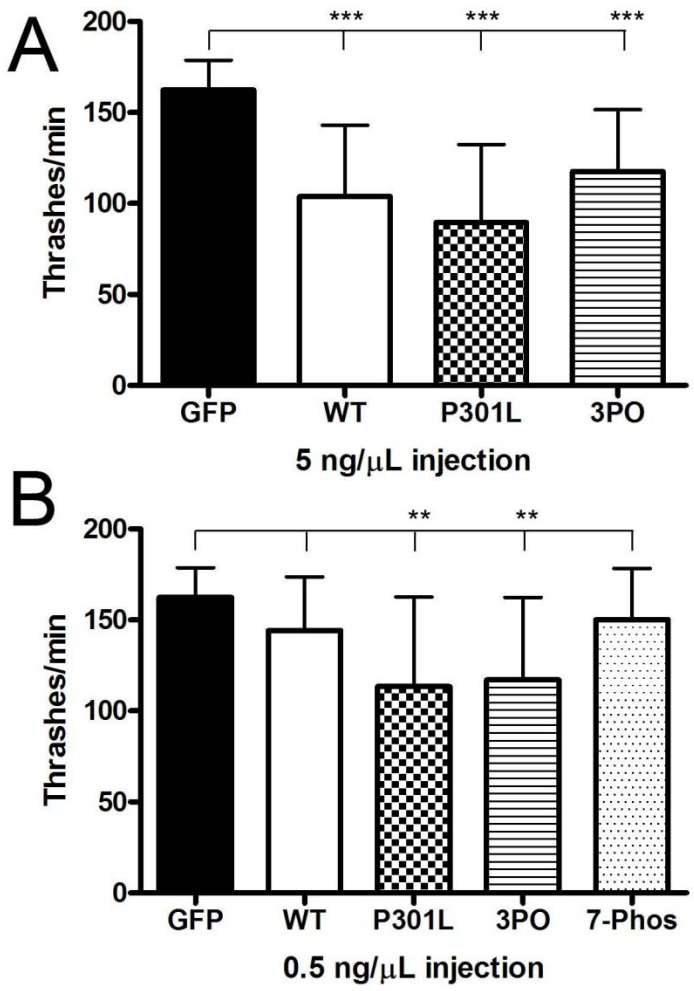

ftd

Figure 4.1. Head thrashes per minute for transgenic tau worms. Worms were placed in M9 buffer and the numbers of head thrashes were counted. The mean number of thrashes per minute are displayed for transgenic worms expressing (A) GFP, wild-type 2N4R tau, P301L tau, and 3PO tau with all tau lines previously injected at 5 ng μL^{-1} and (B) GFP, wild-type 2N4R tau, P301L tau, 3PO tau, and 7-Phos tau with all tau lines previous injected at 0.5 ng μL^{-1}. Error bars represent ±SD with an $n \geq 15$ for (A) and $n \geq 8$ for (B). Stars represent p-value results from Student's unpaired t tests comparing means from each strain. (*), $p < 0.05$; (**), $p < 0.01$; (***), $p < 0.001$.

Figure 4.2

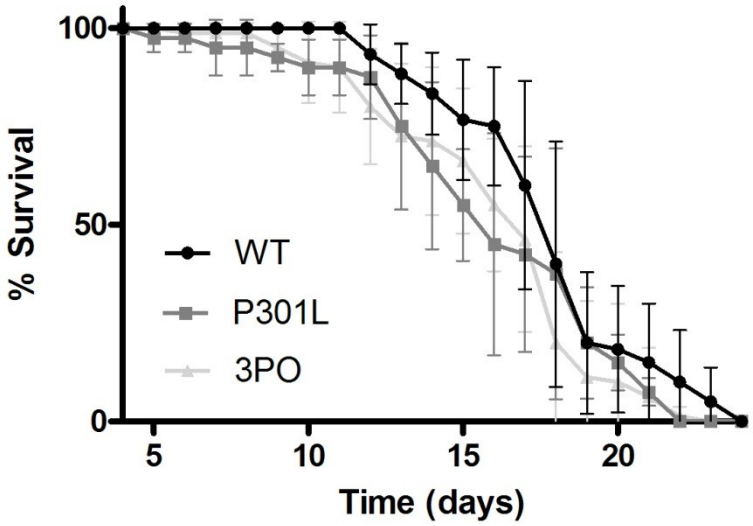

Figure 4.2. Lifespan of transgenic tau worms. This graph displays the percent of worms surviving a number of days after reaching adult the stage. 20 age-matched worms were counted from the time they reached adulthood until death. Error bars represent ±SD with an n=3 for wild-type tau, n=2 for P301L tau, and n=4 for 3PO tau.

4.4.3 Axonal defects associated with P301L and 3PO tau

Confocal microscopy images of individual neurons reveal that GFP-labeled wild-type tau is expressed throughout all neurons in the worms (Figure 4.3). The tau appears to be filamentous, particularly in the axons. Although this has not been confirmed, it is likely that the tau is binding to the microtubules and maintaining its function even in the worms. The axons in tail ganglion appear to be normal in worms expressing wild-type tau (Figure 4.4A). This stands in contrast to worms expressing P301L tau (Figure 4.4B). These worms displayed kinked axons which is an indication of some type of defect. These defects are consistent with the motility defects associated with the P301L strains (Figure 4.1). The P301L tau appears to be more diffuse than the wild-type tau. This pattern could be due to decreased interactions with microtubules and potentially indicative of some aggregation. The aggregate-prone 3PO version of tau displayed very little labeling of axons (Figure 4.5). In this version of tau the sequences associated with tau aggregation have been modified to remove pattern-breaking sequences that inhibit formation of the β-strands. This may affect microtubule-binding but the enhanced β-strands lead to aggregation that can occur very quickly. These aggregates may be apparent in the somatodendritic compartment.

Figure 4.3

Figure 4.3 Expression of wild-type tau. The expression of GFP-labeled wild-type tau under the Prgef-1 promoter is pan-neuronal. The tau appears filamentous, especially throughout the axon. This may indicate binding to microtubules. Images generated by Brian Ackley.

Figure 4.4

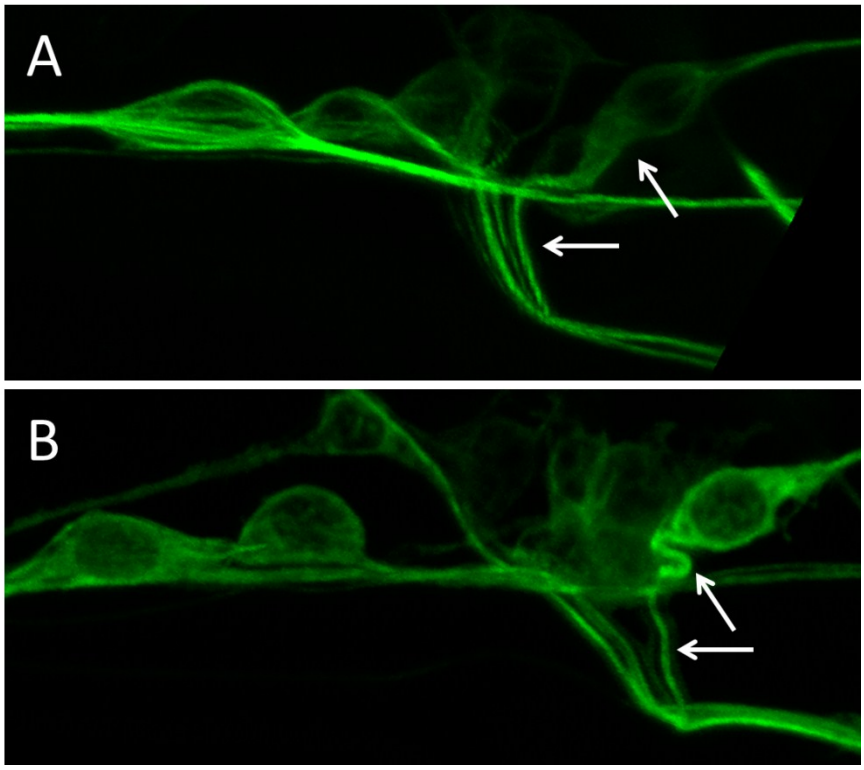

Figure 4.4 Axonal defects associated with P301L tau expression. A) Tail ganglion in worms expressing GFP-tagged wild-type tau. The axons appear similar to non-transgenic worms. B) The same tail ganglion in worms expressing GFP-tagged P301L tau. The axons appear kinked which is consistent with the reduced motility in these worms. Images generated by Brian Ackley.

Figure 4.5

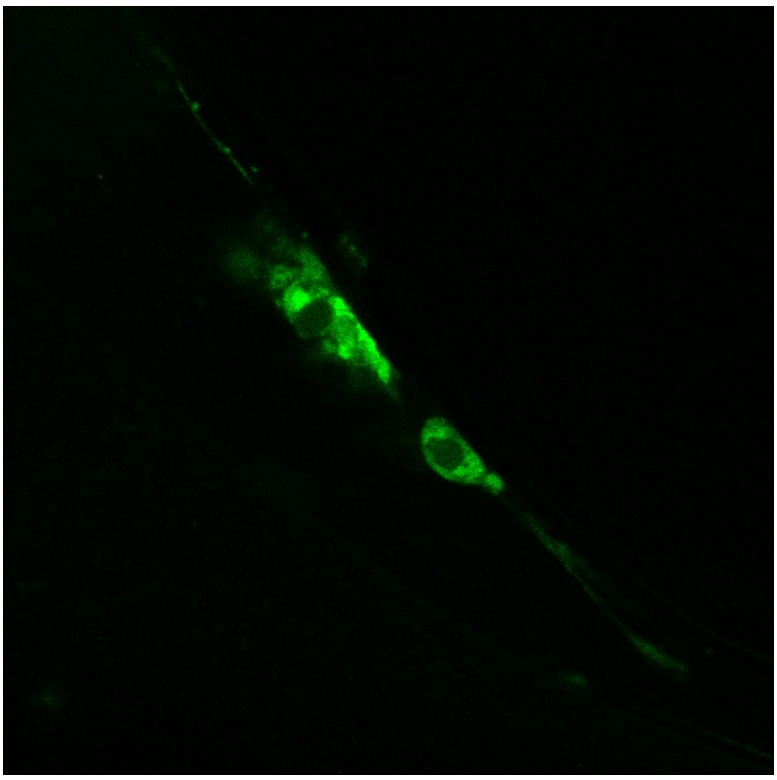

Figure 4.5 Worms expressing GFP-tagged 3PO tau display aggregation and little labeling of axons. The worms expressing the GFP-tagged 3PO tau lack the filamentous labeling on display in worms expressing wild-type and P301L tau variants. This may indicate a lack of binding to microtubules. The clumping in the cell body likely indicates an increase in tau aggregation compared to worms expressing the other forms of tau. Image generated by Brian Ackley.

4.5 Discussion

The results presented above demonstrate that transgenic expression of human tau can induce harmful effects on the neurons of *C. elegans* worms. Expression of those types of tau that have been determined to be pro-aggregant forms, such as P301L and 3PO, typically displayed more severe phenotypes than wild-type tau and, in some cases the 7-Phos pseudophosphorylation mutants. This suggests that tau aggregation is a likely cause of neuronal dysfunction in the worms.

One indication of this neuronal dysfunction is the motility defects detected in the worms. This type of motor defect is not seen in most human tauopathies but is associated with some, such as PSP (*274*). The varying symptoms associated with human tauopathies are affected by which regions of the brain that are affected by the tau pathology. The motor neurons of *C. elegans* can stand in as a model for human neurons with motor defects as an easily detectable phenotype for dysfunction. The causes of this dysfunction should be elucidated in the future. This will require characterization of the aggregates formed in these models in order to determine their similarity to the in vitro results from Chapters II and III. Further imaging of the neurons will occur as well and strains of worms designed to test for pre- and post-synaptic dysfunction are being generated.

Clear differences in the lifespans of the transgenic worms were not detected to a level of statistical significance but it did appear that some of the 3PO and P301L worms may begin dying earlier than those expressing wild-type tau (Figure 4.2). This again suggests that pro-aggregant forms of tau are inducing more toxic effects on the worms that may be shortening their lifespans.

The 3PO and P301L worms appeared to be less mobile than wild-type worms as they aged and further characterization of exacerbated phenotypes in the aged worms may be necessary.

The images of neurons expressing GFP-labeled tau seem to be consistent with the results from motility and lifespan assays. The worms expressing wild-type tau do not seem to exhibit any axonal defects (Figure 4.4A). The tau appears to be labeling microtubules in the axon as it would be expected to. However, in more aggregate-prone versions of tau this labeling appears to be decreased (Figure 4.4B) or completely abolished (Figure 4.5). *C. elegans* do not express endogenous tau but do express a protein with repeat regions similar to tau (*275*). It is unlikely that decreases in the binding of transgenic tau to microtubules are inducing negative effects so the defects are likely related to aggregation of the protein. Further studies will be needed to confirm insoluble tau levels in these worms. The worms expressing 3PO tau did display highly concentrated areas expression that are likely to be aggregates. These appear to be morphologically different than NFTs but further characterization will be required.

The characterization of worms expressing these different forms of tau demonstrates that transgenic worms can be used to model certain simplified aspects of tauopathies. The data from the motility assay indicate that neuronal dysfunction can be detected rather easily. They seem consistent with previous demonstrations that aggregate-prone versions of tau are associated with greater dysfunction and toxicity. In addition, the images of axonal defects and possible tau aggregation are consistent as well. In the future, these same assays can be used to characterize differences that arise due to expression of other types of tau and in other isoforms, including those described in Chapters II and III. The comparisons of the tau isoforms or various FTDP-17

mutations in an in vivo setting will give us the opportunity to take biochemical differences that are evident in our in vitro assays and determine what effects they might be having in a more physiological setting.

Chapter V

Conclusions and Future Directions

Chapter V Conclusions and Future Directions

5.1 Introduction

Tauopathies, including AD, are among the greatest health challenges facing the United States and other industrialized nations. While much progress has been made in treating and preventing other major causes of death, there are no effective treatments that can slow the progression of these diseases. In fact, many important mechanisms of this disease progression have yet to be elucidated. In order for effective treatments to be developed, a more complete understanding of the mechanisms of tau aggregation and toxicity will be needed. This can be addressed by determining what factors initiate the aggregation of tau as well as elucidating the causes of varying pathologies that are associated with tauopathies in humans as well as in animal models of the diseases. The studies described above attempted to address how specific modifications of tau affect its propensity to aggregate and perform its normal functions in order to learn about the initiation of tau aggregation and its resulting pathologies. This information can then be applied to the design of in vivo experiments focused on answering questions about tau toxicity and disease progression.

The most heavily studied post-translational modification of tau is its phosphorylation and many of the links between hyperphosphorylation and tau aggregation are widely characterized. It may be the most important factor in initiating the aggregation of tau in sporadic tauopathies. Prior to aggregation, tau seems to undergo conformational changes that result in an aggregate-prone form (*55*). Changes in phosphorylation patterns seem to have the ability to affect the conformation of the tau protein in different manners (*229*). Hyperphosphorylation, especially at specific sites, may be an initiator of this conformational change and lead to forms of the protein that are

particularly prone to aggregating. However, similar phosphorylation patterns may not induce similar changes in conformation for all of the isoforms due to the presence or absence of certain exons. While hyperphosphorylation of tau is seen in all tauopathies, the diseases can differ according to the tau isoform content found within the aggregates. Specific phosphorylation markers can be identified with particular tauopathies which indicates that the phosphorylation pattern may be important in the development of that particular phenotype. Differences between phosphorylation patterns may affect some tau isoforms differently than others and could induce differential propensities for aggregation. Alterations in the aggregate morphology and isoform content found in various tauopathies may be due to conformational differences induced by certain combinations of phosphorylated residues.

The FTDP-17 mutations are another modification of tau associated with conformational changes and protein aggregation. These are autosomal dominant mutations that lead to very aggressive forms of frontotemporal dementia in which tau pathology occurs much earlier than that which is seen in sporadic tauopathies. The pathologies associated with these mutations are varied but can resemble the pathologies of the more common sporadic tauopathies. Determining the causes of these differences could lead to a better understanding of the progressions of other tauopathies. One of the most obvious differences occurs within the mutations themselves. These mutations are located throughout the protein and induce a variety of intrinsic changes to the biochemical properties of tau. Characterizing how these mutations affect the aggregation and function of tau allows us to directly compare them to each other and helps determine what factors may be particularly important for the initiation and propagation of tau aggregation and how these changes may manifest themselves in the final disease pathologies. A better understanding of the

mechanisms underlying the progression of these diseases will allow for a more targeted approach to therapeutic intervention that will hopefully lead to more successful treatment outcomes.

The results from our studies indicate that the effects of two important modifiers of tau can vary widely based on the isoform background or type of mutation. Many previous in vitro and in vivo experiments focused on tau have been performed with a single isoform or with a single FTDP-17 mutation. Information gathered from these simplified studies has been and will continue to be very valuable. However, when considering how tau is behaving in an actual disease it is prudent to understand that the effects may not be the same for every tau isoform. Furthermore, the effects may also be different when all six isoforms are present or their ratios are altered due to changes in mRNA splicing. Similarly, utilizing a particular FTDP-17 mutation in an in vivo model of tauopathy may not yield the same results as wild-type tau or another FTDP-17 mutated version.

5.2 Phosphorylation and tau isoforms

Hyperphosphorylation is one of the most common characteristics associated with aggregated tau in all tauopathies. Most evidence suggests that hyperphosphorylation of tau is sufficient to induce aggregation of the protein although its role in an in vivo setting is a matter of some debate. Hyperphosphorylation appears to modify the conformation of tau (*229*). This has been postulated to be a tightening of the global hairpin conformation. The tau isoforms display differences in the properties of their aggregation and it stands to reason that modifications that alter their conformation may be affected by the presence or absence of the alternatively spliced exons. Given that some tauopathies are associated with preferential aggregation of certain types

of isoform it is possible that hyperphosphorylation and how it affects the isoforms may play a role in changing how tau aggregates in these diseases.

Indeed, the results from Chapter II indicate that phosphorylation patterns do not necessarily have the same effects on the in vitro polymerization and microtubule interactions of the six tau isoforms. Clear differences exist in how the six isoforms aggregate and interact with microtubules. The most obvious factor affecting functional and dysfunctional differences between isoforms is the presence or absence of exon 10. This exon contains the 1-2 interrepeat region, including the ^{275}VQIINK sequence involved in tau-tau interactions, and the repeat region of the 2nd MTBR. The 4R tau isoforms aggregate quicker and to a larger degree as well as are better able to stabilize the assembly of microtubules than their corresponding 3R isoforms (Figures 2.2, 2.4, and 2.10). The kinetics of aggregation (Figure 2.9) indicate that the mechanisms involved can vary according to isoform type as well. The 7-Phos modifications seemed to enhance tau aggregation in the 4R isoforms while seeming to inhibit aggregation of the 3R isoforms in the assays.

In AD and some other tauopathies, all isoforms are included in the aggregates in roughly the same proportions as found in the normal brain while the aggregates from other tauopathies are primarily made up of 3R or 4R isoforms. The demonstration that a similar phosphorylation pattern can enhance or inhibit tau aggregation depending on the isoform type can have significant implications for the initiation of tauopathies. For example, it could help describe how differential aggregation of the tau isoforms arises in some tauopathies but not in others. It is possible that hyperphosphorylation could occur in different patterns based on the expression

levels of various kinases in certain cell-types or regions of the brain. Specific phosphorylation patterns may enhance aggregation of 4R isoforms while inhibiting aggregation of 3R isoforms or vice versa.

Pseudophosphorylation also induced isoform-specific inhibitory effects on the protein's ability to stabilize assembly of microtubules (Figure 2.10). Changes in the tau isoform ratio can affect the stability of microtubules and are also associated with early-onset forms of tauopathy (*276*). The isoform-specific alterations in function due to hyperphosphorylation demonstrated here could be playing a role in disease initiation by changing the dynamics of microtubules or increasing the concentrations of cytosolic tau.

The evidence from this study clearly suggests that a similar phosphorylation pattern can induce very different effects on the propensity of each isoform to aggregate or stabilize microtubule assembly in our assays (Figures 2.6, 2.7, and 2.10). The SDS-resistant, but urea-sensitive, electrophoretic shift associated with the 7-Phos mutation (Figure 2.1C) provides evidence that the changes induced by pseudophosphorylation are conformational in nature. The differences in magnitude suggest that these changes are unique for each the isoforms. Previous work with fluorescence resonance energy transfer (FRET) demonstrated that pseudophosphorylation mutations, similar to the ones generated in this study, tightened the global hairpin conformation for 2N4R tau and resulted in a conformation recognized by antibodies that detect pathological tau (*229*). The highly flexible nature of tau and the margin of error inherent in the FRET analysis prevent a detailed understanding of the structural characteristics of tau but general conclusions can be drawn. The results from this study indicate that identical phosphorylation

patterns can affect isoforms differently and strongly suggest that this is due to isoform-specific conformational differences. Similar FRET experiments could be utilized to help confirm this and determine specific information about how the 7-Phos pseudophosphorylation mutations are affecting the conformation of the other five isoforms.

5.3 FTDP-17 mutations

The disease phenotypes and pathologies associated with FTDP-17 mutations can vary as widely as those associated with the entire range of sporadic tauopathies. For example, tau aggregates are deposited in different regions on the brain and still typically associate with neurodegeneration in the same regions. These aggregates can appear very different from each other. Straight or helical filaments are formed in some cases while tau fibrils are virtually nonexistent in others. Larger inclusions can resemble NFTs, typically seen in AD, while others are more like Pick bodies or globose tangles. The results from in vitro assays described in Chapter III clearly indicate that the specific mutation can have dramatic effects on the morphology of tau aggregates that are formed. These differences are likely to influence the progression of human tauopathies and may alter results from animal models of the diseases.

In FTDP-17-related disorders, isoform expression in the brain can remain normal or vary. In a similar manner, the aggregates associated with the diseases can be made up of all isoforms or only a particular subset of isoforms even when expression levels of the isoforms have not changed. The age of onset for the familial forms of diseases varies but is typically much earlier than that of sporadic tauopathies. This early age of onset indicates that the initiation of the disease process likely begins earlier than it does for sporadic tauopathies or the diseases progress

much more rapidly once they are initiated. Many of the FTDP-17 forms of tau aggregate much more readily compared to wild-type protein, a property that makes them very useful for transgenic animal models. Despite their uses in animal models, not all FTDP-17 mutations may accurately reflect mechanisms associated with sporadic tauopathies and could, in fact, be very different from other FTDP-17 mutations. The differences between the various FTDP-17 disorders may tell us a lot about how other tauopathies are initiated. Early-onset tauopathies may arise due to enhanced aggregation propensity through direct means, such as alteration of tau conformation, or indirect means, such as increased phosphorylation levels. It may also involve altered mRNA splicing levels or increased soluble levels of tau through inhibited interactions with microtubules. By learning more about the initiation of FTDP-17-related tauopathies we can also learn more about the more common sporadic tauopathies.

This set of experiments was designed to characterize the in vitro aggregation and function of a group of FTDP-17 tau mutants in order to identify differences in how the mutations affected these properties. Based on this information we can begin to determine the role these mutations play in initiating tauopathies and how they may lead to such varying pathologies. The results from these assays demonstrated that the mutants displayed very different profiles in their aggregation and ability to stabilize microtubules. This supports the hypothesis that initiation of these diseases can occur due to a variety of factors.

The most obvious differences between FTDP-17 mutations were displayed in the morphologies of the filaments that were formed in the presence of ARA (Figure 3.3). Several of the mutants formed very few filaments longer than 50 nm while others formed filaments that were much

longer than those formed from wild-type tau. This demonstrates that changes to a single amino acid can greatly enhance or inhibit the propensity for aggregation. Because all mutations do not enhance aggregation it is likely that this is not the sole cause of these diseases or their early-onset compared to sporadic tauopathies. Inhibition of the interactions with microtubules may also play a role by increasing the concentration of unbound tau to levels where nucleation of aggregation may occur. Our assay demonstrated that the effects of the mutants on the abilities to stabilize microtubule polymerization were variable when compared to each other (Figure 3.9). Alterations in splicing ratios may affect the concentrations of unbound tau as well as changing the microtubule dynamics. Effects such as these would not show up in the chosen assays but may be an initiating factor for some of the mutants, particularly those with profiles that appear similar to wild-type tau.

Like the 7-Phos pseudophosphorylation modifications, FTDP-17 mutations are likely affecting the conformation of the tau protein which induces the related effects on aggregation and microtubule interactions. However, unlike the hyperphosphorylation, these changes are likely to involve more direct effects on the local secondary structure. For example, enhancing the β-strand structure at a key location may greatly affect the likelihood that the protein maintains that structure long enough for the monomer to interact with another tau molecule. Certain sites are so common among the known FTDP-17 mutations that it is probable they have a key role somewhere in the process. For example, as part of every MTBR there is a PGGG sequence that may be involved in forming loops when binding to microtubules (*23*). Over a third of the known FTDP-17 mutations (Table 1.1) are located within one of the four PGGG sequences found in tau. Additionally, four more mutations are located at one of the two amino acid residues directly

downstream from these sequences meaning nearly half of all known FTDP-17 mutations reside in or next to one of these sequences (Figure 5.1). The PGGG sequence is highly flexible and may be present, in part, to break up the β-strand character of the sequences that lie just downstream. These sequences appear in the MTBR and may have an important function in the interactions with microtubules. However, due to some of these mutations, the β-strand character in these critical regions is likely enhanced and leading to increases in aggregation. The propensity for β-strand structure is a key factor in the aggregation of tau and the presence of longer β-strands or increased likelihood of forming this secondary structure could alter the kinetics of aggregation. Enhanced aggregation is a likely cause of the early-onset for many of these FTDP-17 related dementias. However, this raises the question of how the different morphologies of aggregates formed from the FTDP-17 mutants in our assays are affecting disease.

The pathologies of the various FTDP-17 diseases are similar yet also dissimilar in many ways. The end result is usually large inclusions of tau but these inclusions can vary morphologically, by isoform content, and type of fibril. The results of our assays demonstrate morphological differences in the type of aggregates formed by the various forms of tau. The tau aggregation is in a setting that is designed to promote aggregation through the addition of inducer molecules. In a disease setting the aggregation of tau takes place over the course of many years. The prion-like model of tau aggregate propagation would predict that a conformational change occurs in tau that is found in a relatively small region of the brain. As this conformationally-distinct form of tau aggregates it can also induce similar conformational changes in tau in neighboring regions of the brain. It stands to reason that the presence of mutated tau that may already be predisposed to

Figure 5.1

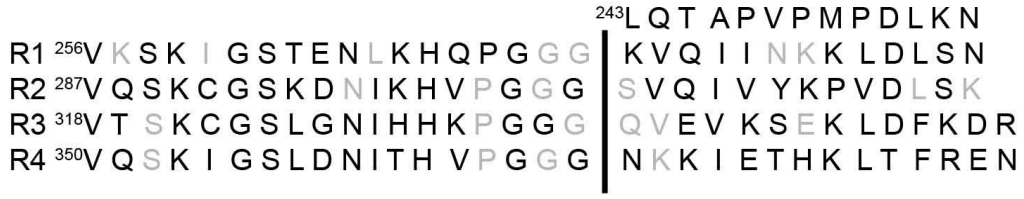

Figure 5.1 FTDP-17 mutations clustered in microtubule-binding repeat regions. Many of the FTDP-17 mutation sites (residues shown in gray) are located in the MTBR. Nearly half of all known mutations are located in or just downstream from one of the PGGG sequences.

exist in an altered conformation would allow for faster propagation and an earlier onset of disease. Even with FTDP-17 tau, the earliest onset of frontotemporal dementias does not typically occur for 2 to 3 decades. Over this long period of time it is likely that aggregates are joining together in order to form longer fibrils and larger inclusions. Mutants like G303V or S320F that typically did not form long filaments in our in vitro assays may still form larger tau aggregates over the course of many years. However, an increased propensity for aggregation that results in formation of small oligomers may instead lead to more aggressive propagation of the tau pathology. Further studies of these mutant forms of tau in an in vivo neuronal setting may answer some of these questions.

Additionally, alterations in the splicing ratio associated with some of these FTDP-17 mutations are likely to play a huge role in how they induce tauopathies but is not something that was addressed by this particular study. Of the mutations studied above, G303V and E342V are associated with increased inclusion of exon 10 while alterations in splicing ratios have not been found or have not been examined for the others. Despite the lack of changes in isoform splicing, differential isoform inclusion in aggregates are associated with several of the mutations. This typically takes the form of increased aggregation of 4R isoforms compared to 3R tau for this group of mutation. Further study into isoform-specific effects, such as those presented in chapter II, may help explain some of the causes behind this selective aggregation.

The negative effects of these mutations are also not likely to be entirely related to aggregation. Other FTDP-17 mutations may be inducing toxicity partially through altered microtubule dynamics. Some of the mutants were able to stabilize microtubule polymerization at a faster rate

than wild-type. In the context of a human neuron, enhancing polymerization of microtubules could be just as likely to induce harmful effects as an inhibited ability to stabilize the polymerization.

5.4 Conformation as destiny?

The evidence presented in the chapters above clearly indicates that relatively minor modifications of tau can induce large effects on the protein's aggregation and function. These modifications can be very small, such as a single amino acid substitution in the FTDP-17 mutations, or they can be larger, such as the effects of phosphorylation at multiple sites throughout the protein. The changes can also have very different effects depending on the isoform background. The electrophoretic shifts associated with the 7-Phos mutations were different for all of the six tau isoforms, likely because the amount of hairpin compaction was different for each of the isoforms (Figure 2.1). The extremely flexible nature of tau makes it extraordinary difficult to determine much information about the state of its secondary structure or global conformation. It is difficult to draw too many specific conclusions about the nature of the conformational change but the evidence seems to suggest that alterations to certain regions of secondary structure or the global hairpin conformation are affecting the kinetics of aggregation, the morphology of the aggregates, and its ability to interact with microtubules.

If tau aggregation is propagated through a prion-like manner of inducing conformational changes in other tau monomers then the specifics of these changes could be important. Conformational changes have been demonstrated to have a direct effect on aggregate morphology and disease phenotype for other proteins associated with aggregation diseases (*277-279*). Altered

conformation of individual tau monomers could be the key factor leading to different fibril morphologies, tau isoform inclusion, and disease progressions (*8, 172, 219*). It is possible that different "strains" of tau conformations may not respond to treatments that are designed to block tau aggregation. This may have to be considered when designing and testing these potential therapeutics.

According to the results described in Chapter II, a similar phosphorylation pattern has very different effects on 3R isoforms than it does on 4R isoforms. Attempts to regulate the phosphorylation levels of tau have been proposed as a potential treatment for these diseases (reviewed in (*280*)). This may still be an effective strategy for preventing aggregation or the buildup of toxic hyperphosphorylated soluble forms of the protein but the same strategies may not work for some of the tauopathies displaying isoform-specific aggregation that is being affected by phosphorylation.

5.5 *C. elegans* models

The current *C. elegans* models of tauopathy indicate that worms expressing the tau variants associated with aggregation appear to develop more severe phenotypes. They are less motile and display axonal dysfunction which supports the idea that tau aggregation is inducing these defects. The work that has been accomplished so far indicates that they can be used as an in vivo experimental system to use in conjunction with our in vitro assays. In this way, information that is learned from the biochemical assays can be used to design in vivo assays that answer questions about the toxic effects of tau aggregation. Differences in motility can indicate more dysfunction and microscopy techniques can directly visualize defects in neurons.

Additionally, the phenotypic differences between the strains of worms indicate that the type of tau expressed in animals can induce varied effects. This may have implications for the design of other animal models as well but further study with more altered forms of tau will be needed and are currently ongoing.

5.6 Future Directions

As mentioned in Chapter IV, the projects described here are ongoing and the next steps will primarily focus on continuing and expanding the *C. elegans* experiments. The initial characterization of the worms expressing wild-type, P301L, 7-Phos, and 3PO tau will continue in order to establish baselines for the motility and lifespan assays described earlier. In addition, more assays will be tested in order to determine if can be used to characterize relative levels of dysfunctions among the different strains. This will allow direct comparison of future *C. elegans* strains to the four established strains. Essentially, worms expressing 3PO tau are acting something like a positive control with very aggressive tau aggregation and severe phenotypes. On the other end of the scale, wild-type tau or I277/308P (incompetent for aggregation) will act as a negative control due to its minimal tau aggregation resulting in less severe phenotypes. There are many potential assays that can serve as readouts for neuronal dysfunction in these animals. Neuronal defects often lead to the Unc phenotype, described in Chapter IV, and other motility assays can detect the severity of the phenotype. The head thrashing assay is one example that has already been utilized (Figure 4.1). Examples of future assays include determining the average velocity of the worms as well as counting the percent that are able to successfully reverse direction when they detect an anterior touch stimulus. As the worms age

these motility defects appear to worsen for worms with the pro-aggregant forms of tau (P301L and 3PO) which means that a more profound effect may be seen with older worms than those that have just reached adulthood. Experiments that measure the phenotype of aged worms could provide a clearer expression of dysfunction.

While these assays can give a quick indication of relative dysfunction among the various lines, further analysis will also be needed. It may be beneficial to determine how these various forms of tau are affecting the neuronal projections of the worms. Axonal dysfunction can be examined through confocal microscopy due to the GFP-labeling of the tau constructs. Additionally, recently generated strains are in backgrounds that contain pre- and post-synaptic markers that will allow us to determine the effects that these various tau variants have on synaptic dysfunction, a problem in AD that may be linked to tau or Aβ oligomer accumulation (*281, 282*). Determining the types of aggregates that are present in the worms will help establish the effects that oligomers or larger fibrils can have on synapse function.

A characterization of insoluble tau will also indicate to what extent the tau variants described in Chapters II and III may contribute to future studies examining the relative toxicities of NFTs and oligomers. One of the major goals of this study was to utilize the in vitro assays for tau aggregation and microtubule stabilization to generate a profile of each of the modified versions of tau in order to apply that information to in vivo studies about their behavior in neurons and disease progression. Confirmation of the filament morphology will be an important initial step and can be performed with in situ oligomer specific antibodies or purification of insoluble tau followed by transmission electron microscopy. The purification of tau will also allow a

determination of total and insoluble levels of the protein for the various strains of worms. This will serve the purpose of validating that expression levels are similar for each of the strains as well as confirming the propensity for aggregation of each of the tau variants.

Following the characterization of the first group of worms, more lines will be generated. These should include several of the other FTDP-17 mutants and will include mutants that represent a cross-section of aggregate lengths and abilities to stabilize microtubule assembly. The DNA constructs of some of these have been completed while others are in the process of being generated at the current time. After they are generated, the new *C. elegans* strains can be characterized in the same manner as the original group described above.

After the completion of the characterization of several C. elegans lines it would be useful to express some of the same variants of tau in cell culture or other model organisms. This would allow comparisons across model systems. Similar results would bolster the argument that there are intrinsic differences between the tau isoforms or the FTDP-17 mutations that directly affect phenotypes in a predictable manner. If the results are dissimilar it would support the idea that organism-specific factors are altering the behavior of tau in other ways.

In addition to strains that express tau variants in all of their neurons, strains that restrict the expression to GABAergic or cholinergic neurons have already been generated and are being characterized. Certain collections of cholinergic neurons may be particularly vulnerable in AD and loss of these neurons can lead to some of the common cognitive impairments associated with the disease (*283, 284*). However, more recent evidence suggests that these neurons are not

affected until later in the disease (*285, 286*). According to some animals models it may, in fact, be the GABAergic neurons that are selectively targeted and the cause of this cognitive impairment but this is relatively untested (*287*). Both types of neurons innervate the hippocampus from the basal forebrain and may play key roles in promoting the memory loss and other deficiencies associated with AD. By testing the effects of limiting tau overexpression to these two types of neurons we hope to address some of the questions surrounding potential selective vulnerability by determining if tau expression has neuronal transmitter-specific effects in the worms.

In addition to the future work with animal models there are in vitro biochemical experiments that can be performed as well. One potential example would be to study some of the effects of the FTDP-17 mutations on the other five tau isoforms. Given the results in Chapter II it is clear that modifications, such as phosophorylation, can induce isoform-specific effects on aggregation and function that can be quite varying when compared to other isoforms. The missing exons may be altering any conformational changes due to the modifications. This same effect would likely happen with mutation-induced alterations. FTDP-17 mutations have several other specific links to tau isoforms that make this a particularly intriguing matter to study. Several of the mutations are associated with altered splicing ratios that increase or decrease the 4R:3R tau ratio. Even some mutations that do not affect mRNA splicing have been associated with preferential aggregation of specific isoforms, similar to that which is seen with several of the sporadic tauopathies discussed in Chapter I. Finally, several of the mutations are found in exon 10 which would make them absent from the 3R isoforms altogether. The vast majority of the mutations are located in the MTBR and the absence of this exon may alter the overall effects of a particular

mutation. Studies using rationally chosen FTDP-17 mutations in the various isoforms could help explain some of the differential aggregation by demonstrating the types of effects that may alter one isoform type but leave another unaffected. This information may be applicable to sporadic tauopathies that display differential aggregation such as progressive supranuclear palsy or Pick's disease.

The results described above indicate that many of the factors surrounding the initiation and propagation of tau aggregation are quite complex. Hyperphosphorylation may induce conformational changes in tau that increase its propensity to aggregate but the changes and their effects may be very different depending on which isoform of tau has been phosphorylated. In humans, FTDP-17 tau mutations can lead to the onset of tauopathies at a much younger age but the mutations may be initiating the disease in different manners. These could include direct or indirect methods of increasing aggregation or through decreased binding to microtubules. Additionally, the type of mutation was able to alter the morphology of the aggregates that are formed as well as its ability to carry out normal functions.

All of this implies that hyperphosphorylation and FTDP-17 mutations may induce conformational changes that affect the behavior of tau in these assays as well as in the afflicted brains. These conformational differences may be a key determinant in the pathologies associated with the different tauopathies. In addition, it may be challenging to directly compare results from animal models that utilize varying methods to induce tau aggregation. The studies described here show that the use of in vitro assays can allow us to determine how modifications of tau may be altering key factors associated with tauopathies, which is information that can then

be used to further analyze their effects in an in vivo setting. Through continuation of these studies we can begin to gain a clearer understanding of the mechanisms of tau toxicity in Alzheimer's disease and other tauopathies which will hopefully lead to advances in treatments of these disorders.

Bibliography

1. Weingarten, M. D., Lockwood, A. H., Hwo, S. Y., and Kirschner, M. W. (1975) A protein factor essential for microtubule assembly, *Proc Natl Acad Sci U S A 72*, 1858-1862.
2. Cleveland, D. W., Hwo, S. Y., and Kirschner, M. W. (1977) Physical and chemical properties of purified tau factor and the role of tau in microtubule assembly, *J Mol Biol 116*, 227-247.
3. Brion, J. P., Couck, A. M., Passareiro, E., and Flament-Durand, J. (1985) Neurofibrillary tangles of Alzheimer's disease: an immunohistochemical study, *J Submicrosc Cytol 17*, 89-96.
4. Alzheimer, A. (1907) Uber eine eigenartige Erkrankung der Hirnrinde, *Allgemeine Zeitschrift fur Psychiatrie und Psychisch-gerichtliche Medizin. 64*, 146-148.
5. Grundke-Iqbal, I., Iqbal, K., Quinlan, M., Tung, Y. C., Zaidi, M. S., and Wisniewski, H. M. (1986) Microtubule-associated protein tau. A component of Alzheimer paired helical filaments, *J Biol Chem 261*, 6084-6089.
6. Feany, M. B., and Dickson, D. W. (1995) Widespread cytoskeletal pathology characterizes corticobasal degeneration, *Am J Pathol 146*, 1388-1396.
7. Pollock, N. J., Mirra, S. S., Binder, L. I., Hansen, L. A., and Wood, J. G. (1986) Filamentous aggregates in Pick's disease, progressive supranuclear palsy, and Alzheimer's disease share antigenic determinants with microtubule-associated protein, tau, *Lancet 2*, 1211.
8. Lee, V. M., Goedert, M., and Trojanowski, J. Q. (2001) Neurodegenerative tauopathies, *Annu Rev Neurosci 24*, 1121-1159.
9. Dotti, C. G., Banker, G. A., and Binder, L. I. (1987) The expression and distribution of the microtubule-associated proteins tau and microtubule-associated protein 2 in hippocampal neurons in the rat in situ and in cell culture, *Neuroscience 23*, 121-130.
10. Papasozomenos, S. C., and Binder, L. I. (1987) Phosphorylation determines two distinct species of Tau in the central nervous system, *Cell Motil Cytoskeleton 8*, 210-226.
11. Binder, L. I., Frankfurter, A., and Rebhun, L. I. (1985) The distribution of tau in the mammalian central nervous system, *J Cell Biol 101*, 1371-1378.
12. Neve, R. L., Harris, P., Kosik, K. S., Kurnit, D. M., and Donlon, T. A. (1986) Identification of cDNA clones for the human microtubule-associated protein tau and chromosomal localization of the genes for tau and microtubule-associated protein 2, *Brain Res 387*, 271-280.
13. Goedert, M., Wischik, C. M., Crowther, R. A., Walker, J. E., and Klug, A. (1988) Cloning and sequencing of the cDNA encoding a core protein of the paired helical filament of Alzheimer disease: identification as the microtubule-associated protein tau, *Proc Natl Acad Sci U S A 85*, 4051-4055.
14. Andreadis, A., Brown, W. M., and Kosik, K. S. (1992) Structure and novel exons of the human tau gene, *Biochemistry 31*, 10626-10633.

15. Andreadis, A., Broderick, J. A., and Kosik, K. S. (1995) Relative exon affinities and suboptimal splice site signals lead to non-equivalence of two cassette exons, *Nucleic Acids Res 23*, 3585-3593.
16. Kosik, K. S., Orecchio, L. D., Bakalis, S., and Neve, R. L. (1989) Developmentally regulated expression of specific tau sequences, *Neuron 2*, 1389-1397.
17. Hong, M., Zhukareva, V., Vogelsberg-Ragaglia, V., Wszolek, Z., Reed, L., Miller, B. I., Geschwind, D. H., Bird, T. D., McKeel, D., Goate, A., Morris, J. C., Wilhelmsen, K. C., Schellenberg, G. D., Trojanowski, J. Q., and Lee, V. M. (1998) Mutation-specific functional impairments in distinct tau isoforms of hereditary FTDP-17, *Science 282*, 1914-1917.
18. Goedert, M., and Jakes, R. (1990) Expression of separate isoforms of human tau protein: correlation with the tau pattern in brain and effects on tubulin polymerization, *EMBO J 9*, 4225-4230.
19. Cleveland, D. W., Hwo, S. Y., and Kirschner, M. W. (1977) Purification of tau, a microtubule-associated protein that induces assembly of microtubules from purified tubulin, *J Mol Biol 116*, 207-225.
20. Lee, G., Cowan, N., and Kirschner, M. (1988) The primary structure and heterogeneity of tau protein from mouse brain, *Science 239*, 285-288.
21. Goode, B. L., and Feinstein, S. C. (1994) Identification of a novel microtubule binding and assembly domain in the developmentally regulated inter-repeat region of tau, *J Cell Biol 124*, 769-782.
22. Goode, B. L., Denis, P. E., Panda, D., Radeke, M. J., Miller, H. P., Wilson, L., and Feinstein, S. C. (1997) Functional interactions between the proline-rich and repeat regions of tau enhance microtubule binding and assembly, *Mol Biol Cell 8*, 353-365.
23. Kar, S., Fan, J., Smith, M. J., Goedert, M., and Amos, L. A. (2003) Repeat motifs of tau bind to the insides of microtubules in the absence of taxol, *The EMBO journal 22*, 70-77.
24. Gustke, N., Trinczek, B., Biernat, J., Mandelkow, E. M., and Mandelkow, E. (1994) Domains of tau protein and interactions with microtubules, *Biochemistry 33*, 9511-9522.
25. Fauquant, C., Redeker, V., Landrieu, I., Wieruszeski, J. M., Verdegem, D., Laprevote, O., Lippens, G., Gigant, B., and Knossow, M. (2011) Systematic Identification of Tubulin-interacting Fragments of the Microtubule-associated Protein Tau Leads to a Highly Efficient Promoter of Microtubule Assembly, *Journal of Biological Chemistry 286*, 33358-33368.
26. Butner, K. A., and Kirschner, M. W. (1991) Tau protein binds to microtubules through a flexible array of distributed weak sites, *J Cell Biol 115*, 717-730.
27. Hirokawa, N., Shiomura, Y., and Okabe, S. (1988) Tau proteins: the molecular structure and mode of binding on microtubules, *J Cell Biol 107*, 1449-1459.
28. Makrides, V., Massie, M. R., Feinstein, S. C., and Lew, J. (2004) Evidence for two distinct binding sites for tau on microtubules, *Proc Natl Acad Sci U S A 101*, 6746-6751.
29. Hiller, G., and Weber, K. (1978) Radioimmunoassay for tubulin: a quantitative comparison of the tubulin content of different established tissue culture cells and tissues, *Cell 14*, 795-804.
30. Chau, M. F., Radeke, M. J., de Ines, C., Barasoain, I., Kohlstaedt, L. A., and Feinstein, S. C. (1998) The microtubule-associated protein tau cross-links to two distinct sites on each alpha and beta tubulin monomer via separate domains, *Biochemistry 37*, 17692-17703.

31. Drubin, D. G., and Kirschner, M. W. (1986) Tau protein function in living cells, *J Cell Biol 103*, 2739-2746.
32. Bre, M. H., and Karsenti, E. (1990) Effects of brain microtubule-associated proteins on microtubule dynamics and the nucleating activity of centrosomes, *Cell Motil Cytoskeleton 15*, 88-98.
33. Panda, D., Goode, B. L., Feinstein, S. C., and Wilson, L. (1995) Kinetic stabilization of microtubule dynamics at steady state by tau and microtubule-binding domains of tau, *Biochemistry 34*, 11117-11127.
34. Caceres, A., and Kosik, K. S. (1990) Inhibition of neurite polarity by tau antisense oligonucleotides in primary cerebellar neurons, *Nature 343*, 461-463.
35. Frappier, T. F., Georgieff, I. S., Brown, K., and Shelanski, M. L. (1994) tau Regulation of microtubule-microtubule spacing and bundling, *J Neurochem 63*, 2288-2294.
36. Kanai, Y., Takemura, R., Oshima, T., Mori, H., Ihara, Y., Yanagisawa, M., Masaki, T., and Hirokawa, N. (1989) Expression of multiple tau isoforms and microtubule bundle formation in fibroblasts transfected with a single tau cDNA, *J Cell Biol 109*, 1173-1184.
37. Chen, J., Kanai, Y., Cowan, N. J., and Hirokawa, N. (1992) Projection domains of MAP2 and tau determine spacings between microtubules in dendrites and axons, *Nature 360*, 674-677.
38. Ebneth, A., Godemann, R., Stamer, K., Illenberger, S., Trinczek, B., and Mandelkow, E. (1998) Overexpression of tau protein inhibits kinesin-dependent trafficking of vesicles, mitochondria, and endoplasmic reticulum: implications for Alzheimer's disease, *J Cell Biol 143*, 777-794.
39. Trinczek, B., Ebneth, A., Mandelkow, E. M., and Mandelkow, E. (1999) Tau regulates the attachment/detachment but not the speed of motors in microtubule-dependent transport of single vesicles and organelles, *J Cell Sci 112 (Pt 14)*, 2355-2367.
40. Seitz, A., Kojima, H., Oiwa, K., Mandelkow, E. M., Song, Y. H., and Mandelkow, E. (2002) Single-molecule investigation of the interference between kinesin, tau and MAP2c, *Embo J 21*, 4896-4905.
41. Morfini, G., Pigino, G., Mizuno, N., Kikkawa, M., and Brady, S. T. (2007) Tau binding to microtubules does not directly affect microtubule-based vesicle motility, *J Neurosci Res 85*, 2620-2630.
42. Brandt, R., Leger, J., and Lee, G. (1995) Interaction of tau with the neural plasma membrane mediated by tau's amino-terminal projection domain, *J Cell Biol 131*, 1327-1340.
43. Moraga, D. M., Nunez, P., Garrido, J., and Maccioni, R. B. (1993) A tau fragment containing a repetitive sequence induces bundling of actin filaments, *J Neurochem 61*, 979-986.
44. Selden, S. C., and Pollard, T. D. (1983) Phosphorylation of microtubule-associated proteins regulates their interaction with actin filaments, *J Biol Chem 258*, 7064-7071.
45. Farias, G. A., Munoz, J. P., Garrido, J., and Maccioni, R. B. (2002) Tubulin, actin, and tau protein interactions and the study of their macromolecular assemblies, *J Cell Biochem 85*, 315-324.
46. Lee, G., Newman, S. T., Gard, D. L., Band, H., and Panchamoorthy, G. (1998) Tau interacts with src-family non-receptor tyrosine kinases, *J Cell Sci 111*, 3167-3177.
47. Ittner, L. M., Ke, Y. D., Delerue, F., Bi, M., Gladbach, A., van Eersel, J., Wolfing, H., Chieng, B. C., Christie, M. J., Napier, I. A., Eckert, A., Staufenbiel, M., Hardeman, E.,

and Gotz, J. (2010) Dendritic function of tau mediates amyloid-beta toxicity in Alzheimer's disease mouse models, *Cell 142*, 387-397.
48. Sontag, E., Nunbhakdi-Craig, V., Lee, G., Brandt, R., Kamibayashi, C., Kuret, J., White, C. L., 3rd, Mumby, M. C., and Bloom, G. S. (1999) Molecular interactions among protein phosphatase 2A, tau, and microtubules. Implications for the regulation of tau phosphorylation and the development of tauopathies, *J Biol Chem 274*, 25490-25498.
49. Dou, F., Netzer, W. J., Tanemura, K., Li, F., Hartl, F. U., Takashima, A., Gouras, G. K., Greengard, P., and Xu, H. (2003) Chaperones Increase Association of Tau Protein with Microtubules, *PNAS 100*, 721-726.
50. Schweers, O., Schonbrunn-Hanebeck, E., Marx, A., and Mandelkow, E. (1994) Structural studies of tau protein and Alzheimer paired helical filaments show no evidence for beta-structure, *J Biol Chem 269*, 24290-24297.
51. Mukrasch, M. D., Bibow, S., Korukottu, J., Jeganathan, S., Biernat, J., Griesinger, C., Mandelkow, E., and Zweckstetter, M. (2009) Structural polymorphism of 441-residue tau at single residue resolution, *PLoS Biol 7*, e34.
52. Fellous, A., Francon, J., Lennon, A. M., and Nunez, J. (1977) Microtubule assembly in vitro. Purification of assembly-promoting factors, *Eur J Biochem 78*, 167-174.
53. Mukrasch, M. D., Biernat, J., von Bergen, M., Griesinger, C., Mandelkow, E., and Zweckstetter, M. (2005) Sites of Tau Important for Aggregation Populate β-Structure and Bind to Microtubules and Polyanions, *Journal of Biological Chemistry 280*, 24978-24986.
54. Jeganathan, S., von Bergen, M., Brutlach, H., Steinhoff, H. J., and Mandelkow, E. (2006) Global hairpin folding of tau in solution, *Biochemistry 45*, 2283-2293.
55. Elbaum-Garfinkle, S., and Rhoades, E. (2012) Identification of an aggregation-prone structure of tau, *J Am Chem Soc 134*, 16607-16613.
56. Sillen, A., Barbier, P., Landrieu, I., Lefebvre, S., Wieruszeski, J. M., Leroy, A., Peyrot, V., and Lippens, G. (2007) NMR investigation of the interaction between the neuronal protein tau and the microtubules, *Biochemistry 46*, 3055-3064.
57. Jancsik, V., Filliol, D., Felter, S., and Rendon, A. (1989) Binding of microtubule-associated proteins (MAPs) to rat brain mitochondria: a comparative study of the binding of MAP2, its microtubule-binding and projection domains, and tau proteins, *Cell Motil Cytoskeleton 14*, 372-381.
58. Littauer, U. Z., Giveon, D., Thierauf, M., Ginzburg, I., and Ponstingl, H. (1986) Common and distinct tubulin binding sites for microtubule-associated proteins, *Proc Natl Acad Sci U S A 83*, 7162-7166.
59. Harada, A., Oguchi, K., Okabe, S., Kuno, J., Terada, S., Ohshima, T., Sato-Yoshitake, R., Takei, Y., Noda, T., and Hirokawa, N. (1994) Altered microtubule organization in small-calibre axons of mice lacking tau protein, *Nature 369*, 488-491.
60. Ikegami, S., Harada, A., and Hirokawa, N. (2000) Muscle weakness, hyperactivity, and impairment in fear conditioning in tau-deficient mice, *Neurosci Lett 279*, 129-132.
61. Lei, P., Ayton, S., Finkelstein, D. I., Spoerri, L., Ciccotosto, G. D., Wright, D. K., Wong, B. X., Adlard, P. A., Cherny, R. A., Lam, L. Q., Roberts, B. R., Volitakis, I., Egan, G. F., McLean, C. A., Cappai, R., Duce, J. A., and Bush, A. I. (2012) Tau deficiency induces parkinsonism with dementia by impairing APP-mediated iron export, *Nat Med 18*, 291-295.

62. Braak, H., and Braak, E. (1991) Neuropathological stageing of Alzheimer-related changes, *Acta Neuropathol 82*, 239-259.
63. Schonheit, B., Zarski, R., and Ohm, T. G. (2004) Spatial and temporal relationships between plaques and tangles in Alzheimer-pathology, *Neurobiol Aging 25*, 697-711.
64. Kidd, M. (1963) Paired helical filaments in electron microscopy of Alzheimer's disease, *Nature 197*, 192-193.
65. Crowther, R. A., and Wischik, C. M. (1985) Image reconstruction of the Alzheimer paired helical filament, *Embo J 4*, 3661-3665.
66. Crowther, R. A. (1991) Straight and paired helical filaments in Alzheimer disease have a common structural unit, *Proc Natl Acad Sci U S A 88*, 2288-2292.
67. Lee, V. M., Balin, B. J., Otvos, L., Jr., and Trojanowski, J. Q. (1991) A68: a major subunit of paired helical filaments and derivatized forms of normal tau, *Science 251*, 675-678.
68. Goedert, M., Spillantini, M. G., Cairns, N. J., and Crowther, R. A. (1992) Tau proteins of Alzheimer paired helical filaments: abnormal phosphorylation of all six brain isoforms, *Neuron 8*, 159-168.
69. Braak, H., and Braak, E. (1997) Frequency of stages of Alzheimer-related lesions in different age categories, *Neurobiol Aging 18*, 351-357.
70. Braak, H., and Del Tredici, K. (2012) Alzheimer's disease: pathogenesis and prevention, *Alzheimers Dement 8*, 227-233.
71. Goate, A., Chartier-Harlin, M. C., Mullan, M., Brown, J., Crawford, F., Fidani, L., Giuffra, L., Haynes, A., Irving, N., James, L., and et al. (1991) Segregation of a missense mutation in the amyloid precursor protein gene with familial Alzheimer's disease [see comments], *Nature 349*, 704-706.
72. Sherrington, R., Rogaev, E. I., Liang, Y., Rogaeva, E. A., Levesque, G., Ikeda, M., Chi, H., Lin, C., Li, G., Holman, K., and et al. (1995) Cloning of a gene bearing missense mutations in early-onset familial Alzheimer's disease [see comments], *Nature 375*, 754-760.
73. Rogaev, E. I., Sherrington, R., Rogaeva, E. A., Levesque, G., Ikeda, M., Liang, Y., Chi, H., Lin, C., Holman, K., Tsuda, T., and et al. (1995) Familial Alzheimer's disease in kindreds with missense mutations in a gene on chromosome 1 related to the Alzheimer's disease type 3 gene, *Nature 376*, 775-778.
74. De Strooper, B., and Annaert, W. (2000) Proteolytic processing and cell biological functions of the amyloid precursor protein, *J Cell Sci 113 (Pt 11)*, 1857-1870.
75. Lewis, J., Dickson, D. W., Lin, W. L., Chisholm, L., Corral, A., Jones, G., Yen, S. H., Sahara, N., Skipper, L., Yager, D., Eckman, C., Hardy, J., Hutton, M., and McGowan, E. (2001) Enhanced neurofibrillary degeneration in transgenic mice expressing mutant tau and APP, *Science 293*, 1487-1491.
76. Delacourte, A., David, J. P., Sergeant, N., Buee, L., Wattez, A., Vermersch, P., Ghozali, F., Fallet-Bianco, C., Pasquier, F., Lebert, F., Petit, H., and Di Menza, C. (1999) The biochemical pathway of neurofibrillary degeneration in aging and Alzheimer's disease, *Neurology 52*, 1158-1165.
77. Braak, H. (1996) Evolution of Alzheimer's disease related intraneuronal changes, In *Fifth International Conference: On Alzheimer's Disease And Related Disorders*, Osaka, Japan.

78. Arriagada, P. V., Growdon, J. H., Hedley-Whyte, E. T., and Hyman, B. T. (1992) Neurofibrillary tangles but not senile plaques parallel duration and severity of Alzheimer's disease, *Neurology 42*, 631-639.
79. Wilcock, G. K., and Esiri, M. M. (1982) Plaques, tangles and dementia. A quantitative study, *J Neurol Sci 56*, 343-356.
80. Hutton, M., Lendon, C. L., Rizzu, P., Baker, M., Froelich, S., Houlden, H., Pickering-Brown, S., Chakraverty, S., Isaacs, A., Grover, A., Hackett, J., Adamson, J., Lincoln, S., Dickson, D., Davies, P., Petersen, R. C., Stevens, M., de Graaff, E., Wauters, E., van Baren, J., Hillebrand, M., Joosse, M., Kwon, J. M., Nowotny, P., Heutink, P., and et al. (1998) Association of missense and 5'-splice-site mutations in tau with the inherited dementia FTDP-17, *Nature 393*, 702-705.
81. Poorkaj, P., Bird, T. D., Wijsman, E., Nemens, E., Garruto, R. M., Anderson, L., Andreadis, A., Wiederholt, W. C., Raskind, M., and Schellenberg, G. D. (1998) Tau is a candidate gene for chromosome 17 frontotemporal dementia, *Ann Neurol 43*, 815-825.
82. Spillantini, M. G., Murrell, J. R., Goedert, M., Farlow, M. R., Klug, A., and Ghetti, B. (1998) Mutation in the tau gene in familial multiple system tauopathy with presenile dementia, *Proc Natl Acad Sci U S A 95*, 7737-7741.
83. Rapoport, M., Dawson, H. N., Binder, L. I., Vitek, M. P., and Ferreira, A. (2002) Tau is essential to beta -amyloid-induced neurotoxicity, *Proc Natl Acad Sci U S A 99*, 6364-6369.
84. Roberson, E. D., Scearce-Levie, K., Palop, J. J., Yan, F., Cheng, I. H., Wu, T., Gerstein, H., Yu, G. Q., and Mucke, L. (2007) Reducing endogenous tau ameliorates amyloid beta-induced deficits in an Alzheimer's disease mouse model, *Science 316*, 750-754.
85. Bandyopadhyay, B., Li, G., Yin, H., and Kuret, J. (2007) Tau aggregation and toxicity in a cell culture model of tauopathy, *J Biol Chem 282*, 16454-16464.
86. Andorfer, C., Acker, C. M., Kress, Y., Hof, P. R., Duff, K., and Davies, P. (2005) Cell-cycle reentry and cell death in transgenic mice expressing nonmutant human tau isoforms, *J Neurosci 25*, 5446-5454.
87. Wittmann, C. W., Wszolek, M. F., Shulman, J. M., Salvaterra, P. M., Lewis, J., Hutton, M., and Feany, M. B. (2001) Tauopathy in Drosophila: neurodegeneration without neurofibrillary tangles, *Science 293*, 711-714.
88. Constantinidis, J., Richard, J., and Tissot, R. (1974) Pick's disease. Histological and clinical correlations, *Eur Neurol 11*, 208-217.
89. Munoz-Garcia, D., and Ludwin, S. K. (1984) Classic and generalized variants of Pick's disease: a clinicopathological, ultrastructural, and immunocytochemical comparative study, *Ann Neurol 16*, 467-480.
90. Dickson, D. W. (1998) Pick's disease: a modern approach, *Brain Pathol 8*, 339-354.
91. Sergeant, N., David, J. P., Lefranc, D., Vermersch, P., Wattez, A., and Delacourte, A. (1997) Different distribution of phosphorylated tau protein isoforms in Alzheimer's and Pick's diseases, *FEBS Lett 412*, 578-582.
92. Probst, A., Tolnay, M., Langui, D., Goedert, M., and Spillantini, M. G. (1996) Pick's disease: hyperphosphorylated tau protein segregates to the somatoaxonal compartment, *Acta Neuropathol (Berl) 92*, 588-596.
93. Goedert, M., Spillantini, M. G., Potier, M. C., Ulrich, J., and Crowther, R. A. (1989) Cloning and sequencing of the cDNA encoding an isoform of microtubule-associated

protein tau containing four tandem repeats: differential expression of tau protein mRNAs in human brain, *Embo J 8*, 393-399.
94. Hauw, J. J., Daniel, S. E., Dickson, D., Horoupian, D. S., Jellinger, K., Lantos, P. L., McKee, A., Tabaton, M., and Litvan, I. (1994) Preliminary NINDS neuropathologic criteria for Steele-Richardson-Olszewski syndrome (progressive supranuclear palsy), *Neurology 44*, 2015-2019.
95. Cervos-Navarro, J., and Schumacher, K. (1994) Neurofibrillary pathology in progressive supranuclear palsy (PSP), *J Neural Transm Suppl 42*, 153-164.
96. Tellez-Nagel, I., and Wisniewski, H. M. (1973) Ultrastructure of neurofibrillary tangles in Steele-Richardson-Olszewski syndrome, *Arch Neurol 29*, 324-327.
97. Roy, S., Datta, C. K., Hirano, A., Ghatak, N. R., and Zimmerman, H. M. (1974) Electron microscopic study of neurofibrillary tangles in Steele-Richardson-Olszewski syndrome, *Acta Neuropathol 29*, 175-179.
98. Spillantini, M. G., Goedert, M., Crowther, R. A., Murrell, J. R., Farlow, M. R., and Ghetti, B. (1997) Familial multiple system tauopathy with presenile dementia: a disease with abundant neuronal and glial tau filaments, *Proc Natl Acad Sci U S A 94*, 4113-4118.
99. Sergeant, N., Wattez, A., and Delacourte, A. (1999) Neurofibrillary degeneration in progressive supranuclear palsy and corticobasal degeneration: tau pathologies with exclusively "exon 10" isoforms, *J Neurochem 72*, 1243-1249.
100. Chambers, C. B., Lee, J. M., Troncoso, J. C., Reich, S., and Muma, N. A. (1999) Overexpression of four-repeat tau mRNA isoforms in progressive supranuclear palsy but not in Alzheimer's disease, *Ann Neurol 46*, 325-332.
101. Ksiezak-Reding, H., Morgan, K., Mattiace, L. A., Davies, P., Liu, W. K., Yen, S. H., Weidenheim, K., and Dickson, D. W. (1994) Ultrastructure and biochemical composition of paired helical filaments in corticobasal degeneration, *Am J Pathol 145*, 1496-1508.
102. Rebeiz, J. J., Kolodny, E. H., and Richardson, E. P., Jr. (1968) Corticodentatonigral degeneration with neuronal achromasia, *Arch Neurol 18*, 20-33.
103. McKee, A. C., Cantu, R. C., Nowinski, C. J., Hedley-Whyte, E. T., Gavett, B. E., Budson, A. E., Santini, V. E., Lee, H. S., Kubilus, C. A., and Stern, R. A. (2009) Chronic traumatic encephalopathy in athletes: progressive tauopathy after repetitive head injury, *J Neuropathol Exp Neurol 68*, 709-735.
104. McKee, A. C., Stein, T. D., Nowinski, C. J., Stern, R. A., Daneshvar, D. H., Alvarez, V. E., Lee, H. S., Hall, G., Wojtowicz, S. M., Baugh, C. M., Riley, D. O., Kubilus, C. A., Cormier, K. A., Jacobs, M. A., Martin, B. R., Abraham, C. R., Ikezu, T., Reichard, R. R., Wolozin, B. L., Budson, A. E., Goldstein, L. E., Kowall, N. W., and Cantu, R. C. (2012) The spectrum of disease in chronic traumatic encephalopathy, *Brain*.
105. Luethcke, C. A., Bryan, C. J., Morrow, C. E., and Isler, W. C. (2011) Comparison of concussive symptoms, cognitive performance, and psychological symptoms between acute blast-versus nonblast-induced mild traumatic brain injury, *J Int Neuropsychol Soc 17*, 36-45.
106. Omalu, B., Bailes, J., Hamilton, R. L., Kamboh, M. I., Hammers, J., Case, M., and Fitzsimmons, R. (2011) Emerging histomorphologic phenotypes of chronic traumatic encephalopathy in American athletes, *Neurosurgery 69*, 173-183; discussion 183.
107. Clark, L. N., Poorkaj, P., Wszolek, Z., Geschwind, D. H., Nasreddine, Z. S., Miller, B., Li, D., Payami, H., Awert, F., Markopoulou, K., Andreadis, A., D'Souza, I., Lee, V. M., Reed, L., Trojanowski, J. Q., Zhukareva, V., Bird, T., Schellenberg, G., and Wilhelmsen,

K. C. (1998) Pathogenic implications of mutations in the tau gene in pallido-ponto- nigral degeneration and related neurodegenerative disorders linked to chromosome 17, *Proc Natl Acad Sci U S A 95*, 13103-13107.
108. Spillantini, M. G., Crowther, R. A., Kamphorst, W., Heutink, P., and van Swieten, J. C. (1998) Tau pathology in two Dutch families with mutations in the microtubule- binding region of tau, *Am J Pathol 153*, 1359-1363.
109. Ingram, E. M., and Spillantini, M. G. (2002) Tau gene mutations: dissecting the pathogenesis of FTDP-17, *Trends Mol Med 8*, 555-562.
110. von Bergen, M., Friedhoff, P., Biernat, J., Heberle, J., and Mandelkow, E. (2000) Assembly of tau protein into Alzheimer paired helical filaments depends on a local sequence motif (306VQIVYK311) forming beta structure, *Proc Natl Acad Sci U S A 97*, 5129-5134.
111. Giannetti, A. M., Lindwall, G., Chau, M. F., Radeke, M. J., Feinstein, S. C., and Kohlstaedt, L. A. (2000) Fibers of tau fragments, but not full length tau, exhibit a cross beta-structure: implications for the formation of paired helical filaments, *Protein Sci 9*, 2427-2435.
112. Li, L., von Bergen, M., Mandelkow, E. M., and Mandelkow, E. (2002) Structure, stability, and aggregation of paired helical filaments from tau protein and FTDP-17 mutants probed by tryptophan scanning mutagenesis, *J Biol Chem 277*, 41390-41400.
113. Lasagna-Reeves, C. A., Castillo-Carranza, D. L., Sengupta, U., Sarmiento, J., Troncoso, J., Jackson, G. R., and Kayed, R. (2012) Identification of oligomers at early stages of tau aggregation in Alzheimer's disease, *FASEB J 26*, 1946-1959.
114. Delacourte, A., and Defossez, A. (1986) Alzheimer's disease: Tau proteins, the promoting factors of microtubule assembly, are major components of paired helical filaments, *J Neurol Sci 76*, 173-186.
115. Montpetit, V., Clapin, D. F., and Guberman, A. (1985) Substructure of 20 nm filaments of progressive supranuclear palsy, *Acta Neuropathol 68*, 311-318.
116. Yamazaki, M., Nakano, I., Imazu, O., Kaieda, R., and Terashi, A. (1994) Astrocytic straight tubules in the brain of a patient with Pick's disease, *Acta Neuropathol 88*, 587-591.
117. Wischik, C. M., Novak, M., Edwards, P. C., Klug, A., Tichelaar, W., and Crowther, R. A. (1988) Structural characterization of the core of the paired helical filament of Alzheimer disease, *Proc Natl Acad Sci U S A 85*, 4884-4888.
118. Sillen, A., Leroy, A., Wieruszeski, J. M., Loyens, A., Beauvillain, J. C., Buee, L., Landrieu, I., and Lippens, G. (2005) Regions of tau implicated in the paired helical fragment core as defined by NMR, *Chembiochem 6*, 1849-1856.
119. Takauchi, S., Hosomi, M., Marasigan, S., Sato, M., Hayashi, S., and Miyoshi, K. (1984) An ultrastructural study of Pick bodies, *Acta Neuropathol 64*, 344-348.
120. Steele, J., Richardson, J., and Olszewski, J. (1964) Progressive Supranuclear Palsy, *Archives of Neurology 10*, 333-359.
121. Kopke, E., Tung, Y. C., Shaikh, S., Alonso, A. C., Iqbal, K., and Grundke-Iqbal, I. (1993) Microtubule-associated protein tau. Abnormal phosphorylation of a non-paired helical filament pool in Alzheimer disease, *J Biol Chem 268*, 24374-24384.
122. Lindwall, G., and Cole, R. D. (1984) Phosphorylation affects the ability of tau protein to promote microtubule assembly, *J Biol Chem 259*, 5301-5305.

123. Grundke-Iqbal, I., Iqbal, K., Tung, Y. C., Quinlan, M., Wisniewski, H. M., and Binder, L. I. (1986) Abnormal phosphorylation of the microtubule-associated protein tau (tau) in Alzheimer cytoskeletal pathology, *Proc Natl Acad Sci U S A 83*, 4913-4917.
124. Kosik, K. S., Joachim, C. L., and Selkoe, D. J. (1986) Microtubule-associated protein tau (tau) is a major antigenic component of paired helical filaments in Alzheimer disease, *Proc Natl Acad Sci U S A 83*, 4044-4048.
125. Wood, J. G., Mirra, S. S., Pollock, N. J., and Binder, L. I. (1986) Neurofibrillary tangles of Alzheimer disease share antigenic determinants with the axonal microtubule-associated protein tau (tau) [published erratum appears in Proc Natl Acad Sci U S A 1986 Dec;83(24):9773], *Proc Natl Acad Sci U S A 83*, 4040-4043.
126. Ihara, Y., Nukina, N., Miura, R., and Ogawara, M. (1986) Phosphorylated tau protein is integrated into paired helical filaments in Alzheimer's disease, *J Biochem (Tokyo) 99*, 1807-1810.
127. Ishiguro, K., Takamatsu, M., Tomizawa, K., Omori, A., Takahashi, M., Arioka, M., Uchida, T., and Imahori, K. (1992) Tau protein kinase I converts normal tau protein into A68-like component of paired helical filaments, *J Biol Chem 267*, 10897-10901.
128. Ishiguro, K., Shiratsuchi, A., Sato, S., Omori, A., Arioka, M., Kobayashi, S., Uchida, T., and Imahori, K. (1993) Glycogen synthase kinase 3 beta is identical to tau protein kinase I generating several epitopes of paired helical filaments, *FEBS Lett 325*, 167-172.
129. Imahori, K., and Uchida, T. (1997) Physiology and pathology of tau protein kinases in relation to Alzheimer's disease, *J Biochem (Tokyo) 121*, 179-188.
130. Lew, J., Huang, Q. Q., Qi, Z., Winkfein, R. J., Aebersold, R., Hunt, T., and Wang, J. H. (1994) A brain-specific activator of cyclin-dependent kinase 5, *Nature 371*, 423-426.
131. Pei, J. J., Gong, C. X., Iqbal, K., Grundke-Iqbal, I., Wu, Q. L., Winblad, B., and Cowburn, R. F. (1998) Subcellular distribution of protein phosphatases and abnormally phosphorylated tau in the temporal cortex from Alzheimer's disease and control brains, *J Neural Transm 105*, 69-83.
132. Pei, J. J., Braak, E., Braak, H., Grundke-Iqbal, I., Iqbal, K., Winblad, B., and Cowburn, R. F. (1999) Distribution of active glycogen synthase kinase 3beta (GSK-3beta) in brains staged for Alzheimer disease neurofibrillary changes, *J Neuropathol Exp Neurol 58*, 1010-1019.
133. Lovestone, S., Hartley, C. L., Pearce, J., and Anderton, B. H. (1996) Phosphorylation of tau by glycogen synthase kinase-3 beta in intact mammalian cells: the effects on the organization and stability of microtubules, *Neuroscience 73*, 1145-1157.
134. Spittaels, K., Van den Haute, C., Van Dorpe, J., Geerts, H., Mercken, M., Bruynseels, K., Lasrado, R., Vandezande, K., Laenen, I., Boon, T., Van Lint, J., Vandenheede, J., Moechars, D., Loos, R., and Van Leuven, F. (2000) Glycogen synthase kinase-3beta phosphorylates protein tau and rescues the axonopathy in the central nervous system of human four-repeat tau transgenic mice, *J Biol Chem 275*, 41340-41349.
135. Greenberg, S. M., and Kosik, K. S. (1995) Secreted beta-APP stimulates MAP kinase and phosphorylation of tau in neurons, *Neurobiol Aging 16*, 403-407; discussion 407-408.
136. Busciglio, J., Lorenzo, A., Yeh, J., and Yankner, B. A. (1995) beta-amyloid fibrils induce tau phosphorylation and loss of microtubule binding, *Neuron 14*, 879-888.
137. Perez, M., Cuadros, R., Smith, M. A., Perry, G., and Avila, J. (2000) Phosphorylated, but not native, tau protein assembles following reaction with the lipid peroxidation product, 4-hydroxy-2-nonenal, *FEBS Lett 486*, 270-274.

138. Jackson, G. R., Wiedau-Pazos, M., Sang, T. K., Wagle, N., Brown, C. A., Massachi, S., and Geschwind, D. H. (2002) Human wild-type tau interacts with wingless pathway components and produces neurofibrillary pathology in Drosophila, *Neuron 34*, 509-519.
139. Song, J. S., and Yang, S. D. (1995) Tau protein kinase I/GSK-3 beta/kinase FA in heparin phosphorylates tau on Ser199, Thr231, Ser235, Ser262, Ser369, and Ser400 sites phosphorylated in Alzheimer disease brain, *J Protein Chem 14*, 95-105.
140. Biernat, J., and Mandelkow, E. M. (1999) The development of cell processes induced by tau protein requires phosphorylation of serine 262 and 356 in the repeat domain and is inhibited by phosphorylation in the proline-rich domains, *Mol Biol Cell 10*, 727-740.
141. Drewes, G., Trinczek, B., Illenberger, S., Biernat, J., Schmitt-Ulms, G., Meyer, H. E., Mandelkow, E. M., and Mandelkow, E. (1995) Microtubule-associated protein/microtubule affinity-regulating kinase (p110mark). A novel protein kinase that regulates tau-microtubule interactions and dynamic instability by phosphorylation at the Alzheimer-specific site serine 262, *J Biol Chem 270*, 7679-7688.
142. Cho, J. H., and Johnson, G. V. (2003) Glycogen synthase kinase 3beta phosphorylates tau at both primed and unprimed sites. Differential impact on microtubule binding, *J Biol Chem 278*, 187-193.
143. Wagner, U., Utton, M., Gallo, J. M., and Miller, C. C. (1996) Cellular phosphorylation of tau by GSK-3 beta influences tau binding to microtubules and microtubule organisation, *J Cell Sci 109 (Pt 6)*, 1537-1543.
144. Sontag, E., Nunbhakdi-Craig, V., Lee, G., Bloom, G. S., and Mumby, M. C. (1996) Regulation of the phosphorylation state and microtubule-binding activity of Tau by protein phosphatase 2A, *Neuron 17*, 1201-1207.
145. Bramblett, G. T., Goedert, M., Jakes, R., Merrick, S. E., Trojanowski, J. Q., and Lee, V. M. (1993) Abnormal tau phosphorylation at Ser396 in Alzheimer's disease recapitulates development and contributes to reduced microtubule binding, *Neuron 10*, 1089-1099.
146. Leger, J., Kempf, M., Lee, G., and Brandt, R. (1997) Conversion of serine to aspartate imitates phosphorylation-induced changes in the structure and function of microtubule-associated protein tau, *J Biol Chem 272*, 8441-8446.
147. Eidenmuller, J., Fath, T., Hellwig, A., Reed, J., Sontag, E., and Brandt, R. (2000) Structural and functional implications of tau hyperphosphorylation: information from phosphorylation-mimicking mutated tau proteins, *Biochemistry 39*, 13166-13175.
148. Eidenmuller, J., Fath, T., Maas, T., Pool, M., Sontag, E., and Brandt, R. (2001) Phosphorylation-mimicking glutamate clusters in the proline-rich region are sufficient to simulate the functional deficiencies of hyperphosphorylated tau protein, *Biochem J 357*, 759-767.
149. Okawa, Y., Ishiguro, K., and Fujita, S. C. (2003) Stress-induced hyperphosphorylation of tau in the mouse brain, *FEBS Lett 535*, 183-189.
150. Rankin, C. A., Sun, Q., and Gamblin, T. C. (2005) Pseudo-phosphorylation of tau at Ser202 and Thr205 affects tau filament formation, *Brain Res Mol Brain Res*.
151. Necula, M., and Kuret, J. (2005) Site-specific pseudophosphorylation modulates the rate of tau filament dissociation, *FEBS Lett 579*, 1453-1457.
152. Abraha, A., Ghoshal, N., Gamblin, T. C., Cryns, V., Berry, R. W., Kuret, J., and Binder, L. I. (2000) C-terminal inhibition of tau assembly in vitro and in Alzheimer's disease, *J Cell Sci 113 Pt 21*, 3737-3745.

153. Augustinack, J. C., Schneider, A., Mandelkow, E. M., and Hyman, B. T. (2002) Specific tau phosphorylation sites correlate with severity of neuronal cytopathology in Alzheimer's disease, *Acta Neuropathol (Berl) 103*, 26-35.
154. Fath, T., Eidenmuller, J., and Brandt, R. (2002) Tau-mediated cytotoxicity in a pseudohyperphosphorylation model of Alzheimer's disease, *J Neurosci 22*, 9733-9741.
155. Steiner, B., Mandelkow, E. M., Biernat, J., Gustke, N., Meyer, H. E., Schmidt, B., Mieskes, G., Soling, H. D., Drechsel, D., Kirschner, M. W., and et al. (1990) Phosphorylation of microtubule-associated protein tau: identification of the site for Ca2(+)-calmodulin dependent kinase and relationship with tau phosphorylation in Alzheimer tangles, *Embo J 9*, 3539-3544.
156. Fischer, D., Mukrasch, M. D., Biernat, J., Bibow, S., Blackledge, M., Griesinger, C., Mandelkow, E., and Zweckstetter, M. (2009) Conformational changes specific for pseudophosphorylation at serine 262 selectively impair binding of tau to microtubules, *Biochemistry 48*, 10047-10055.
157. Bibow, S., Ozenne, V., Biernat, J., Blackledge, M., Mandelkow, E., and Zweckstetter, M. (2011) Structural Impact of Proline-Directed Pseudophosphorylation at AT8, AT100, and PHF1 Epitopes on 441-Residue Tau, *J Am Chem Soc*.
158. Braak, H., Braak, E., and Strothjohann, M. (1994) Abnormally phosphorylated tau protein related to the formation of neurofibrillary tangles and neuropil threads in the cerebral cortex of sheep and goat, *Neurosci Lett 171*, 1-4.
159. Schneider, A., Biernat, J., von Bergen, M., Mandelkow, E., and Mandelkow, E. M. (1999) Phosphorylation that detaches tau protein from microtubules (Ser262, Ser214) also protects it against aggregation into Alzheimer paired helical filaments, *Biochemistry 38*, 3549-3558.
160. Sun, Q., and Gamblin, T. C. (2009) Pseudohyperphosphorylation causing AD-like changes in tau has significant effects on its polymerization, *Biochemistry 48*, 6002-6011.
161. Novak, M. (1994) Truncated tau protein as a new marker for Alzheimer's disease, *Acta Virol 38*, 173-189.
162. Ding, H., Matthews, T. A., and Johnson, G. V. (2006) Site-specific phosphorylation and caspase cleavage differentially impact tau-microtubule interactions and tau aggregation, *J Biol Chem 281*, 19107-19114.
163. Gamblin, T. C., Chen, F., Zambrano, A., Abraha, A., Lagalwar, S., Guillozet, A. L., Lu, M., Fu, Y., Garcia-Sierra, F., LaPointe, N., Miller, R., Berry, R. W., Binder, L. I., and Cryns, V. L. (2003) Caspase cleavage of tau: linking amyloid and neurofibrillary tangles in Alzheimer's disease, *Proc Natl Acad Sci U S A 100*, 10032-10037.
164. Bondareff, W., Wischik, C. M., Novak, M., Amos, W. B., Klug, A., and Roth, M. (1990) Molecular analysis of neurofibrillary degeneration in Alzheimer's disease. An immunohistochemical study, *Am J Pathol 137*, 711-723.
165. Morishima-Kawashima, M., Hasegawa, M., Takio, K., Suzuki, M., Titani, K., and Ihara, Y. (1993) Ubiquitin is conjugated with amino-terminally processed tau in paired helical filaments, *Neuron 10*, 1151-1160.
166. David, D. C., Layfield, R., Serpell, L., Narain, Y., Goedert, M., and Spillantini, M. G. (2002) Proteasomal degradation of tau protein, *J Neurochem 83*, 176-185.
167. Novak, M., Kabat, J., and Wischik, C. M. (1993) Molecular characterization of the minimal protease resistant tau unit of the Alzheimer's disease paired helical filament, *Embo J 12*, 365-370.

168. Min, S. W., Cho, S. H., Zhou, Y., Schroeder, S., Haroutunian, V., Seeley, W. W., Huang, E. J., Shen, Y., Masliah, E., Mukherjee, C., Meyers, D., Cole, P. A., Ott, M., and Gan, L. (2010) Acetylation of tau inhibits its degradation and contributes to tauopathy, *Neuron 67*, 953-966.
169. Cohen, T. J., Guo, J. L., Hurtado, D. E., Kwong, L. K., Mills, I. P., Trojanowski, J. Q., and Lee, V. M. (2011) The acetylation of tau inhibits its function and promotes pathological tau aggregation, *Nat Commun 2*, 252.
170. Wang, J. Z., Grundke-Iqbal, I., and Iqbal, K. (1996) Glycosylation of microtubule-associated protein tau: an abnormal posttranslational modification in Alzheimer's disease [see comments], *Nat Med 2*, 871-875.
171. Schweers, O., Mandelkow, E. M., Biernat, J., and Mandelkow, E. (1995) Oxidation of cysteine-322 in the repeat domain of microtubule-associated protein tau controls the in vitro assembly of paired helical filaments, *Proc Natl Acad Sci U S A 92*, 8463-8467.
172. Goedert, M., Jakes, R., Spillantini, M. G., Hasegawa, M., Smith, M. J., and Crowther, R. A. (1996) Assembly of microtubule-associated protein tau into Alzheimer-like filaments induced by sulphated glycosaminoglycans, *Nature 383*, 550-553.
173. Wilson, D. M., and Binder, L. I. (1997) Free fatty acids stimulate the polymerization of tau and amyloid beta peptides. In vitro evidence for a common effector of pathogenesis in Alzheimer's disease, *Am J Pathol 150*, 2181-2195.
174. Kampers, T., Friedhoff, P., Biernat, J., Mandelkow, E. M., and Mandelkow, E. (1996) RNA stimulates aggregation of microtubule-associated protein tau into Alzheimer-like paired helical filaments, *FEBS Lett 399*, 344-349.
175. Duan, A. R., and Goodson, H. V. (2012) Taxol-stabilized microtubules promote the formation of filaments from unmodified full-length Tau in vitro, *Mol Biol Cell 23*, 4796-4806.
176. Frost, B., Jacks, R. L., and Diamond, M. I. (2009) Propagation of tau misfolding from the outside to the inside of a cell, *J Biol Chem 284*, 12845-12852.
177. Clavaguera, F., Bolmont, T., Crowther, R. A., Abramowski, D., Frank, S., Probst, A., Fraser, G., Stalder, A. K., Beibel, M., Staufenbiel, M., Jucker, M., Goedert, M., and Tolnay, M. (2009) Transmission and spreading of tauopathy in transgenic mouse brain, *Nat Cell Biol 11*, 909-913.
178. Liu, L., Drouet, V., Wu, J. W., Witter, M. P., Small, S. A., Clelland, C., and Duff, K. (2012) Trans-synaptic spread of tau pathology in vivo, *PLoS One 7*, e31302.
179. de Calignon, A., Polydoro, M., Suarez-Calvet, M., William, C., Adamowicz, D. H., Kopeikina, K. J., Pitstick, R., Sahara, N., Ashe, K. H., Carlson, G. A., Spires-Jones, T. L., and Hyman, B. T. (2012) Propagation of tau pathology in a model of early Alzheimer's disease, *Neuron 73*, 685-697.
180. Iba, M., Guo, J. L., McBride, J. D., Zhang, B., Trojanowski, J. Q., and Lee, V. M. (2013) Synthetic Tau Fibrils Mediate Transmission of Neurofibrillary Tangles in a Transgenic Mouse Model of Alzheimer's-Like Tauopathy, *J Neurosci 33*, 1024-1037.
181. Cummings, J. L., and Altman, J. (2005) Genotype, proteotype, phenotype relationships in neurodegenerative diseases. Highlights from the 21st Ipsen Foundation Alzheimer's Disease Symposium, September 13, 2004, Paris, France, *Rev Neurol Dis 2*, 80-84.
182. Alonso Adel, C., Mederlyova, A., Novak, M., Grundke-Iqbal, I., and Iqbal, K. (2004) Promotion of hyperphosphorylation by frontotemporal dementia tau mutations, *J Biol Chem 279*, 34873-34881.

183. Connell, J. W., Gibb, G. M., Betts, J. C., Blackstock, W. P., Gallo, J., Lovestone, S., Hutton, M., and Anderton, B. H. (2001) Effects of FTDP-17 mutations on the in vitro phosphorylation of tau by glycogen synthase kinase 3beta identified by mass spectrometry demonstrate certain mutations exert long-range conformational changes, *FEBS Lett 493*, 40-44.
184. van Herpen, E., Rosso, S. M., Serverijnen, L. A., Yoshida, H., Breedveld, G., van de Graaf, R., Kamphorst, W., Ravid, R., Willemsen, R., Dooijes, D., Majoor-Krakauer, D., Kros, J. M., Crowther, R. A., Goedert, M., Heutink, P., and van Swieten, J. C. (2003) Variable phenotypic expression and extensive tau pathology in two families with the novel tau mutation L315R, *Ann Neurol 54*, 573-581.
185. Rosso, S. M., van Herpen, E., Deelen, W., Kamphorst, W., Severijnen, L. A., Willemsen, R., Ravid, R., Niermeijer, M. F., Dooijes, D., Smith, M. J., Goedert, M., Heutink, P., and van Swieten, J. C. (2002) A novel tau mutation, S320F, causes a tauopathy with inclusions similar to those in Pick's disease, *Ann Neurol 51*, 373-376.
186. Ishihara, T., Zhang, B., Higuchi, M., Yoshiyama, Y., Trojanowski, J. Q., and Lee, V. M. (2001) Age-dependent induction of congophilic neurofibrillary tau inclusions in tau transgenic mice, *Am J Pathol 158*, 555-562.
187. Kins, S., Crameri, A., Evans, D. R., Hemmings, B. A., Nitsch, R. M., and Gotz, J. (2001) Reduced protein phosphatase 2A activity induces hyperphosphorylation and altered compartmentalization of tau in transgenic mice, *J Biol Chem 276*, 38193-38200.
188. Santacruz, K., Lewis, J., Spires, T., Paulson, J., Kotilinek, L., Ingelsson, M., Guimaraes, A., DeTure, M., Ramsden, M., McGowan, E., Forster, C., Yue, M., Orne, J., Janus, C., Mariash, A., Kuskowski, M., Hyman, B., Hutton, M., and Ashe, K. H. (2005) Tau suppression in a neurodegenerative mouse model improves memory function, *Science 309*, 476-481.
189. Ittner, L. M., Fath, T., Ke, Y. D., Bi, M., van Eersel, J., Li, K. M., Gunning, P., and Gotz, J. (2008) Parkinsonism and impaired axonal transport in a mouse model of frontotemporal dementia, *Proc Natl Acad Sci U S A 105*, 15997-16002.
190. Schindowski, K., Bretteville, A., Leroy, K., Begard, S., Brion, J. P., Hamdane, M., and Buee, L. (2006) Alzheimer's disease-like tau neuropathology leads to memory deficits and loss of functional synapses in a novel mutated tau transgenic mouse without any motor deficits, *Am J Pathol 169*, 599-616.
191. Zhang, B., Higuchi, M., Yoshiyama, Y., Ishihara, T., Forman, M. S., Martinez, D., Joyce, S., Trojanowski, J. Q., and Lee, V. M. (2004) Retarded axonal transport of R406W mutant tau in transgenic mice with a neurodegenerative tauopathy, *J Neurosci 24*, 4657-4667.
192. Tanemura, K., Akagi, T., Murayama, M., Kikuchi, N., Murayama, O., Hashikawa, T., Yoshiike, Y., Park, J. M., Matsuda, K., Nakao, S., Sun, X., Sato, S., Yamaguchi, H., and Takashima, A. (2001) Formation of filamentous tau aggregations in transgenic mice expressing V337M human tau, *Neurobiol Dis 8*, 1036-1045.
193. Oddo, S., Caccamo, A., Shepherd, J. D., Murphy, M. P., Golde, T. E., Kayed, R., Metherate, R., Mattson, M. P., Akbari, Y., and LaFerla, F. M. (2003) Triple-transgenic model of Alzheimer's disease with plaques and tangles: intracellular Abeta and synaptic dysfunction, *Neuron 39*, 409-421.

194. Kosmidis, S., Grammenoudi, S., Papanikolopoulou, K., and Skoulakis, E. M. (2010) Differential effects of Tau on the integrity and function of neurons essential for learning in Drosophila, *J Neurosci 30*, 464-477.
195. Papanikolopoulou, K., Kosmidis, S., Grammenoudi, S., and Skoulakis, E. M. (2010) Phosphorylation differentiates tau-dependent neuronal toxicity and dysfunction, *Biochem Soc Trans 38*, 981-987.
196. Colodner, K. J., and Feany, M. B. (2010) Glial fibrillary tangles and JAK/STAT-mediated glial and neuronal cell death in a Drosophila model of glial tauopathy, *J Neurosci 30*, 16102-16113.
197. Kraemer, B. C., Zhang, B., Leverenz, J. B., Thomas, J. H., Trojanowski, J. Q., and Schellenberg, G. D. (2003) Neurodegeneration and defective neurotransmission in a Caenorhabditis elegans model of tauopathy, *Proc Natl Acad Sci U S A 100*, 9980-9985.
198. Miyasaka, T., Ding, Z., Gengyo-Ando, K., Oue, M., Yamaguchi, H., Mitani, S., and Ihara, Y. (2005) Progressive neurodegeneration in C. elegans model of tauopathy, *Neurobiol Dis 20*, 372-383.
199. Fatouros, C., Pir, G. J., Biernat, J., Koushika, S. P., Mandelkow, E., Mandelkow, E. M., Schmidt, E., and Baumeister, R. (2012) Inhibition of tau aggregation in a novel Caenorhabditis elegans model of tauopathy mitigates proteotoxicity, *Hum Mol Genet 21*, 3587-3603.
200. Lu, M., and Kosik, K. S. (2001) Competition for microtubule-binding with dual expression of tau missense and splice isoforms, *Mol Biol Cell 12*, 171-184.
201. King, M. E., Gamblin, T. C., Kuret, J., and Binder, L. I. (2000) Differential assembly of human tau isoforms in the presence of arachidonic acid, *J Neurochem 74*, 1749-1757.
202. Dinkel, P. D., Siddiqua, A., Huynh, H., Shah, M., and Margittai, M. (2011) Variations in Filament Conformation Dictate Seeding Barrier between Three- and Four-Repeat Tau, *Biochemistry*.
203. Goedert, M., Spillantini, M. G., Jakes, R., Rutherford, D., and Crowther, R. A. (1989) Multiple isoforms of human microtubule-associated protein tau: sequences and localization in neurofibrillary tangles of Alzheimer's disease, *Neuron 3*, 519-526.
204. Himmler, A., Drechsel, D., Kirschner, M. W., and Martin, D. W., Jr. (1989) Tau consists of a set of proteins with repeated C-terminal microtubule-binding domains and variable N-terminal domains, *Mol Cell Biol 9*, 1381-1388.
205. Sergeant, N., Delacourte, A., and Buee, L. (2005) Tau protein as a differential biomarker of tauopathies, *Biochim Biophys Acta 1739*, 179-197.
206. Mailliot, C., Sergeant, N., Bussiere, T., Caillet-Boudin, M. L., Delacourte, A., and Buee, L. (1998) Phosphorylation of specific sets of tau isoforms reflects different neurofibrillary degeneration processes, *FEBS Lett 433*, 201-204.
207. Iqbal, K., Alonso Adel, C., Chen, S., Chohan, M. O., El-Akkad, E., Gong, C. X., Khatoon, S., Li, B., Liu, F., Rahman, A., Tanimukai, H., and Grundke-Iqbal, I. (2005) Tau pathology in Alzheimer disease and other tauopathies, *Biochim Biophys Acta 1739*, 198-210.
208. Rankin, C. A., Sun, Q., and Gamblin, T. C. (2008) Pre-assembled tau filaments phosphorylated by GSK-3b form large tangle-like structures, *Neurobiol Dis 31*, 368-377.
209. Carlson, S. W., Branden, M., Voss, K., Sun, Q., Rankin, C. A., and Gamblin, T. C. (2007) A complex mechanism for inducer mediated tau polymerization, *Biochemistry 46*, 8838-8849.

210. Balaraman, Y., Limaye, A. R., Levey, A. I., and Srinivasan, S. (2006) Glycogen synthase kinase 3beta and Alzheimer's disease: pathophysiological and therapeutic significance, *Cell Mol Life Sci 63*, 1226-1235.
211. Kobayashi, S., Ishiguro, K., Omori, A., Takamatsu, M., Arioka, M., Imahori, K., and Uchida, T. (1993) A cdc2-related kinase PSSALRE/cdk5 is homologous with the 30 kDa subunit of tau protein kinase II, a proline-directed protein kinase associated with microtubule, *FEBS Lett 335*, 171-175.
212. Mi, K., and Johnson, G. V. (2006) The role of tau phosphorylation in the pathogenesis of Alzheimer's disease, *Curr Alzheimer Res 3*, 449-463.
213. Necula, M., and Kuret, J. (2004) Pseudophosphorylation and glycation of tau protein enhance but do not trigger fibrillization in vitro, *J Biol Chem 279*, 49694-49703.
214. Gamblin, T. C., King, M. E., Dawson, H., Vitek, M. P., Kuret, J., Berry, R. W., and Binder, L. I. (2000) In vitro polymerization of tau protein monitored by laser light scattering: method and application to the study of FTDP-17 mutants, *Biochemistry 39*, 6136-6144.
215. Voss, K., and Gamblin, T. C. (2009) GSK-3β phosphorylation of functionally distinct tau isoforms has differential, but mild effects, *Mol Neurodegener 4*, 1-12.
216. Friedhoff, P., Schneider, A., Mandelkow, E. M., and Mandelkow, E. (1998) Rapid assembly of Alzheimer-like paired helical filaments from microtubule-associated protein tau monitored by fluorescence in solution, *Biochemistry 37*, 10223-10230.
217. Berne, B. J. (1974) Interpretation of the light scattering from long rods, *J Mol Biol 89*, 755-758.
218. Santa-Maria, I., Perez, M., Hernandez, F., Avila, J., and Moreno, F. J. (2006) Characteristics of the binding of thioflavin S to tau paired helical filaments, *J Alzheimers Dis 9*, 279-285.
219. Barghorn, S., and Mandelkow, E. (2002) Toward a unified scheme for the aggregation of tau into Alzheimer paired helical filaments, *Biochemistry 41*, 14885-14896.
220. Gamblin, T. C., Berry, R. W., and Binder, L. I. (2003) Tau polymerization: role of the amino terminus, *Biochemistry 42*, 2252-2257.
221. Witman, G. B., Cleveland, D. W., Weingarten, M. D., and Kirschner, M. W. (1976) Tubulin requires tau for growth onto microtubule initiating sites, *Proc Natl Acad Sci U S A 73*, 4070-4074.
222. Esmaeli-Azad, B., McCarty, J. H., and Feinstein, S. C. (1994) Sense and antisense transfection analysis of tau function: tau influences net microtubule assembly, neurite outgrowth and neuritic stability, *J Cell Sci 107*, 869-879.
223. Biernat, J., Gustke, N., Drewes, G., Mandelkow, E. M., and Mandelkow, E. (1993) Phosphorylation of Ser262 strongly reduces binding of tau to microtubules: distinction between PHF-like immunoreactivity and microtubule binding, *Neuron 11*, 153-163.
224. Lu, P. J., Wulf, G., Zhou, X. Z., Davies, P., and Lu, K. P. (1999) The prolyl isomerase Pin1 restores the function of Alzheimer-associated phosphorylated tau protein, *Nature 399*, 784-788.
225. Yoshida, H., and Ihara, Y. (1993) Tau in paired helical filaments is functionally distinct from fetal tau: assembly incompetence of paired helical filament-tau, *J Neurochem 61*, 1183-1186.

226. Leroy, K., Yilmaz, Z., and Brion, J. P. (2007) Increased level of active GSK-3beta in Alzheimer's disease and accumulation in argyrophilic grains and in neurones at different stages of neurofibrillary degeneration, *Neuropathol Appl Neurobiol 33*, 43-55.
227. Gong, C. X., Shaikh, S., Wang, J. Z., Zaidi, T., Grundke-Iqbal, I., and Iqbal, K. (1995) Phosphatase activity toward abnormally phosphorylated tau: decrease in Alzheimer disease brain, *J Neurochem 65*, 732-738.
228. Gong, C. X., Singh, T. J., Grundke-Iqbal, I., and Iqbal, K. (1993) Phosphoprotein phosphatase activities in Alzheimer disease brain, *J Neurochem 61*, 921-927.
229. Jeganathan, S., Hascher, A., Chinnathambi, S., Biernat, J., Mandelkow, E. M., and Mandelkow, E. (2008) Proline-directed pseudo-phosphorylation at AT8 and PHF1 epitopes induces a compaction of the paperclip folding of Tau and generates a pathological (MC-1) conformation, *J Biol Chem 283*, 32066-32076.
230. Haase, C., Stieler, J. T., Arendt, T., and Holzer, M. (2004) Pseudophosphorylation of tau protein alters its ability for self-aggregation, *J Neurochem 88*, 1509-1520.
231. Jicha, G. A., Bowser, R., Kazam, I. G., and Davies, P. (1997) Alz-50 and MC-1, a new monoclonal antibody raised to paired helical filaments, recognize conformational epitopes on recombinant tau, *J Neurosci Res 48*, 128-132.
232. Goode, B. L., Chau, M., Denis, P. E., and Feinstein, S. C. (2000) Structural and functional differences between 3-repeat and 4-repeat tau isoforms. Implications for normal tau function and the onset of neurodegenerative disease, *J Biol Chem 275*, 38182-38189.
233. Berry, R. W., Abraha, A., Lagalwar, S., LaPointe, N., Gamblin, T. C., Cryns, V. L., and Binder, L. I. (2003) Inhibition of tau polymerization by its carboxy-terminal caspase cleavage fragment, *Biochemistry 42*, 8325-8331.
234. Gauthier-Kemper, A., Weissmann, C., Golovyashkina, N., Sebo-Lemke, Z., Drewes, G., Gerke, V., Heinisch, J. J., and Brandt, R. (2011) The frontotemporal dementia mutation R406W blocks tau's interaction with the membrane in an annexin A2-dependent manner, *J Cell Biol 192*, 647-661.
235. Wischik, C. M., Novak, M., Thogersen, H. C., Edwards, P. C., Runswick, M. J., Jakes, R., Walker, J. E., Milstein, C., Roth, M., and Klug, A. (1988) Isolation of a fragment of tau derived from the core of the paired helical filament of Alzheimer disease, *Proc Natl Acad Sci U S A 85*, 4506-4510.
236. Gamblin, T. C., Berry, R. W., and Binder, L. I. (2003) Modeling tau polymerization in vitro: a review and synthesis, *Biochemistry 42*, 15009-15017.
237. Sawaya, M. R., Sambashivan, S., Nelson, R., Ivanova, M. I., Sievers, S. A., Apostol, M. I., Thompson, M. J., Balbirnie, M., Wiltzius, J. J., McFarlane, H. T., Madsen, A. O., Riekel, C., and Eisenberg, D. (2007) Atomic structures of amyloid cross-beta spines reveal varied steric zippers, *Nature 447*, 453-457.
238. von Bergen, M., Barghorn, S., Biernat, J., Mandelkow, E. M., and Mandelkow, E. (2005) Tau aggregation is driven by a transition from random coil to beta sheet structure, *Biochim Biophys Acta 1739*, 158-166.
239. King, M. E., Ahuja, V., Binder, L. I., and Kuret, J. (1999) Ligand-dependent tau filament formation: implications for Alzheimer's disease progression, *Biochemistry 38*, 14851-14859.

240. Congdon, E. E., Kim, S., Bonchak, J., Songrug, T., Matzavinos, A., and Kuret, J. (2008) Nucleation-dependent tau filament formation: the importance of dimerization and an estimation of elementary rate constants, *J Biol Chem 283*, 13806-13816.
241. Arrasate, M., Perez, M., Armas-Portela, R., and Avila, J. (1999) Polymerization of tau peptides into fibrillar structures. The effect of FTDP-17 mutations, *FEBS Lett 446*, 199-202.
242. Barghorn, S., Zheng-Fischhofer, Q., Ackmann, M., Biernat, J., von Bergen, M., Mandelkow, E. M., and Mandelkow, E. (2000) Structure, microtubule interactions, and paired helical filament aggregation by tau mutants of frontotemporal dementias, *Biochemistry 39*, 11714-11721.
243. DeTure, M., Ko, L. W., Yen, S., Nacharaju, P., Easson, C., Lewis, J., van Slegtenhorst, M., Hutton, M., and Yen, S. H. (2000) Missense tau mutations identified in FTDP-17 have a small effect on tau-microtubule interactions, *Brain Res 853*, 5-14.
244. Nacharaju, P., Lewis, J., Easson, C., Yen, S., Hackett, J., Hutton, M., and Yen, S. H. (1999) Accelerated filament formation from tau protein with specific FTDP-17 missense mutations, *FEBS Lett 447*, 195-199.
245. Nagiec, E. W., Sampson, K. E., and Abraham, I. (2001) Mutated tau binds less avidly to microtubules than wildtype tau in living cells, *J Neurosci Res 63*, 268-275.
246. Sahara, N., Tomiyama, T., and Mori, H. (2000) Missense point mutations of tau to segregate with FTDP-17 exhibit site-specific effects on microtubule structure in COS cells: a novel action of R406W mutation, *J Neurosci Res 60*, 380-387.
247. Vogelsberg-Ragaglia, V., Bruce, J., Richter-Landsberg, C., Zhang, B., Hong, M., Trojanowski, J. Q., and Lee, V. M. (2000) Distinct FTDP-17 missense mutations in tau produce tau aggregates and other pathological phenotypes in transfected CHO cells, *Mol Biol Cell 11*, 4093-4104.
248. Yen, S. H., Hutton, M., DeTure, M., Ko, L. W., and Nacharaju, P. (1999) Fibrillogenesis of tau: insights from tau missense mutations in FTDP-17, *Brain Pathol 9*, 695-705.
249. Shulman, J. M., and Feany, M. B. (2003) Genetic modifiers of tauopathy in Drosophila, *Genetics 165*, 1233-1242.
250. Delobel, P., Flament, S., Hamdane, M., Jakes, R., Rousseau, A., Delacourte, A., Vilain, J. P., Goedert, M., and Buee, L. (2002) Functional characterization of FTDP-17 tau gene mutations through their effects on Xenopus oocyte maturation, *J Biol Chem 277*, 9199-9205.
251. Lee, V. M., Kenyon, T. K., and Trojanowski, J. Q. (2005) Transgenic animal models of tauopathies, *Biochim Biophys Acta 1739*, 251-259.
252. Rankin, C. A., and Gamblin, T. C. (2008) Assessing the toxicity of tau aggregation, *J Alzheimers Dis 14*, 411-416.
253. Goedert, M., and Jakes, R. (2005) Mutations causing neurodegenerative tauopathies, *Biochimica et biophysica acta 1739*, 240-250.
254. Hasegawa, M., Smith, M. J., and Goedert, M. (1998) Tau proteins with FTDP-17 mutations have a reduced ability to promote microtubule assembly, *FEBS Lett 437*, 207-210.
255. Wszolek, Z. K., Slowinski, J., Golan, M., and Dickson, D. W. (2005) Frontotemporal dementia and parkinsonism linked to chromosome 17, *Folia Neuropathol 43*, 258-270.
256. Kyte, J., and Doolittle, R. F. (1982) A simple method for displaying the hydropathic character of a protein, *J Mol Biol 157*, 105-132.

257. Chou, P. Y., and Fasman, G. D. (1974) Conformational parameters for amino acids in helical, beta-sheet, and random coil regions calculated from proteins, *Biochemistry 13*, 211-222.
258. Chiti, F., Stefani, M., Taddei, N., Ramponi, G., and Dobson, C. M. (2003) Rationalization of the effects of mutations on peptide and protein aggregation rates, *Nature 424*, 805-808.
259. Morris, A. M., Watzky, M. A., Agar, J. N., and Finke, R. G. (2008) Fitting neurological protein aggregation kinetic data via a 2-step, minimal/"Ockham's razor" model: the Finke-Watzky mechanism of nucleation followed by autocatalytic surface growth, *Biochemistry 47*, 2413-2427.
260. Combs, B., Voss, K., and Gamblin, T. C. (2011) Pseudohyperphosphorylation has differential effects on polymerization and function of tau isoforms, *Biochemistry 50*, 9446-9456.
261. Li, W., and Lee, V. M. (2006) Characterization of two VQIXXK motifs for tau fibrillization in vitro, *Biochemistry 45*, 15692-15701.
262. von Bergen, M., Barghorn, S., Li, L., Marx, A., Biernat, J., Mandelkow, E. M., and Mandelkow, E. (2001) Mutations of tau protein in frontotemporal dementia promote aggregation of paired helical filaments by enhancing local beta-structure, *J Biol Chem 276*, 48165-48174.
263. Mirra, S. S., Murrell, J. R., Gearing, M., Spillantini, M. G., Goedert, M., Crowther, R. A., Levey, A. I., Jones, R., Green, J., Shoffner, J. M., Wainer, B. H., Schmidt, M. L., Trojanowski, J. Q., and Ghetti, B. (1999) Tau pathology in a family with dementia and a P301L mutation in tau, *J Neuropathol Exp Neurol 58*, 335-345.
264. Liu, F., and Gong, C. X. (2008) Tau exon 10 alternative splicing and tauopathies, *Mol Neurodegener 3*, 8.
265. LeBoeuf, A. C., Levy, S. F., Gaylord, M., Bhattacharya, A., Singh, A. K., Jordan, M. A., Wilson, L., and Feinstein, S. C. (2008) FTDP-17 mutations in Tau alter the regulation of microtubule dynamics: an "alternative core" model for normal and pathological Tau action, *The Journal of biological chemistry 283*, 36406-36415.
266. Barghorn, S., Zheng-Fischhofer, Q., Ackmann, M., Biernat, J., von Bergen, M., and Mandelkow, E. (2000) Structure, microtubule interactions, and paired helical filament aggregation by tau mutants of frontotemporal dementias, *Biochemistry 39*, 11714-11721.
267. Grover, A., DeTure, M., Yen, S. H., and Hutton, M. (2002) Effects on splicing and protein function of three mutations in codon N296 of tau in vitro, *Neurosci Lett 323*, 33-36.
268. Neumann, M., Schulz-Schaeffer, W., Crowther, R. A., Smith, M. J., Spillantini, M. G., Goedert, M., and Kretzschmar, H. A. (2001) Pick's disease associated with the novel Tau gene mutation K369I, *Ann Neurol 50*, 503-513.
269. Ishihara, T., Hong, M., Zhang, B., Nakagawa, Y., Lee, M. K., Trojanowski, J. Q., and Lee, V. M. (1999) Age-dependent emergence and progression of a tauopathy in transgenic mice overexpressing the shortest human tau isoform, *Neuron 24*, 751-762.
270. Hall, G. F., Chu, B., Lee, G., and Yao, J. (2000) Human tau filaments induce microtubule and synapse loss in an in vivo model of neurofibrillary degenerative disease, *J Cell Sci 113 (Pt 8)*, 1373-1387.
271. Mocanu, M. M., Nissen, A., Eckermann, K., Khlistunova, I., Biernat, J., Drexler, D., Petrova, O., Schonig, K., Bujard, H., Mandelkow, E., Zhou, L., Rune, G., and

Mandelkow, E. M. (2008) The potential for beta-structure in the repeat domain of tau protein determines aggregation, synaptic decay, neuronal loss, and coassembly with endogenous Tau in inducible mouse models of tauopathy, *J Neurosci 28*, 737-748.
272. Iliev, A. I., Ganesan, S., Bunt, G., and Wouters, F. S. (2006) Removal of pattern-breaking sequences in microtubule binding repeats produces instantaneous tau aggregation and toxicity, *J Biol Chem 281*, 37195-37204.
273. Brenner, S. (1974) The genetics of Caenorhabditis elegans, *Genetics 77*, 71-94.
274. Steele, J. C., Richardson, J. C., and Olszewski, J. (1964) Progressive Supranuclear Palsy. A Heterogeneous Degeneration Involving the Brain Stem, Basal Ganglia and Cerebellum with Vertical Gaze and Pseudobulbar Palsy, Nuchal Dystonia and Dementia, *Arch Neurol 10*, 333-359.
275. Chew, Y. L., Fan, X., Gotz, J., and Nicholas, H. R. (2013) Protein with tau-like repeats regulates neuronal integrity and lifespan in C. elegans, *J Cell Sci*.
276. Bunker, J. M., Wilson, L., Jordan, M. A., and Feinstein, S. C. (2004) Modulation of microtubule dynamics by tau in living cells: implications for development and neurodegeneration, *Mol Biol Cell 15*, 2720-2728.
277. Nekooki-Machida, Y., Kurosawa, M., Nukina, N., Ito, K., Oda, T., and Tanaka, M. (2009) Distinct conformations of in vitro and in vivo amyloids of huntingtin-exon1 show different cytotoxicity, *Proc Natl Acad Sci U S A 106*, 9679-9684.
278. Angers, R. C., Kang, H. E., Napier, D., Browning, S., Seward, T., Mathiason, C., Balachandran, A., McKenzie, D., Castilla, J., Soto, C., Jewell, J., Graham, C., Hoover, E. A., and Telling, G. C. (2010) Prion strain mutation determined by prion protein conformational compatibility and primary structure, *Science 328*, 1154-1158.
279. Petkova, A. T., Leapman, R. D., Guo, Z., Yau, W. M., Mattson, M. P., and Tycko, R. (2005) Self-propagating, molecular-level polymorphism in Alzheimer's beta-amyloid fibrils, *Science 307*, 262-265.
280. Badiola, N., Suarez-Calvet, M., and Lleo, A. (2010) Tau phosphorylation and aggregation as a therapeutic target in tauopathies, *CNS Neurol Disord Drug Targets 9*, 727-740.
281. Terry, R. D., Masliah, E., Salmon, D. P., Butters, N., DeTeresa, R., Hill, R., Hansen, L. A., and Katzman, R. (1991) Physical basis of cognitive alterations in Alzheimer's disease: synapse loss is the major correlate of cognitive impairment, *Ann Neurol 30*, 572-580.
282. Coleman, P. D., and Yao, P. J. (2003) Synaptic slaughter in Alzheimer's disease, *Neurobiol Aging 24*, 1023-1027.
283. Lehericy, S., Hirsch, E. C., Cervera-Pierot, P., Hersh, L. B., Bakchine, S., Piette, F., Duyckaerts, C., Hauw, J. J., Javoy-Agid, F., and Agid, Y. (1993) Heterogeneity and selectivity of the degeneration of cholinergic neurons in the basal forebrain of patients with Alzheimer's disease, *J Comp Neurol 330*, 15-31.
284. Whitehouse, P. J., Price, D. L., Clark, A. W., Coyle, J. T., and DeLong, M. R. (1981) Alzheimer disease: evidence for selective loss of cholinergic neurons in the nucleus basalis, *Ann Neurol 10*, 122-126.
285. Davis, K. L., Mohs, R. C., Marin, D., Purohit, D. P., Perl, D. P., Lantz, M., Austin, G., and Haroutunian, V. (1999) Cholinergic markers in elderly patients with early signs of Alzheimer disease, *JAMA 281*, 1401-1406.
286. Gilmor, M. L., Erickson, J. D., Varoqui, H., Hersh, L. B., Bennett, D. A., Cochran, E. J., Mufson, E. J., and Levey, A. I. (1999) Preservation of nucleus basalis neurons containing

choline acetyltransferase and the vesicular acetylcholine transporter in the elderly with mild cognitive impairment and early Alzheimer's disease, *J Comp Neurol 411*, 693-704.
287. Loreth, D., Ozmen, L., Revel, F. G., Knoflach, F., Wetzel, P., Frotscher, M., Metzger, F., and Kretz, O. (2012) Selective degeneration of septal and hippocampal GABAergic neurons in a mouse model of amyloidosis and tauopathy, *Neurobiol Dis 47*, 1-12.